ABSTRACT

Title of dissertation: SOCIAL AND ECOLOGICAL FACTORS INFLUENCING COLLECTIVE BEHAVIOR IN GIANT DANIO

Amanda Megan Chicoli, Doctor of Philosophy, 2016

Dissertation directed by: Professor Derek Paley
Neuroscience and Cognitive Science Program

A fundamental problem in biology is understanding how and why things group together. Collective behavior is observed on all organismic levels — from cells and slime molds, to swarms of insects, flocks of birds, and schooling fish, and in mammals, including humans. The *long-term goal* of this research is to understand the functions and mechanisms underlying collective behavior in groups.

This dissertation focuses on shoaling (aggregating) fish. Shoaling behaviors in fish confer foraging and anti-predator benefits through social cues from other individuals in the group. However, it is not fully understood what information individuals receive from one another or how this information is propagated throughout a group. It is also not fully understood how the environmental conditions and perturbations affect group behaviors. The *specific research objective* of this dissertation is to gain

a better understanding of how certain social and environmental factors affect group behaviors in fish.

I focus on two ecologically relevant decision-making behaviors: (i) rheotaxis, or orientation with respect to a flow, and (ii) startle response, a rapid response to a perceived threat.

By integrating behavioral and engineering paradigms, I detail specifics of behavior in giant danio *Devario aequipinnatus* (McClelland 1893), and numerically analyze mathematical models that may be extended to group behavior for fish in general, and potentially other groups of animals as well. These models that predict behavior data, as well as generate additional, testable hypotheses.

One of the primary goals of neuroethology is to study an organism's behavior in the context of evolution and ecology. Here, I focus on studying ecologically relevant behaviors in giant danio in order to better understand collective behavior in fish. The experiments in this dissertation provide contributions to fish ecology, collective behavior, and biologically-inspired robotics.

Social and Ecological Factors Influencing Collective Behavior in Giant Danio

by

Amanda Megan Chicoli

Dissertation submitted to the Faculty of the Graduate School of the
University of Maryland, College Park in partial fulfillment
of the requirements for the degree of
Doctor of Philosophy
2016

Advisory Committee:
Dr. Derek Paley, Chair/Advisor
Dr. Arthur Popper, Co-Advisor
Dr. Jens Herberholz, Dean's Representative
Dr. Catherine Carr
Dr. Jonathan Simon

Preface

Versions of Chapters 3 and 6 of this dissertation has been previously published. At the time of writing, material from other chapters is in preparation for submission to peer-reviewed journals.

Peer-reviewed publications included in this dissertation:

1. A. Chicoli, J. Bak-Coleman, S. Coombs, & D. A. Paley (2015). Rheotaxis performance increases with group size in a coupled phase model with sensory noise. *European Physics Journal Special Topics* 224:17 3233-3244. The final publication is available at Springer via http://dx.doi.org/[10.1140/epjst/e2015-50080-x]

2. A. Chicoli, S. Butail, Y. Lun, J. Bak-Coleman, S. Coombs & D. A. Paley (2014). The effects of flow on schooling *Devario aequipinnatus*: school structure, startle response and information transmission. *Journal of Fish Biology* 84:5 1401-1421 .

Peer-reviewed publications not included in the dissertation:

1. S. Butail, A. Chicoli, & D. A. Paley (2012). Putting the fish in the fish tank: Immersive VR for animal behavior experiments. *Proc. IEEE International Conference on Robotics and Automation* 5018-5023

Dedication

To my family

Acknowledgments

I owe my greatest gratitude to my advisor, Dr. Derek Paley for his unwavering support and guidance. Dr. Paley took the risk of hiring me, knowing I had little background in engineering or computer science — skills necessary to complete this dissertation. Not only have I learned a great deal thanks to his patience, but the research and opportunities I have had during my graduate career have sparked a passion and interest in engineering problems that will continue throughout my career. It is rare to find a mentor who is enthusiastic, full of ideas, and has a genuine interest in their student's research, so I am especially grateful to have had Dr. Paley as a mentor, who is all of the above. As a mentor, Dr. Paley is a champion of all his students and has been incredibly supportive of me not only in my research endeavors, but also encouraged a work-life balance, and allowed me to pursue outreach and committee activities as well. Dr. Paley has created a lab family and work environment that has been a great pleasure to work in. Thanks for the lab meetings, bbqs, and CDCL vs the Wild adventures. I couldn't have survived the outdoor rope course or this dissertation without your guidance.

I would also like to thank my co-advisor, Dr. Arthur Popper. From the first interview at Maryland where he insisted I download when2meet, to providing the equipment and lab space necessary for the work in this dissertation, he has been providing valuable advise and resources, and has always been willing to meet. As a fellow New Yorker, it always felt like home walking into Dr. Popper's office.

In addition to two incredible mentors, my time at Maryland has provided me with countless colleagues and role models whose time, advice, and interactions have provided solutions to research problems, and helped shape my perspective. In this I must especially thank faculty members who have served on various committees, including this dissertation defense: Professors Jens Herberholz, Catherine Carr, Jonathan Simon, Daphne Soares, Dan Butts, and Sheryl Coombs. Thanks to Dr. Eric Tytell and Dr. Avis Cohen as well for lending the high frame rate camera used in several experiments.

My colleagues at the Collective Dynamics and Control Laboratory have enriched my graduate life in many ways and deserve a special mention. I thank current and former CDCL lab members Dr. Sachit Butail, Dr. Levi DeVries, Seth Napora, Dr. Nitin Sydney, Dr. Cammy Peterson, Dr. Tracy Severson, Daigo Shishika, William Craig, Frank Lagor, Chin Gian Hooi, Steve Sherman, Dr. Feitian Zhang, Dr. Derrick Yeo, Brian Free, and Brett Barkley. You have all provided countless laughs, chess games, coffee, and discussions. I also owe special thanks to the undergraduates who have worked with me over the years, including Jen (Yu) Lun, Hongyi

Xia, Patrick Washington, Steven Tennyson, Michael Baeder, and Sajni Patel, as well as to the numerous past and present undergraduate members of the CDCL who contributed to discussions.

I also owe a great deal of gratitude to everyone in the Neuroscience and Cognitive Science Program. While too many to name, the students in the program, while spread across campus and different institutions have provided a home and tight-knit community. Through committees, student seminars, happy hours, rock climbing, and parties at Kenesaw and Patricia Court, I have made many lasting friendships, and learned a lot more about linguistics, cognitive science, and electrophysiology thanks to all of you.

Thank you to Pam Komarek and Emerald Brooks for answering numerous questions, organizing NACS events, and supplying plenty of snacks for seminars. I would like to thank the NACS grant specialists Beth Brittan-Powell, Katie Sacksteder, and Gaelle Kolb for their advice on fellowships and career guidance.

Thanks to everyone in the Aerospace Engineering department. Thanks to LaVita Williams for handling countless equipment orders, and always making my day brighter, to Laura Thornsen, who trekked across campus to learn how to submit an NRSA fellowship, to Tom Hurst for organizing student events, to Michael Jones for switching my payroll and insurance almost every semester without issue, to Kevin Lewy for fixing numerous lab computers, and to Otto Fandino for making everything run smoothly.

My housemates at my places of residence have been a crucial factor in my finishing smoothly. I'd like to express my gratitude to Michelle Arthur, Jeffrey Chrabaszcz, and Kyle Wakayama for introducing me to rock climbing and mountain biking, (as terrible as I am at both of those activities), for whiskey, statistics, and Shakespeare. Rita Lee, Naomi Kane, Margalit Haber, Gregory Perrin, and Sameen Farooq have all remained close friends from both near and far despite all our busy schedules. Thank you for your continued friendship.

I owe my deepest thanks to my family. To my mom for nourishing my interest in science at an early age, and for instilling a strong work ethic. To my Dad for always reminding me to accomplish goals one step at a time. I also owe a great deal of thanks to my boyfriend, John Stanley, who has kept me afloat the past two years.

As the only biologist in an engineering lab, I often found myself traveling to conferences solo. I owe a great thanks to all the great friends I have met during these travels, who welcomed me to their lab groups, provided ears for practice talks, and made every conference an enjoyable adventure. I hope to continue to see you all for years to come.

I would like to acknowledge financial support from the National Science Founda-

tion, grant CMMI 0954361, and training grant DC00046 from the National Institute of Deafness and Communicative Disorders of the National Institutes of Health.

It is impossible to remember all, and I apologize to those I've inadvertently left out.

Table of Contents

List of Tables xi

List of Figures xii

1 Introduction and general background 1
1.1 Motivation . . . 1
1.2 Objectives . . . 4
1.3 Behavioral ecology of giant danio *Devario aequipinnatus* . . . 5
1.4 Relation to previous literature . . . 8
1.4.1 Shoaling and schooling behavior in fish . . . 9
1.4.2 Rheotaxis . . . 15
1.4.3 Startle response . . . 18
1.5 Approach . . . 22
1.6 Contributions of dissertation . . . 23
1.7 Organization of dissertation . . . 25
1.8 Statement about the use of experimental animals . . . 28

2 Mathematical background 29
2.1 Individual-based tracking . . . 30
2.2 Analysis of spatial data . . . 32
2.2.1 Nearest neighbor distance . . . 32
2.2.2 Spatial autocorrelations . . . 33
2.2.3 The convex hull . . . 34
2.3 Analysis of orientation and heading . . . 36
2.3.1 Quantitative analysis of circular data . . . 36
2.3.2 Polarization and the phase order parameter . . . 37

2.3.3 External and internal disagreement . . . 38
2.3.4 Characterizing a startle response . . . 39
2.4 Graph theory . . . 40
2.5 Synchronization and coupled oscillator models . . . 42
2.6 Susceptible-Infected-Removed (SIR) models . . . 45

Part I: Group Rheotaxis 51

3 Rheotaxis performance increases with group size in a coupled phase model with sensory noise 51
3.1 Introduction . . . 51
3.2 Noisy synchronization model . . . 52
3.3 Modeling Results . . . 56
3.3.1 No gain on reference direction . . . 56
3.3.2 No gain on neighbor orientation . . . 58
3.3.3 Equal gain on reference direction and neighbor orientation . . . 58
3.3.4 Higher gain on neighbor orientation . . . 59
3.3.5 Higher gain on the reference direction . . . 60
3.4 Discussion . . . 60
3.4.1 Effect of sensory noise on synchronization . . . 62
3.4.2 Effect of group size on synchronization . . . 63

4 Effects of flow speed and group size on rheotaxis and shoaling in giant danio 67
4.1 Introduction . . . 67
4.2 Materials and methods . . . 68
4.2.1 Experimental animal care . . . 68
4.2.2 Experimental set-up . . . 68
4.2.3 Experimental design . . . 69
4.2.4 Experimental protocol . . . 71
4.2.5 Statistical analysis . . . 72
4.2.6 Aggregation model . . . 73
4.3 Experimental Results . . . 75
4.3.1 Effects of flow speed and group size on rheotaxis . . . 75
4.3.2 Effects of flow speed and group size on group alignment . . . 77
4.3.3 Effects of flow speed and group size on group aggregation . . . 79
4.3.4 Space utilization . . . 80
4.3.5 Results of the aggregation model . . . 80
4.4 Discussion . . . 83

4.4.1 Flow speed, group size and rheotaxis performance 83
4.4.2 Increased aggregation with group size 86

Part II: Startle Response and Information Transmission 91

5 Probabilistic information transmission in a network of coupled oscillators 91
5.1 Introduction 91
5.2 Methods 93
5.2.1 Coupled oscillator synchronization model 93
5.2.2 Probabilistic model of information transmission 94
5.2.3 Behavioral Rules 96
5.2.4 Parameter space 97
5.2.5 Shoaling types 97
5.2.6 Analysis metrics 99
5.3 Results 100
5.3.1 Startle propagation 101
5.3.2 Orientation dynamics 103
5.4 Discussion 106

6 Effect of flow on group structure, startle response and information transmission 111
6.1 Introduction 111
6.2 Experimental design 113
6.3 Experimental approach 116
6.3.1 Experimental set-up 116
6.3.2 Stimulus design 119
6.3.3 Statistical analysis 120
6.3.4 Model of information transmission 120
6.4 Results 122
6.4.1 Alignment in flow and no flow 122
6.4.2 Neighbor position and school structure 124
6.4.3 Response probability 125
6.4.4 Model including social information fits experimental data . . . 126
6.5 Discussion 128
6.5.1 The effect of flow on group formation and polarity 129
6.5.2 Startle response probability and information transmission . . . 131
6.5.3 Variability of startle responses 134
6.5.4 Modeling information transmission 136

Summary and Conclusions 145

7 Conclusions and suggestions for future work 145
7.1 Summary of contributions 145
7.2 Ongoing work and suggestions for future research 148
7.2.1 Synchronization in noisy environments 148
7.2.2 Group size benefits 149
7.2.3 Information transmission in groups 150
7.2.4 Modeling multi-sensory integration 152
7.2.5 Individual differences 153

Appendix A 157

Bibliography 164

List of Tables

3.1 Summary of model parameters 56

5.1 Parameter space of probabilistic startle model 98
5.2 Shoaling categories 99

6.1 Linear mixed-effects model investigating the effect of stimulus speed, group size and flow condition on response. Replicate groups were controlled for as a random effect 127

A.1 Linear mixed effects model investigating the effect of group size, flow speed and flow direction on external disagreement (ED). Replicate groups were controlled for as a random effect. 157
A.2 Linear mixed effects model investigating the effect of group size, flow speed and flow direction on internal disagreement (ID). Replicate groups were controlled for as a random effect. 158
A.3 Linear mixed effects model investigating the effect of group size, flow speed and flow direction on standard deviation in x-position (cross-stream). Replicate groups were controlled for as a random effect. . . . 159
A.4 Linear mixed effects model investigating the effect of group size, flow speed and flow direction on the standard deviation in y-position (stream-wise). Replicate groups were controlled for as a random effect. 160
A.5 Linear mixed effects model investigating the effect of group size, flow speed and flow direction on NND. Replicate groups were controlled for as a random effect. 161
A.6 Linear mixed effects model investigating the effect of group size, flow speed and flow direction on shoal density. Replicate groups were controlled for as a random effect. 162

A.7 Linear mixed effects model investigating the effect of group size, flow speed and flow direction on shoal area. Replicate groups were controlled for as a random effect. 163

List of Figures

1.1 a) Photo of giant danio, used from Wikipedia through a Creative Commons license; b) staining photo of giant danio superficial lateral line with DASPEI, used with permission from the laboratory of Dr. Sheryl Coombs, and c) photo of a shoal of giant danio in a laboratory tank. 8
1.2 An illustration depicting the approach I use to investigate both rheotactic and startle response behaviors. 23
1.3 Illustration of the organization of this dissertation. Each part pertains to a different behavior, either group rheotaxis or startle response. There are two chapters within each part: a chapter on mathematical modeling, followed by an experiment that either explicitly tests model predictions, or is fit to the model detailed in the preceding chapter. . 26

2.1 Sample of individually tracked fish, showing the fish silhouette, the series of elliptical cross-sections used to estimate the midline and the midline of eight fish. 31

2.2 Illustration of neighbor distance and bearing. Each focal fish k fish has a position in space notated by x_k and y_k coordinates. Time is not included in this schematic. Note that the positional coordinates here can also be referenced in the complex plane for compactness, as an alternative to Cartesian coordinates. Each fish has an orientation notated by θ. I measure the distance to a neighboring fish as the distance from the head (between the eyes) of the focal fish k to the same location on the neighboring fish, l. The bearing of the focal fish relative to the neighboring fish is given by δ, the angle between agent l's orientation and agent k's orientation. 33
2.3 Illustration of the convex hull for a group of fish. Fish positions are marked. The outermost fish are the coordinate points for the polygon of the convex hull. This is illustrated by the purple line. The area within the purple bounds would be the calculated area of the shoal. . 35
2.4 Illustrating the magnitude component of polarization, the vector strength. Low vector strength indicates weak alignment, whereas high vector strength indicates strong alignment. 37
2.5 Fish orientations lie on the circle, as shown by the black lines extending from the fish. When calculating the difference between orientations, there are two potential answers, α and β. The chord length, in green, is a unique answer to the difference in orientations between agents. Since the diameter (purple dashed line) of the unit circle is equal to 2, the maximum difference between any two agents would be 2. The chord length divided by 2 bounds the difference in orientation between two agents between 0 and 1. 40
2.6 Depiction of (a) metric and (b) topological interaction topologies. The focal fish is in red, fish affected the focal fish's behavior are in yellow. 42
2.7 (a) Fixed interaction between agents (fish) depicted by a graph. Nodes of the graph are fish, and arrows are directional edges of the graph. (b) Another representation of the graph in (a). Red filled agents or outlined circles are in a startled state, and can spread the startle to connected agents. 48

3.1 Example von Mises distributions with concentration values 10^2, 10^0 and 10^{-2}. 54
3.2 Typical runs (N=4, N=32) in the presence of low noise, $\sigma = \sigma_0 = 10^2$ (a,c) and moderate noise, $\sigma = \sigma_0 = 10^0$ (b,d). 57

3.3 (a,b) Synchronization results when the gain on flow is zero ($\kappa_0 = 0$). (c,d) Gain on neighbors is zero ($\kappa_0 = 1$). (a,c) ED and (b,d) ID, over all group sizes, N and noise values. Noise values are as follows: (a,b) $\sigma = 10^2$ and (c,d) $\sigma_0 = 10^2$ (yellow), (a,b) $\sigma = 10^0$ and (c,d) $\sigma_0 = 10^0$ (orange online), and (a,b) $\sigma = 10^{-2}$ and (c,d) $\sigma_0 = 10^{-2}$ (blue). Length of bars represent the upper and lower quartiles. 64
3.4 The effect of group size on synchronization results when there is both neighbor and flow information ($\kappa_0 = 1/2$) for low (a,b), moderate (c,d) and high (e,f) flow noise levels and for low (yellow), moderate (orange) and high (blue) levels of neighbor noise within each of these flow noise conditions. Length of bars represent the upper and lower quartiles. 65
3.5 The effect of group size on internal disagreement (ID) when there is a slight preference for neighbor orientation ($\kappa_0 = 1/3$) (a), or a slight preference for the reference direction ($\kappa_0 = 2/3$) (b) in the presence of high flow noise ($\sigma_0 = 10^{-2}$). Low (yellow), moderate (orange) and high (blue) levels of neighbor noise is shown for each condition. Length of bars represent the upper and lower quartiles. 66

4.1 Experimental set-up, illustrating the Loligo flow tunnel, overhead camera and mirror placement. 70
4.2 Experimental protocol 72
4.3 Sample data, showing fish, head and nose positions (green dots and stars, respectively) as well as fish orientation, and the direction into the flow. 74
4.4 Effect of flow speed, group size and replicate on dependent variables of (a) ED, (b) ID. Increasing and decreasing flow speed changes are pooled together. 76
4.5 Rose histograms of fish orientation over group sizes and flow speeds. Note that these histograms are not scaled. 78
4.6 Effect of flow speed, group size and replicate on dependent variables of (a) std x-position, (b) std y-position. Increasing and decreasing flow speed changes are pooled together. 79
4.7 Effect of flow speed, group size and replicate on dependent variables of (a) NND (b) density of shoal, (c) area of shoal, and (d) image of experimental data with 32 fish demonstrating aggregation. For (a)-(c), increasing and decreasing flow speed changes are pooled together. . . 81

4.8 Aggregation model predictions in nearest neighbor distance. The yellow line with triangles shows the trend in the experimental data, in which NND decreases as a function of $1/\sqrt{N}$. The line with blue crosses shows the model results run with all-to-all interaction topology. The line with red squares shows the model run with a limited interaction topology of the four closest neighbors. The line with purple stars is the standard deviation in xy-position for the limited interaction topology. 82

5.1 The transition diagrams illustrating how agents change state. 95
5.2 Image depicting change in agent state over time as a cellular automata. Blue indicates a non-startled state and yellow indicates a startled state. On the first time step, ten agents startle due to the external threat via P^{ext}. On subsequent time steps, the startle propagates throughout the shoal. 95
5.3 Categorization of shoaling behavior in the model. 99
5.4 Exemplary plots depicting proportion of shoal startling over time. . . 100
5.5 Bar plot illustrating the max proportion of the shoal startled (averaged over 300 Monte Carlo runs) for sample values of P^{ext} and P^{int}. Error bars are 95% confidence intervals. 102
5.6 Bar plot illustrating the average proportion (over 300 Monte Carlo runs) of the shoal oriented $\pm 20°$ from the reference direction at the time of the last startle response. Error bars are 95% confidence intervals. 104
5.7 Bar plot illustrating the average proportion (over 300 Monte Carlo runs) of the shoal oriented $\pm 20°$ from the reference direction at the last time step of the simulation. Error bars are 95% confidence intervals. 105
5.8 Waterfall plots displaying orientation histograms over time for all three shoaling types, $P^{ext} = 0.05$, $P^{ext} = 0.05$ Note the time scale plots the first five time steps when most startles occur, then plots once every 10 time steps up until 50, by which time the startles have long ended. 109

6.1 Experimental arena depicted working area, and verification screen, showing a stimulus. The side of the screen where the black square is located is the side where the stimulus is being shown. 115

6.2 (a) Schematic of the flow tank (adapted from (Vogel and Labarbera, 1978). An impeller drives water through a return tube. The collimators reduce turbulence and fish were tested in the 25.4 × 25.4 cm working area. The working area is backlit with evenly distributed fluorescent lighting. (b) Top view of the working area during a flow trial. Arrows illustrate the direction of flow. (c) Three-dimensional illustration of the flow tank with overhead mounted camera, connected to a computer outside the experimental room. Stimuli are presented to either side of the tank by the computer monitors attached to a computer that generates the stimulus movies (Chicoli et al., 2014). . . . 117
6.3 Time-averaged vector strength and direction associated with groups of eight fish in flow (a) and no-flow (b), where the orientation 0° is in the upstream direction. Vector strength ranges from 0 to 1, with 1 being the highest degree of alignment. Probability of individuals in solitary trials responding to a looming stimulus according to orientation with respect to the stimulus location at stimulus onset in flow (c) and no-flow (d), where the orientation 0° is in the stimulus direction. Length of rose histogram indicates the frequency with which individual fish are oriented in any given direction at the time of stimulus onset, whereas the color indicates the probability of a response, computed from the total number of solitary trials (Chicoli et al., 2014). 137
6.4 (a) and (b) Probability density functions of relative position. Color corresponds to the number of points in each bin, normalized by the bin with the most points. Red circles are one standard deviation away from the mean, white circles are the average nearest-neighbor distance. (a) flow (b) no-flow; (c) and (d) Scatterplots and corresponding histograms of individual position in the tank (Chicoli et al., 2014). . . . 138
6.5 Response probabilities of at least one fish startling at various stimulus speeds in individual (squares) and groups of eight fish (circles). Error bars are the standard error of the mean. There were eight blocks for each condition and, within each of the blocks, each stimulus was shown twice (16 measurements per point). Filled black symbols indicate flow and empty symbols indicate no-flow (Chicoli et al., 2014). 139

6.6 Frequency distributions of the number of giant danio responding in (a) flow and (b) no flow. (c) Cumulative probability distribution of the number of fish responding (black squares are flow trials, empty squares are no-flow trials). Dotted lines with corresponding black and empty symbols for flow and no-flow, respectively, show polynomial model fits to the distributions 140
6.7 Example of an optimal fit of a probabilistic model (empty bars, simulated data) to the cumulative probability distributions of a certain number of giant danio startling in (a) flow and (b) no flow (black squares, experimental data; grey shaded region, mean fit of the model $\pm s.d.$ 141
6.8 Semi-log plots of optimized values of P^{ext} (the probability of directly responding to a threat) and P^{int} (the probability of responding to cues from other individuals) in flow (black squares) and no flow (white circles) for (a) and (c) n-neighbor and (b) and (d) metric distance topologies. In the n-neighbour topology, fish receive signals from the closest n number of neighbors, whereas in the metric distance topology networks, fish receive signals from all neighboring fish within a given radial distance. 142

Chapter 1: Introduction and general background

1.1 Motivation

A group of fish darts away from a predator in a silvery flash, a flock of birds morphs and twists in the sky, and crowds of pedestrians brush past each other on the streets of New York. Collective behaviors[1] are mesmerizing to watch and have fascinated philosophers and scientists for centuries. As early as the 4^{th} century B.C., Aristotle wrote on the collective behavior of fishes. In his work *Historia Animalium*, he described the behavior of a shoal of fish as apolitical in that the advantages of being a member in the school were passive, resulting from baseline coordination among members (Peck, 1970). Aside from inspiring philosophers and being fascinating to watch, the investigation into the collective behavior — in particular the collective behaviors of fish — has many potential applications, specifically (i) in the protection of fish shoals from man-made hazards, (ii) application to group behavior in other

[1]Collective behavior is defined as the behavior of aggregates who do not have procedures for selecting or identifying leaders or members and where emergent behaviors not seen at the individual level can be observed (Turner and Killian, 1957).

species, including humans, and (iii) the design of sensors and controls for autonomous vehicles.

Fish are a key part of the marine ecosystem and likely to be affected by hydrokinetic tidal turbines and hydrodams (Viehman and Zydlewski, 2015). However, little is known about fish behavior around these fluid obstacles (Goodwin et al., 2014; Hammar et al., 2013). Viehman and Zydlewski (2015) found that shoals of fish had a lower probability of entering a turbine than individual fish, and also reacted at greater distances from the turbine. This suggests that communities and groups of fish differ from individuals in their behavior around obstacles. In order to better protect fish, we must first understand the behavior of both individual and groups of fish in different environmental conditions.

By quantifying both the behavior of groups and individuals in different ecological environments, we may also gain a better understanding of group behaviors in other animal groups as well, including humans. Humans are a social group-living species. Although there are many differences in how humans and fish group together, there are also shared characteristics in group behavior. The investigation of how shoals of fish move and make decisions in groups can influence city and emergency planning (Faria et al., 2009; Helbing et al., 2005), and lend potential insights into political(Conradt and Roper, 2003, 2005; Couzin et al., 2011, 2012; Sumpter et al.,

2008) and economic processes (Cont and Bouchaud, 1997; Orlean, 1995). Studying fish cognition and behavior in groups may also help us understand more about the evolution of human culture (Laland et al., 2011) and human decision-making (Conradt et al., 2009; Kurvers et al., 2013).

With the investigation of emergent behaviors in fish, there is also the potential application to bio-inspired robotics (Lauder and Madden, 2006). Because fish shoals can coordinate without a specific leader, understanding fish interaction rules can help influence the design of autonomous controls for multiple vehicles (Rubenstein et al., 2014; Schmicl and Crailsheim, 2008). (Although leadership does seem to play a role in fish and other group behaviors (Biro et al., 2010; Couzin et al., 2005; Krause et al., 2000; Reebs, 2000)). The lateral line of fish (see Section 1.4.1) is also of interest to engineers. Vision is currently the main sensory modality used for autonomous vehicles. In cluttered, dark, or murky environments many autonomous vehicles have trouble navigating, making environmental sampling, and rescue attempts difficult in these environments. Use of a lateral-line inspired sensor for autonomous vehicles may improve performance in these otherwise unfavorable conditions (Yang et al., 2011; Zhang et al., 2015).

1.2 Objectives

Advances in tracking software, including automated tracking and the ability to deal with occlusions of individual agents (Butail and Paley, 2011; Perez-Escudero et al., 2014) have allowed for quantitative results on individual movements to be obtained. As a result, over the past decade there has been a surge of quantitative data on group behavior. However, we still do not fully understand how or why groups form, how information is transmitted between group members, or how the environment modulates group behaviors.

While there has been extensive research on shoaling behaviors, much less attention has been given to investigating what happens when a shoal is perturbed (e.g., from a predator attack). Additionally, there has been almost no research investigating the effects of how the fluid environment in which fish live affects group behaviors (Rieucau et al., 2014a).

This research seeks to better understand how social and ecological factors influence decision-making behaviors in groups of fish and how information may propagate through a group. Specifically, this dissertation combines tools from biology, engineering, and computer science to investigate the roles of group size, sensory noise, and flow on rheotaxis and startle response behavior.

The existing gaps of knowledge addressed in this dissertation are

1. Investigation of the effects of unbounded noise on synchronization;

2. Quantification of the effects of group size and flow on shoaling, rheotaxis and startle response behaviors;

3. Prediction of the spread of information transmission through a group that includes dynamics.

1.3 Behavioral ecology of giant danio *Devario aequipinnatus*

The phylogeny of giant danio has been debated over the years. The most recent detailing of the phylogeny of the genus *Danio* has been detailed by (Fang, 2003; Mayden et al., 2006), in which several species of fish were determined to belong to a related genus, *Devario*. *Devario aequippinatus* was agreed to be the scientific name for the species of giant danio.

Giant danio *Devario aequipinnatus* McClelland 1839 are a cyprinid minnow species. They are surface-dwelling tropical fish species naturally occurring in South and Southeast Asia, including northern India, Nepal, Bangladesh, Myanmar, and Thailand. They inhabit freshwater, in flowing rivers or streams of moderate flow speeds of up to two body lengths per second (BL^{-s}) (McClure et al., 2006), and

form loose aggregations or schools. They feed mainly on insects (McClure et al., 2006). The giant danio reflect blue, green, and yellow tones. There is a bright yellow central strip that extends along the body of the fish (Figure 1.1), and individuals tend to have different body patterning. Their most common natural predators are kingfishers (McClure field notes).

Giant danio were selected for these studies because their ecology and shoaling behaviors make them ideal for studies of collective behavior in flow. Additionally, giant danio have been previously used for a variety of behavioral studies investigating their rheotactic, startle response, and shoaling behaviors.

With regards to foraging behavior and rheotaxis, Chapman and Kramer (1996) investigated competitive tactics in giant danio when responding to zebrafish *Danio rerio* intruders to a food source. They found that an individual giant danio was able to successfully defend a food source agains a group of five zebrafish, but as the number of zebrafsh intruders increased up to 20, the defense rate dropped, as indicated by the precent of chases of intruder fish. Bak-Coleman et al. (2013) investigated rheotactic behavior in giant danio with different sensory modalities and found that giant danio exhibit rheotaxis even in the absence of light, and with the hair cells of the lateral line ablated.

In experiments involving shoaling, Viscido et al. (2004) measured shoal charac-

teristics in groups of four and eight giant danio in order to study individual behavior and emergent properties in fish schools. Paley et al. (2007) detailed a coupled oscillator system with particles to model shoaling behavior, and used giant danios to validate the model. They found that giant danios tended to show higher alignment with close neighbors, while the overall group polarization remained low. Stienessen and Parrish (2013) investigated shoal decision-making based on heterogeneity with regard to information about a food source and detailed resulting shoal dynamics. They found that the fish behavior was a combination of behaviors found in both the trained or informed fish (searching behavior) and the uninformed fish (aggregating tightly). By varying the number of uninformed giant danios, they provided evidence that information is shared between individuals, and that uninformed fish play an active role in the decision-making process. Bartolini et al. (2015) investigated the effect of temperature on shoaling giant danios, and found that lower temperatures lead to tighter shoals with reduced activity.

In order to visualize flow fields during swimming and startle response behaviors, Zhu et al. (2002) used giant danio in examining three-dimensional flows during normal fish swimming. Epps and Techet (2007) studied the relation of kinematics and the vortex wakes resulting from an escape response using particle image velocimetry (PIV), again using giant danio.

These studies and more demonstrate the rich social behaviors of giant danio, and provide a basis for which to form additional hypotheses about group behavior.

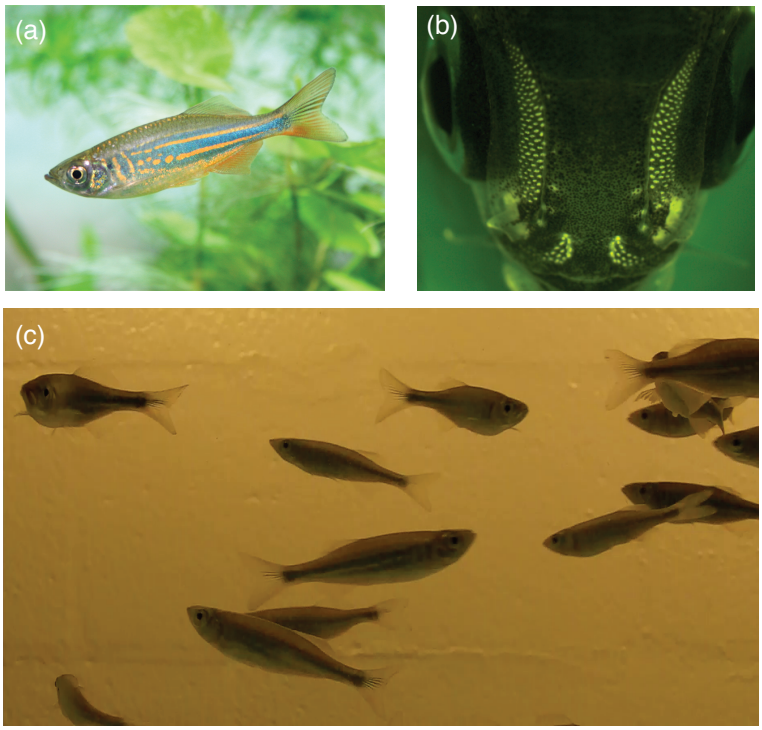

Figure 1.1: a) Photo of giant danio, used from Wikipedia through a Creative Commons license; b) staining photo of giant danio superficial lateral line with DASPEI, used with permission from the laboratory of Dr. Sheryl Coombs, and c) photo of a shoal of giant danio in a laboratory tank.

1.4 Relation to previous literature

In order to appreciate the significance of the studies contained in this dissertation, it is necessary to discuss the basic ecology of shoaling and why fish group

together, as well as what is known about the particular behaviors of interest. There is a vast, interdisciplinary literature on shoaling behavior, rheotaxis, and startle response behaviors in fish. The following sections will succinctly cover these topics, focusing on studies most closely related to the research covered in this dissertation.

1.4.1 Shoaling and schooling behavior in fish

In the literature, several definitions have been used for schooling and shoaling behavior. Breder (1967) used the word school to refer to any aggregate group fish. However, this could then also refer to any group of fish that has come together for a resource. Some scholars had thought that a school should only refer to groups of fish that were both aggregating, and strongly aligned with each other. Shaw (1970) defined a school of fish as any aggregation of fish that were mutually attracted to each other. More nuanced definitions of schools and shoals later defined a school of fish as a specific subset of a shoal in which individuals in the group show a high degree of polarization, or alignment (Pitcher, 1983). This definition is also not easily interpretable, since it may be difficult to tell *why* fish are aggregating. Additionally, it is unclear what is a sufficient degree of polarization to distinguish between a shoal and a school. Groups of fish typically show a spectrum of alignment that oscillates over time (Miller and Gerlai, 2008). These definitions of groups of fish continue to

be debated and criticized because of their lack of clarity and precision in terms of quantification (Delcourt and Poncin, 2012). For the purposes of this dissertation, I refer to all groups of fish as a shoal.

In general, shoaling behavior seems to be a result of a combination of three forces acting on individuals in a groups: attraction, repulsion, and orientation (alignment). Attraction draws individuals to aggregate, where a repulsive force minimizes the distance between individuals and may help reduce collisions, and the orientation force allows groups to align their headings, creating a polarized shoal (Reynolds, 1987).

Benefits of shoaling behavior

Many species of animals live or forage in groups (see (Sumpter, 2006) for review). In fishes, shoaling behavior is exhibited by almost half of all species at some point in their lives (Shaw, 1978) and has been proposed to confer multiple advantages, including predator avoidance, foraging, and hydrodynamic benefits.

The benefits of shoaling have been largely cast in terms of reducing predation risk (Hamilton, 1971; Krause and Ruxton, 2002; Lima, 1995; Magurran, 1986; McNamara and Houston, 1992; Pitcher and Parrish, 1993; Pulliam, 1973), and there are several mechanisms by which shoaling can confer anti-predator benefits.

A large shoal is more likely to detect a predator, and detect one faster than an individual, through an expanded sensory range. A group of animals, including fishes, is capable of transferring directional information about discrete sources in the external environment (Breder, 1959; Couzin et al., 2006; Magurran and Higham, 1988; Radakov, 1973; Ryer and Olla, 1991; Ward et al., 2008). Rapid predator evasion and waves of information transmission have been observed in schooling fish in the lab (Radakov, 1973), and in the field (Axelson et al., 2001; Gerlotto et al., 2006) with model or natural predators. This evasion tactic, also known as the Trafalgar effect (Godin and Morgan, 1985; Treherne and Foster, 1981), transmits information within the school via waves of response that can spread faster than the speed of an approaching predator (Radakov, 1973). Thus, social information transmission is likely to play a role in the collective response to a predator, and allow for rapid predator escape once a threat has been detected. However, the information content (e.g., whether it conveys general alarm, the direction and speed of the approaching predator, or the escape direction of nearby fish) is not well understood, including the sensory mechanisms by which information is transmitted through the school.

Another hypothesis for a reduced predation risk benefit of shoaling is the dilution of risk (Bertram, 1978; Krause and Ruxton, 2002), which is based on the assumption that, at a given time, only one group member is preyed upon during a

solitary predator's attack. This is debated to play a significant role for much larger group sizes (i.e., massive marine shoals) (Rieucau et al., 2014a). Additionally, predators attacking a large school may experience a confusion effect (Ioannou et al., 2007; Krakauer, 1995; Landeau and Terborgh, 1986; Milinski, 1984; Miller, 1922) by which it is difficult to find and select a target to attack. However, very large shoals may stand out in an open ocean, and laboratory experiments suggest that predatory fish select for coordinated, collective motion in virtual prey (Ioannou et al., 2012).

The proposed foraging advantages of shoaling have not been as clearly demonstrated as the anti-predatory ones. Shoaling can improve foraging activity when information can be obtained from the foraging behavior of others to improve an individual's own exploitation of a patchy resource (Berdahl et al., 2013). It has also been shown that individual fish choose to shoal with individual fish with whom they have had previous foraging success (Krause et al., 2000), or with whom they are familiar (Lachlan et al., 1998). Pitcher et al. (1982) found that groups of fish were able to locate food faster than individuals.

Shoaling may also facilitate locating potential mates and may provide hydrodynamic advantages including decreased energy use (Hemelrijk et al., 2014; Weihs, 1973), although this is is difficult to measure empirically, and has been debated (Pitcher and Parrish, 1993).

Sensory basis of shoaling

While those are the reasons *why* fish group together, we also know a bit about *how* they choose to aggregate, and how information might be shared between group members.

In order to shoal, a fish must be aware of the locations (and possibly the velocity) of its shoal-mates. Shoaling appears to be maintained through both vision and the lateral line, although the lateral line seems to play an especially important role. Partridge and Pitcher (1980) found a role of the lateral line in the positioning of neighbors (shoals without a lateral line had increased frequency of a 90° bearing, as well as effects on nearest neighbor distance and information propagation. Cahn and Phyllis (1972) also found a role of the lateral line in the side by side spacing of groups of tuna *Euthynnus affinis*.

Additionally, fish can sense their environment with their lateral line. The lateral line is a system of flow-sensing sensory organs (neuromasts) found in many aquatic vertebrates, especially fish. Each neuromast is composed of directionally sensitive hair cells (stereovillae) embedded in a gelatinous cupula. The cupula couples the movement of near-field water to the embedded hairs. Within each cupula, there is a bidirectional axis of motion, based on hair cell orientation. Deflection of the hair cell bundle in its preferred direction of motion results in ion channel opening

and increased firing rate. Conversely, movement in the opposite direction produce an inhibitory response (Dijkgraaf, 1963; Flock, 1965). Displacement of the hair cell bundle orthogonal to the preferred direction of motion yields no response. Thus, these hair cells are directional along a bi-directional axis, and when arrayed over the body can allow directional sensing in multiple directions. There are two submodalities of the lateral line system, categorized by the location of the neuromasts. When the neuromasts protrude from the surface of the skin, they are referred to as superficial neuromasts, and when these sensors are located in fluid-filled channels beneath the surface of the fish, they are called canal neuromasts. The signals from superficial neuromasts correspond to local flow velocity, and the sensory signals from the canal neuromasts correspond to the pressure gradient between the pores. When examined over the population of neurons, the fish is able to sense the pressure gradient length body. The lateral line is important for the ecology and behavior of fish, and has been shown to play a role in a variety of fish behaviors (Montgomery et al., 1995), including shoaling (Cahn et al., 1965; Partridge, 1980) (also see Section 1.4.1), but also startle response behavior (McHenry et al., 2009; Olszewski et al., 2012; Pitcher, 1980), prey capture (Kanter and Coombs, 2003), rheotaxis (Bak-Coleman et al., 2013; Baker and Montgomery, 1999; Montgomery et al., 1997; Trump and Mchenry, 2013), and object localization (Goulet et al., 2008; Windsor et al., 2010).

Given the demonstrated importance of the lateral line in shoaling behavior and information transmission (Partridge and Pitcher, 1980), the fact that local flow fields influence lateral line sensing, and that many fish encounter a variety of fluid environments, it follows that there should be further investigation of fish shoaling and information transmission in flow. This dissertation addresses some of these gaps in the literature by investigating the effect of uniform flow on shoaling behavior and information transmission during predator escape.

1.4.2 Rheotaxis

Rheotaxis is a robust, multi-sensory behavior in which fish and other aquatic organisms tend to align themselves in the direction of flow (Arnold, 1974; Lyon, 1904). This form of taxis is generally positive (orienting upstream), but can be negative (orienting downstream). Positive rheotaxis confers many potential benefits to fish, including capture of downstream drifting prey (Gardiner and Atema, 2007; Kleerekoper, 1978), orientation to currents for migration (Thorpe et al., 1981; Tytler et al., 1978), aiding odor searches (Carton and Montgomery, 2003), and energetic cost savings for fish attempting to maintain stream-wise positions in strong currents (Montgomery et al., 1995).

Although rheotaxis is an important behavior in the survival of many fish and

aquatic species, the benefits of group behavior have largely focused on anti-predation (Hamilton, 1971; Krause and Ruxton, 2002). According to a review of schooling behavior by Rieucau et al. (2014b), there has been conflicting evidence for some of the anti-predator hypotheses, and little experimental evidence obtained for larger groups. Thus, further work is necessary to investigate other possible benefits for the evolution of shoaling behavior.

While the primary focus of previous research on collective behavior has been on anti-predator benefits, there have been several studies investigating group benefits of taxis. Grünbaum (1998) developed asocial and social random-walk models for chemotaxis along a gradient using attractive and repulsive forces to mimic collective behavior; this study demonstrated that collective behaviors have the potential to enhance taxis by providing a mechanism for averaging instantaneous movement decisions over neighbors rather than averaging over time. Torney et al. (2009) investigated context-dependent search of a chemical gradient with fluctuating gradients defined by patchy, heterogeneous information; by including social interaction terms and observed that a group acts as a non-local spatial gradient sensor. Berdahl et al. (2013) investigated emergent environmental sampling by moving animal groups; they found that a group of fish has the ability to track a fluctuating environmental gradient.

These studies are versions of the many-wrongs hypothesis (Codling et al., 2007; Simons, 2004), which states that individuals average their preferred direction, leading to a compromise in route choice that leads to an improvement in navigational performance. In one of the earliest studies of the many-wrongs hypothesis, Sir Francis Galton made a near-perfect estimate of the weight of an ox by using 787 guesses made by others (Galton, 1907). The results of these studies support the hypothesis that group behavior enhances taxis, as compared to solitary individuals, and provide some possible mechanisms by which this benefit emerges.

Additionally, of these previous studies only Berdahl et al. (2013) tested their modeling predictions experimentally. While theoretical results are generalizable, testing modeling predictions is an important step in identifying what behavioral rules animal groups use to make decisions (Sumpter et al., 2012). Testing model predictions may also uncover species-specific navigational strategies based on ecology, sociality, or sensory biology.

While rheotaxis has been extensively studied and is of interest to neuroethologists and fisheries biologists, it has yet to be fully appreciated as a group behavior, despite ample evidence of group rheotaxis in nature (e.g., the upstream migration of salmon to their natal spawning sites) and evidence of collective benefits in migration (Berdahl et al., 2013; Ojima and Iwata, 2009). It has been shown that individuals

in a group may gain additional information about the environment from observing the behavior of their neighbors (Breder, 1959; Couzin et al., 2006; Radakov, 1973). During rheotaxis, individual fish may use a combination of visual and lateral-line sensing to perceive the relative motion of nearby fish in order to gain information about the directionality of the local flow field (Partridge, 1980; Strandburg-Peshkin et al., 2013). This dissertation investigates the effect of group size and sensory noise on rheotaxis, from theoretical and experimental perspectives.

1.4.3 Startle response

In teleost fishes, the neural basis of startle-escape behavior has been studied in much detail (Eaton et al., 2001; Korn and Faber, 2005). The behavior is controlled by a system of reticulospinal neurons, including a pair of large Mauthner neurons on which multimodal (auditory, visual and lateral line) inputs converge (Eaton and Emberley, 1991; Fukami et al., 1965; Preuss et al., 2006; Zottoli et al., 1995). A single action potential in one Mauthner cell reliably activates contralateral spinal motor neurons causing a fast startle response away from a potential threat (Eaton et al., 1977; Preuss and Faber, 2003; Preuss et al., 2006; Weiss et al., 2009). Startle probability is a quantifiable behavioral measure that reflects the excitability of the Mauthner cell system remarkably well (Neumeister et al., 2008, 2010; Preuss and

Faber, 2003). In fact, Mauthner cells are regarded as decision-making neurons for the execution of the startle response, and there is evidence for both ecological and social regulation of the decision to startle at the level of the Mauthner cell (Neumeister et al., 2010).

While quantification of startle probability has been investigated frequently in individual fish, the evaluation of startle probability of groups of fish, as well as how the startle probability varies under different flow conditions, has been rarely studied. Godin et al. (1988) measured the probability as a function of school size of at least one individual startling in a school of glowlight tetra *Hemigrammus erythrozonus* subjected to an artificial threat stimulus (a brief flash of light); this study provides evidence that the probability of detection increases with group size. Domenici and Blake (1997) compared the kinematics of startle responses of solitary herring to schooling herring and found that when responding to a sound stimulus, schooling herring had longer latencies, but improved directionality. Marras and Domenici (2013) found that in shoaling fish, some fish are more likely to lead or initial a startle response before others. Studies of startle response behavior have been conducted in various ecological conditions including turbid water (Meager et al., 2006), and hypoxic conditions (Domenici et al., 2007). Turbidity decreased locomotor performance, and likeliness of predator escape (Meager et al., 2006), and hypoxia decreased aggrega-

tion behavior during shoaling, and increased latency for escape responses (Domenici et al., 2007).

In addition to these experimental studies, there have been several modeling studies investigating predator attack on a group. Godin et al. (1988) used classical theories of signal detection to predict the number of fish responding. However, these predictions underestimate the experimentally observed number of *H. erythrozonus* responding. One explanation for the disagreement between model and experiment is that the independent probability signal detection model used by Godin et al. (1988) fails to take into account socially transmitted information. It could thus be hypothesized that the probability of an individual fish responding in a group may depend on the behavior of other shoal mates.

There have also been several models that simulate anti-predator behavior. Vabø and Nøttestad (1997) developed a two-dimensional cellular automata to observe patterns of group behavior in two dimensions that resembled patterns of prey escape previously observed. Inada and Kawachi (2002) used a model of repulsion, attraction and orientation to simulate the behavior of homogenous shoals of fish with and without the presence of a predator and also observed various patterns of escape based on the movement of the predator. Zheng et al. (2005) used a similar ROA model as Inada and Kawachi (2002), but included the ability of a predator to catch prey

agents, and investigated selfish or cooperative escape behaviors by prey on probability of capture. They found that individuals behaving selfishly may lead to increased predator confusion (as indicated by their simulated predator's target switching). Lee et al. (2006) investigated the dynamics of prey-flock escaping behavior in response to a predator attack similarly to Inada and Kawachi (2002) and Zheng et al. (2005), but in a molecular dynamics model. Some models of predator-prey interactions have included evolutionary dynamics (Wood and Ackland, 2007).

However, there are few modeling approaches that have explicitly studied the rapid information transmission that occurs during the startle response. A notable exception is Kolpas et al. (2013) in which the authors modeled perturbations on a group of fish by changing the heading of only one individual, then examining how other individuals responded to the heading change based on different interaction topologies. This model did not explicitly include startle behavior or transmission of startle response behavior through a group. This dissertation develops a model of information transmission in groups and uses it to investigate the influence of social influence in the rapid escape from a predator. Additionally, experiments are performed to investigate the effects of flow on information transmission in groups.

1.5 Approach

A defining characteristic in the study of collective animal behavior is the interplay between experiment and theory, coined the modeling cycle (Sumpter et al., 2012). In their review paper, Sumpter et al. (2012) classifies modeling approaches as either theory-driven, data-driven, or model selection. The theory-driven approach starts from models informed by previous data and used to make predictions about future experimental results. The data-driven approach attempts to explain experimental data. Patterns are identified using informal models. The model selection approach evaluates models based on how closely each approximates the data (Sumpter et al., 2012).

This dissertation incorporates elements of all these approaches. I generally start from a theoretical standpoint, then collect experimental data to test theoretical predictions. I then assess whether the experimental data can be predicted by the model, and where the collected experimental data may lie in the parameter space of the model. Figure 1.3 provides a simple schematic of my approach. I apply this approach to each behavior of interest: rheotaxis, and startle response behavior.

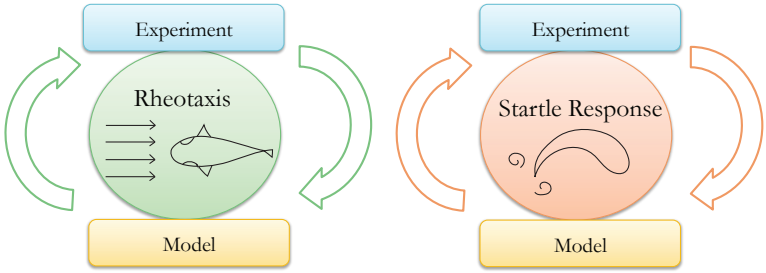

Figure 1.2: An illustration depicting the approach I use to investigate both rheotactic and startle response behaviors.

1.6 Contributions of dissertation

This dissertation advances the current body of knowledge in the general fields of collective behavior and fish ecology by integrating theoretical models with experimental data on fish behaviors.

The contributions of this dissertation are

1. *The extension of a noisy, non-Euclidean synchronization model to include a reference direction and unbounded sensory noise.* The classic Kuramoto model (Kuramoto, 1975) of synchronization on the circle (see Section 2.5) is modified to include unbounded sensory noise and a reference direction in order to model rheotactic behavior in fish. Weak synchronization is demonstrated to be able to occur in the presence of unbounded noise.

2. *Investigation of the influence of sensory noise and group size on synchroniza-*

tion using novel measures of internal disagreement (ID) and external disagreement (ED). Using the rheotactic model, the effect of group size and unspecified sensory noise on both rheotaxis and shoal alignment are investigated. A gain parameter in the model is used to specify whether agents are attending to the external flow stimulus, neighbor information, or some combination of both, in order to assess the role of social information in rheotaxis. Behavioral predictions are generated from model results.

3. *Quantification of the role of group size and flow speed on rheotaxis and shoaling behaviors.* Predictions from the theoretical results of the rheotaxis model, namely that group size improves rheotaxis in noisy sensory conditions, is tested experimentally. Fish of various group sizes are filmed in a flow tunnel under different flow speeds. Measures of spatial and orientation characteristics were measured. In order to better characterize the experimental data, a simple aggregation model is formulated to complement the orientation-based rheotaxis model.

4. *Development and application of a probabilistic model for predicting information transmission in groups.* Modeling techniques from epidemiology and computer science are applied novelly to the field of collective behavior to explicitly model

the probabilistic nature of information transmission through a group, as well as the resulting dynamics. This study makes multiple predictions about both the propagation of information as well as group response to a threat, based on different shoaling characteristics.

5. *Experimental test of the role of uniform flow on shoal structure and startle response probability in groups of fish.* Hypotheses are formulated for how rheotaxis (alignment with respect to a flow) may affect startle response behavior and shoal structure. Individual and groups of giant danio are exposed to looming fright stimuli in both a flow and a no-flow condition. Shoal characteristics, and startle response characteristics are then measured. The results of the experiment are fit to the model detailed in the previous chapter.

1.7 Organization of dissertation

The outline of the rest of this dissertation is as follows

In the first half of this dissertation, I discuss theoretical and experimental studies investigating group rheotactic behavior. In the second half of the dissertation, I detail experimental and theoretical studies on startle response behavior. Finally, I summarize the dissertation contributions and suggest avenues for future research.

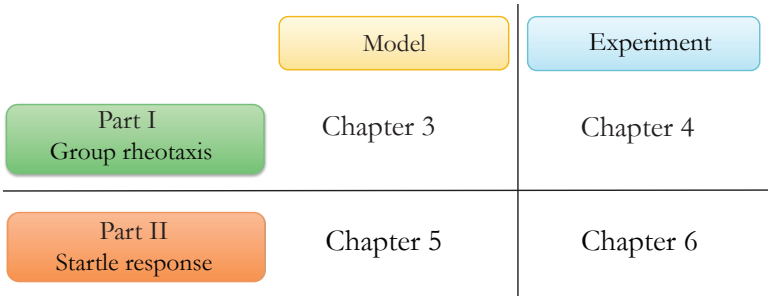

Figure 1.3: Illustration of the organization of this dissertation. Each part pertains to a different behavior, either group rheotaxis or startle response. There are two chapters within each part: a chapter on mathematical modeling, followed by an experiment that either explicitly tests model predictions, or is fit to the model detailed in the preceding chapter.

Chapter 2 provides background and justification for the choice of empirical analysis techniques as well as modeling methods used. This chapter will serve as a reference throughout the dissertation.

Chapter 3 presents a mathematical model in the form of an all-to-all, coupled-oscillator framework over the non-Euclidean space of fish orientations to model group rheotactic behavior. Individuals in the model measure the orientation of their neighbors and the flow direction relative to their own orientation. These measures are corrupted by sensory noise. The effects of sensory noise and group size on internal (i.e., within the school) and external (i.e., with the flow) disagreement in orientation are discussed, and model predictions are framed in the context of biological processes.

Chapter 4 tests the hypothesis that group size and flow speed affect shoaling and rheotaxis. Group size and flow speed are varied. Measures of rheotaxis and

shoaling are performed, including orientation with respect to neighbors and respect to the direction of the flow, as well as the spatial variables of nearest neighbor distance, shoal density, and shoal area. Results are placed in the context of previous research, including the theoretical predictions of the previous chapter.

Chapter 5 develops a probabilistic model of information transmission and couples this model with the dynamic model described in Chapter 3. Three different shoaling behaviors are categorized within the parameter space: non-shoaling, facultative shoaling, and obligate shoaling, depending on whether the group follows the synchronization model (shoaling), and whether the group has polarized initial orientations (obligate shoaling) or random initial orientations (facultative shoaling). The parameter space is explored, including inattentive and attentive behavioral states in the model, defined by the value of the probability of information transmission among neighbors. The percent of the group startling, the directionality of the escape response over time, as well as internal and external (from the threat) disagreement values over time are measured. This model generates predictions for behavioral results in comparative studies between different fish species.

Chapter 6 tests the experimental hypotheses that a uniform flow field will affect startle response, shoal structure and information transmission. Competing hypotheses are outlined, and the experiment is described. In the experiment, small

groups of fish are startled by a looming stimulus in flow and no-flow contexts. Results are stated and discussed. The experimental data is fit to the probabilistic model of information transmission described in the previous chapter.

Chapter 7 summarizes the conclusions and contributions of the dissertation and then discusses ongoing and future research ideas.

1.8 Statement about the use of experimental animals

The protocols for the research contained in this dissertation have been approved by the Institutional Care and Use Committee the University of Maryland, College Park. Relevant protocols were also approved by the Institutional Care and Use Committee at Bowling Green State University for the experiments conducted on that campus.

Chapter 2: Mathematical background

The goal of this chapter is to provide background and justification for the choice of empirical analysis techniques, as well as modeling methods used throughout this dissertation. Some of the topics covered here briefly are extensive fields of research in their own right. This chapter will only cover what is immediately relevant to understand the methods used within the dissertation, and why the methods used were chosen over other potential options. For readers seeking additional information, further references are provided.

It should also be noted that for the study of collective behavior, analysis often must borrow ideas and concepts from other fields. Typically, these ideas have come from engineering or physics. In order to model and analyze some of the behavioral phenomena of interest, I have borrowed mathematical concepts from engineering, physics, epidemiology, and computer science. Some of the methods described here are being novelly applied to the study of fish shoaling behavior.

2.1 Individual-based tracking

For the experimental data in Chapter 6, in which the startle responses of individual fish were quantified, I used a custom individual-based, multi-fish tracking system developed in MATLAB by Dr. Sachit Butail (Butail and Paley, 2011). This tracking system automatically reconstructs the full-body trajectories of fishes using two-dimensional silhouettes. The first step of the tracker is a background subtraction, in which the dark silhouettes of the fish are detected against a white background. The shape of each fish is then modeled as a series of elliptical cross-sections along a flexible midline (Figure 2.1). The size of each ellipse is estimated using an iterated extended Kalman filter (note that for a single overhead view, only one of the elliptical axes is estimated and the other is assumed to be constant). The shape model informs an optimization algorithm that locates the fish midline in each frame. The tracking system was used to monitor the head position (the point midway between the eyes) and head orientation of each fish throughout each trial. Verification and correction of tracking error was performed with a custom MATLAB interface by manually selecting points on the midline overlaid on the raw video frames.

For the rheotaxis experiments described in Chapter 4, data was tracked by hand at a sampling rate of once per second for five seconds. While this provides less

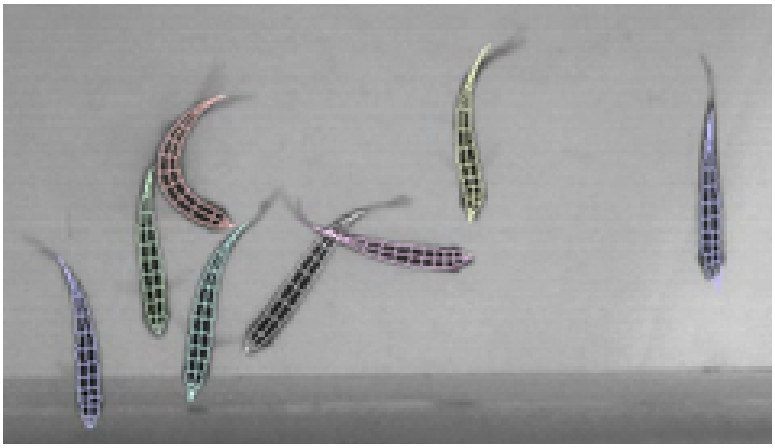

Figure 2.1: Sample of individually tracked fish, showing the fish silhouette, the series of elliptical cross-sections used to estimate the midline and the midline of eight fish.

data than reconstructing the individual body shape and trajectory of the fish, the additional data would not have provided much more information and would have been costly in terms of time and computational power.

Calibration

Camera calibration must be performed in order to get the transformation function from the camera view to the world view. A distance between two points in the camera view will be given in units of pixels, whereas we generally prefer length in metric units. Ballerini et al. (2008) provides a thorough manual for both the reasoning and execution of camera calibration up to three-dimensions. Intrinsic calibration (to obtain the camera parameters of focal length, distortion, skew coefficients and

principal point) was performed once at the start of experiments, and again any time the camera may have been moved. Extrinsic calibration (rotations, translations) was performed once daily.

For camera calibration, I used the MATLAB Camera Calibration Tool Box (Bouguet, 2008). Errors in the calibration were kept at less than half a pixel in x or y coordinates. When limited to a single overhead camera view, the calibration conversion from pixels to centimeters is restricted to a two-dimensional plane. Thus, in a three-dimensional tank, when the actual depth of the fish are unknown, the depth must be assumed. For the behavioral experiments described in the following chapters, I assume the fish are located in a plane in the center of the tank. Calibration was verified against a known image (a checkerboard pattern).

2.2 Analysis of spatial data

2.2.1 Nearest neighbor distance

The nearest neighbor distance (NND) is the distance from a focal fish to its n^{th} nearest neighbor. Figure 2.2 illustrates how the distance between two fish is calculated. The NND measure has been used widely in collective behavior research, mainly to ask how many neighbors influence an individual's movement decisions. The depression between peaks of the NND distribution has also been used to determine

if different sub-groups were present Aoki (1980).

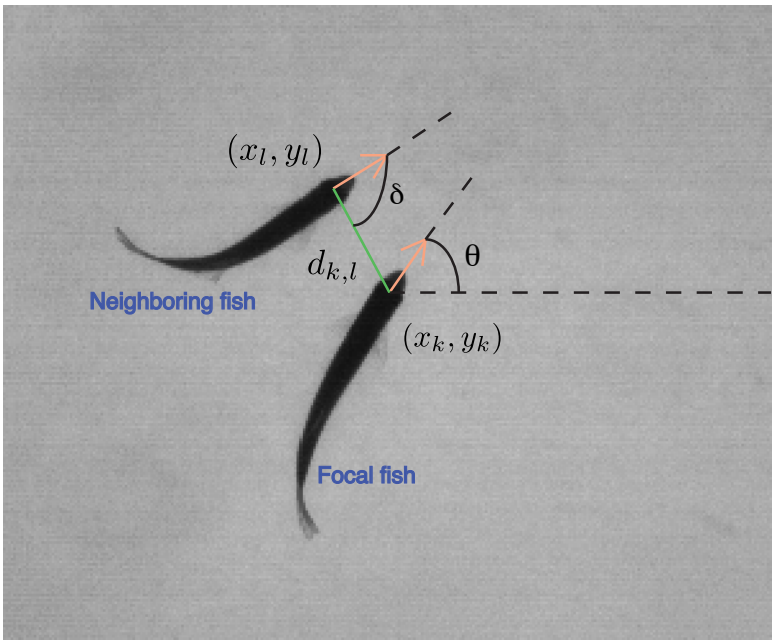

Figure 2.2: Illustration of neighbor distance and bearing. Each focal fish k fish has a position in space notated by x_k and y_k coordinates. Time is not included in this schematic. Note that the positional coordinates here can also be referenced in the complex plane for compactness, as an alternative to Cartesian coordinates. Each fish has an orientation notated by θ. I measure the distance to a neighboring fish as the distance from the head (between the eyes) of the focal fish k to the same location on the neighboring fish, l. The bearing of the focal fish relative to the neighboring fish is given by δ, the angle between agent l's orientation and agent k's orientation.

2.2.2 Spatial autocorrelations

I calculated the spatial probability of neighbor position by considering each fish in the shoal as a focal individual; the relative position and relative orientation of every other fish in the shoal were considered over all time points of the undisturbed

shoal (e.g, before fish were startled, when applicable). Therefore, each time the neighbor was in a particular position, one count was added to the corresponding bin. The relative position of a neighbor is expressed in Cartesian coordinates with the focal fish at the origin oriented along the positive y-axis. Relative positions were binned into 60×60 bins using Matlab's *hist* function. The probabilities for each bin were computed by normalizing bin counts by the bin with the highest count (i.e., the most visited bin). Elliptical contours of the first and second standard deviations of a bivariate Gaussian distribution were fitted to these probabilities.

Wall effects may play a role in shoal structure. In order to minimize the effect of possible wall effects, statistics on shoal structure excluded data points within one body length of the wall. The distance of one body length was chosen, because the range of lateral line sensing is approximately one body length. However, it is certainly possible that visualizing walls or the shape of the working arena may influence shoal structure as well.

2.2.3 The convex hull

The convex hull, Delaunay triangulation, and Voronoi diagram are all concepts in computational geometry that are closely related to each other (de Berg et al., 2008). In the field of collective behavior all three of these concepts are widely used;

however in this dissertation I focus on the convex hull.

A convex set is the region such that, for every pair of points within it, the straight line segment that joins pairs of points is contained within the region. The convex hull is the set of points that is the smallest convex set in Euclidean space (Preparata and Shamos, 1985). The convex hull is useful in studies of collective behavior in several ways. The interior of the convex hull is the area contained by the group. Dividing this area by the number of individuals in the group yields an estimation of density. In order to calculate the convex hull of groups of fish, I used the built-in MATLAB functions *convhull*, which also generates the area of the convex hull. Figure 2.3 illustrates an example of the convex hull for a small group of fish.

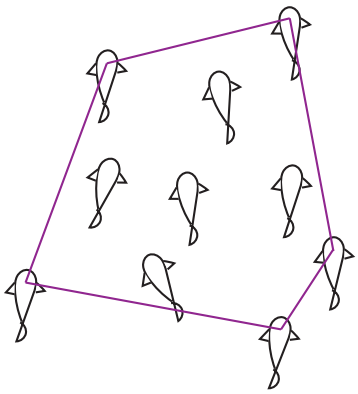

Figure 2.3: Illustration of the convex hull for a group of fish. Fish positions are marked. The outermost fish are the coordinate points for the polygon of the convex hull. This is illustrated by the purple line. The area within the purple bounds would be the calculated area of the shoal.

2.3 Analysis of orientation and heading

2.3.1 Quantitative analysis of circular data

The orientations of fish and simulated agents lies on the circle. Every chapter in this dissertation deals with circular data, whether it be the analysis of fish orientations or modeling orientations of simulated agents. As such, the treatment of circular data deserves some mention here.

Analytical and statistical methods used for points on a line will not always be effective for points on the circle. Fisher (1993) provides techniques for handling circular data. Visualization of circular data generally occurs on a circular plot. Compass plots use arrows to indicate a direction and magnitude of a vector; rose histograms plot frequency of angular data. In order to statistically assess if a distribution is uniform on a circle, I use Rayleigh tests. More advanced statistics involving circular data are not used in the dissertation. In order to sample sensory noise on the circle, I use a von Mises (VM) distribution (Mardia and Jupp, 1999). A normal Gaussian distribution when placed on the circle would lead to overlapping tail ends, increasing the probability of extreme values being selected. Thus, a distribution meant for the circle should be used. The two main options are the wrapped Gaussian or the VM, which is a close approximation of the wrapped Gaussian, avoids overlapping tails,

and is straightforward to implement. A VM distribution is characterized by its mean and concentration, σ^{kl} (roughly, the reciprocal of variance).

2.3.2 Polarization and the phase order parameter

In the multi-agent model described by Kuramoto (1975), synchrony is quantified using the complex phase order parameter defined as

$$p_\theta \triangleq \frac{1}{N}\sum_{k=1}^{N}\exp^{i\theta_k^t} = \frac{1}{N}\sum_{k=1}^{N}(\cos\theta_k^t + i\sin\theta_k^t) \tag{2.1}$$

where θ_k^t is the orientation at time t of agent k, N is the number of agents, and $i = \sqrt{-1}$. The magnitude $|p_\theta|$ represents the level of alignment in orientation and ranges from 0 to 1, with values of one to represent fully aligned (see Figure 2.4). (The magnitude of p_θ is also referred to as vector strength.) The orientation of p_θ indicates the direction of the average velocity.

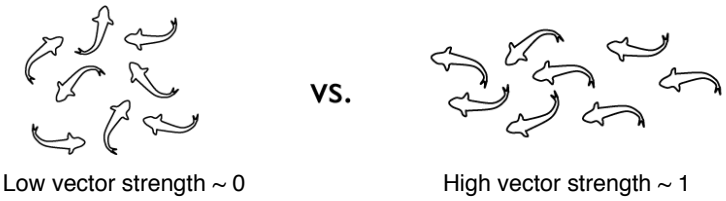

Figure 2.4: Illustrating the magnitude component of polarization, the vector strength. Low vector strength indicates weak alignment, whereas high vector strength indicates strong alignment.

2.3.3 External and internal disagreement

In the coupled oscillator model introduced by Kuramoto (1975), synchrony is quantified using a complex-phase order parameter p_θ. In the stochastic consensus literature (Huang and Manton, 2009), the following definition is used to characterize the asymptotic behavior in weak consensus: $\mathbb{E}|\theta_k^t|^2 < \infty$ for all t and k and $\lim_{t\to\infty} \mathbb{E}|\theta_k^t - \theta_l^t|^2 = 0$ for all pairs k, l, where $\mathbb{E}$ is the expected value operator.

However, the roots of a complex number are multi-valued, as seen in the simple example of $z^{1/2} = \pm\sqrt{z}$. In order to achieve a single difference between two angles, this dissertation introduces two alternative measures of disagreement in orientation used in combination with measures previously discussed. These measures are based on chord length on the unit circle, illustrated in Figure 2.5. The internal disagreement (ID) measure quantifies the median level of disagreement within the school, and the external disagreement (ED) measure quantifies the median level of disagreement between each fish and a reference direction (e.g., the direction of flow, or the direction away from threat). To compute ED and ID, I use the median statistic because the distribution of chord lengths was highly skewed, and the median captures highly skewed or bimodal data better than other statistics such as the mean or mode.

Let $z_{k,l}^T \triangleq |e^{i\theta_l^T} - e^{i\theta_k^T}|/2 \in [0, 1]$, where T is a sufficiently large time such that weak consensus is reached. The orientation θ_k^T of fish k at time step T is converted

to $e^{i\theta_k^T}$, a complex unit phasor. When taking the difference between two angular values, there is no unique answer; thus the chord length is used instead. The value $z_{k,l}^T$ is half of the chord length between points $e^{i\theta_l^T}$ and $e^{i\theta_k^T}$ on the unit circle; the maximum chord length equals two.

For ID, I take the median of $z_{k,l}^T$ over all pairwise differences in orientation within each trial, $\tilde{Z}^T = \text{median}\{z_{1,2}^T, z_{1,3}^T ..., z_{1,N}^T, z_{2,2}^T, z_{2,3}^T, ..., z_{N-1,N}^T\}$. For ED, I compute $\tilde{Z}_0^T = \text{median}\{z_{0,1}^T, z_{0,2}^T, ..., z_{0,N}^T\}$. The number of values in the ID set is $N^2 - N/2$ and, in the ED set, N. Let ${}^m\tilde{Z}^T$ denote the median disagreement in synchronization for Monte Carlo trial m. The ID value is the median disagreement in orientation over all Monte Carlo trials, i.e., $ID = \text{median}\{{}_1\tilde{Z}^T, {}_2\tilde{Z}^T, ..., {}_M\tilde{Z}^T\}$. Similarly, the ED value is $ED = \text{median}\{{}_1\tilde{Z}_0^T, ..., {}_M\tilde{Z}_0^T\}$.

2.3.4 Characterizing a startle response

Detecting a startle response is a problem of peak detection in a time-varying signal. I first characterized a startle response using the angular rate of rotation of the fish's head orientation (Domenici and Blake, 1997), which is estimated by the tracking system (Butail and Paley, 2011). I then compared a numerical (two-point) differencing method over time to a threshold of 3000°/sec to determine whether a startle response occurred. I determined the threshold by measuring the angular rate

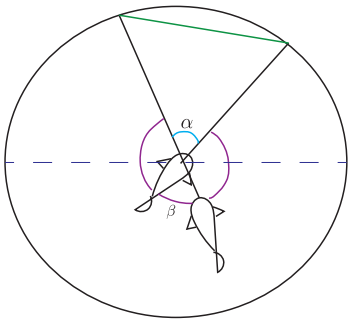

Figure 2.5: Fish orientations lie on the circle, as shown by the black lines extending from the fish. When calculating the difference between orientations, there are two potential answers, α and β. The chord length, in green, is a unique answer to the difference in orientations between agents. Since the diameter (purple dashed line) of the unit circle is equal to 2, the maximum difference between any two agents would be 2. The chord length divided by 2 bounds the difference in orientation between two agents between 0 and 1.

of rotation during rapid turning in a sample of fish, and by reviewing all videos with another reviewer. Another potential method that was not used in Chicoli et al. (2014) to detect startles is to finding all peaks in the data. Any peaks that do not differ significantly from the average angular rotation rate of fish during the control (no stimulus) may be discarded as slower swimming turns.

2.4 Graph theory

A graph G is a series of nodes and edges (Mesbahi and Egerstedt, 2010), which provide a representation of how information is shared between agents in a network. In the simplest case, an all-to-all communication graph, each agent interacts with every

other agent, $\mathcal{G} = (\mathcal{N},\mathcal{E})$ with nodes $\mathcal{N} = \{1, ..., N\}$ and edges $(k, l) \in \mathcal{E} \subseteq \mathcal{N} \times \mathcal{N}$ such that the graph $\mathcal{G}$ satisfies $(k, l) \in \mathcal{E}$ for all $k \neq l$. However, graphs can take many forms. The edges between nodes can be associated with a direction, as in a directed graph, and a weight, as in a weighted graph. There may also be special nodes in a graph.

With regards to fish behavior, the graph of fish interactions is usually termed the interaction topology. We do not yet fully understand the interaction topologies of fish schools (or other animal groups), but there are several hypotheses. The two main theories for interaction in groups have been a topological based interaction model and metric distance based interaction model. In the topological model, focal individuals attend to a certain number of nearest neighbors, irrespective of their distance from the focal individual. The metric distance model hypothesizes that individuals attended to all neighbors within a given distance. Figure 2.6 gives an illustration of these two topology types. Interactions between agents are also likely to be sensory-based (Strandburg-Peshkin et al., 2013).

Partridge (1980) showed that velocities and headings of saithe *Pollachius virens* correlate with those of their first two nearest neighbors at slow speeds, but only with those of the first nearest neighbor at high speeds. Partridge (1980) also demonstrated that bearing to the first three nearest neighbors in saithe and herring *Clupea haren-*

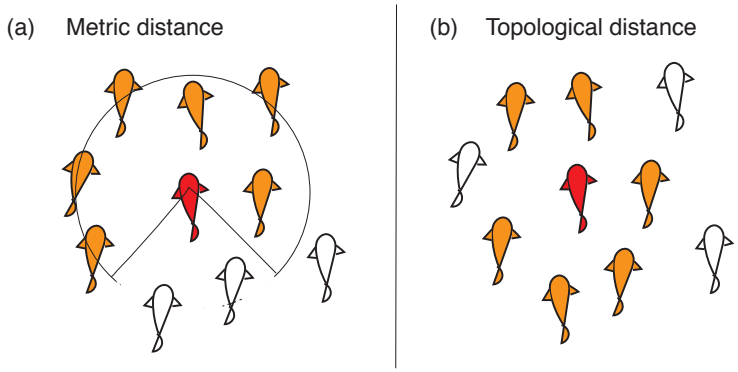

Figure 2.6: Depiction of (a) metric and (b) topological interaction topologies. The focal fish is in red, fish affected the focal fish's behavior are in yellow.

gus is non-random, implying that at least the first three neighbors are influential. Herbert-read et al. (2011) found that individual mosquitofish seem to attend to the closest individual fish. Ballerini et al. (2008) found evidence that starlings *Sturnus vulgaris* may pay attention to as many as six or seven nearest neighbors, which the authors note corresponds to their cognitive capacity. Patrtridge et al. (1983) showed that the distribution of neighbors is affected by shoal size in bluefin tuna *Thynnus thynnus*.

2.5 Synchronization and coupled oscillator models

I investigate the effects of sensory noise and group size on rheotactic performance using a mathematical model of coupled phase oscillators based on Kuramoto (1975). Originally developed in physics, the Kuramoto model has been adopted in

neuroscience to investigate neural control and information processing (Rosbash et al., 2004). It has also been applied to the study of collective behavior in biological groups (Leonard et al., 2012; Nabet et al., 2009). Phase oscillator models have motivated studies on stability analysis (Jadbabaie et al., 2003; Moreau, 2005) and stabilization of planar collective motion (Paley et al., 2007; Sepulchre et al., 2008). Previously, Mahmoudian and Paley (2011) investigated phase synchronization in the presence of bounded noise.

In cooperative controls theory, synchronization differs from consensus in the following sense: consensus takes place in a Euclidean space, such as the real line, whereas synchronization takes place in a non-Euclidean space, such as the circle. Synchronization is connected to the biologically relevant behaviors of alignment and rheotaxis in fish because these quantities are described by phase angles, and a phase angle is a point on a circle. In collective behavior, each fish synchronizes its orientation with that of its neighbors so that the school heads in a common direction. In rheotaxis, individuals also synchronize with the direction of the flow.

The original Kuramoto model (in discrete time) is given by

$$\theta_k^t = \theta_k^{t-1} + \psi_k + \frac{\kappa}{N} \sum_{l \in N_k} \sin(\theta_l - \theta_k), k = 1, ..., N. \tag{2.2}$$

where θ_k is the orientation of agent k, and ψ_k is the natural frequency of agent k,

κ/N is the gain, normalized by the number of agents, and N_k denotes the neighbor set of k.

I modify this model in Chapter 3 to model noisy synchronization and rheotaxis behavior in fish. The noisy synchronization model is written as:

$$\theta_k^t = \theta_k^{t-1} + 0 + \sum_{l=0, l \in N_k} \kappa_{kl}^t \sin(\theta_l^t - \theta_k^t + \omega_{kl}^t), k = 1, ..., N. \tag{2.3}$$

Note that in the noisy synchronization model, I have dropped the natural frequency parameter ψ. This term is the agent's natural frequency. If included, each agent would rotate at the specified frequency rate without any external input. Since rotating about in circles without a stimulus is not a behavior generally observed in fish, it is excluded. There is also the addition of the reference direction, $l = 0$, which can be interpreted as the direction of the flow when modeling rheotaxis, or an escape direction when modeling startle response behavior. Finally, the gain κ moves inside the sum, making the gain dependent on the value of l, and an unbounded noise term ω^{kl} is included, which is also dependent on the value of l. The purpose of setting the gain and the noise to be dependent on l is so that these parameters can be adjusted independently for when a focal agent is comparing its orientation to the reference direction, or to the orientations of other agents. This allows for evaluation of the relative roles of external versus internal cues in the process of synchronization. This

model is detailed more extensively in Chapter 3.

2.6 Susceptible-Infected-Removed (SIR) models

I use a model of information transmission to study startle propagation in groups, focusing on fish schools. The model used is known in computer science and epidemiology literature as a susceptible-infected-remove (SIR) model. SIR models are based on three main probabilities (i) the probability of an individual being susceptible to infection, (ii) the probability of being infected, and (iii) the probability of being cured (Billings et al., 2002; Kermack and McKendrick, 1927; Mesbahi and Egerstedt, 2010). Here, I change the terminology slightly to refer to (i) the probability of a fish being susceptible to startle response, (ii) the probability of a fish being startled by either a directly perceived threat or cues from its neighbors, and (iii) the probability of remaining in a startled state, if previously startled. Once out of the startled state (completed the startle response), agents cannot be re-startled, hence the removed portion of the model name. Theoretically and biologically, if left for a long enough period of time, startles could occur again. However, my goal here is to examine the spread of a single, isolated startle event.

An important aspect of this model is the inclusion of time t. Let $P^{ext} = P_k^t$ be the probability that agent k detects and responds to an external signal, such as

a predation threat, at time t, where $k = 1, ..., N$ and N is the number of agents in the group. P_k, the probability of agent k being in a startled state includes the probability of indirect detection of threatening stimuli through the interactions with other agents. Let P^{int}=$P_{k,l}$ be the probability that agent k perceives (and responds to) a cue from agent l and P^{sus}=$P_{k,k}$ be the probability that agent k sustains the response state from one time step to the next. The notation N_k denotes the neighbor set of k, which is the set of agents that generate information received by agent k. Suppose, without loss of generality, that the stimulus occurs at time $t = 0$, and this is the only time instant in which agents can directly perceive and respond to the threat directly. P_k^t, for $t > 0$, is thus the probability at time t that agent k sustains a response from the previous time step $t-1$, or detects and responds to a neighboring agent that is in the response state at time $t-1$. While there are multiple ways to be informed of the presence of a threat, there are still binary states of startled and not startled in the model. The probability of being in a startled or not startled state at $t > 0$ is based on the probabilities of P^{sus} and P^{int}. The probability of not startling is given by

$$P(\text{not startle}) = 1 - (P^{sus} \cup P^{int} - P^{sus} \cap P^{int}), \tag{2.4}$$

where $P^{sus} \cup P^{int} = 1 - (1 - P^{sus})(1 - P^{int})$. Equation 2.4 can then be re-written as

the following:

$$P(\text{not startle}) = 1 - (1 - (1 - P^{sus})(1 - P^{int})). \tag{2.5}$$

The probability of startle is then

$$P(\text{startle}) = 1 - (1 - P^{sus})(1 - P^{int}). \tag{2.6}$$

At any time step t, each agent k thus has the following probability of being startled

$$P_k^t = 1 - (1 - P_{k,k}P_k^{t-1}) \prod_{l \in \mathcal{N}_k^t} (1 - P_{k,l}P_l^{t-1})(1 - P_k^{t-1}), \tag{2.7}$$

where $1 - P_k^{t-1}$ is the probability that agent k was not startled at the previous time step.

Figure 2.7 illustrates how a startle response can spread through a group, in graph form. Figure 2.7(a) shows the fixed, directional, interaction topology. Startle state is indicated by a red fill in (a) and a red-outlined circle in (b). Agent 1 startles at $t = 0$, and it can then spread the startle to connected agents 2, 4, and 5. At time $t = 5$ the startle spreads to agent 4, who can now spread the startle to agents 2, 3, and 5. At $t = 10$, agents 2 and 5 have become startled as well.

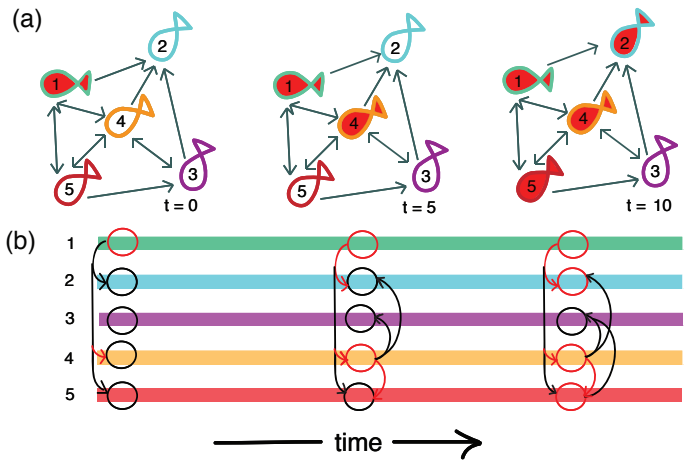

Figure 2.7: (a) Fixed interaction between agents (fish) depicted by a graph. Nodes of the graph are fish, and arrows are directional edges of the graph. (b) Another representation of the graph in (a). Red filled agents or outlined circles are in a startled state, and can spread the startle to connected agents.

Part I: Group Rheotaxis

Chapter 3: Rheotaxis performance increases with group size in a coupled phase model with sensory noise

3.1 Introduction

This chapter presents a mathematical model in the form of an all-to-all, coupled-oscillator framework over the non-Euclidean space of fish orientations to model group rheotactic behavior. I expand on our current understanding of the factors governing rheotaxis in flow and on taxis in uncertain environments, by investigating synchronization of particles with sensory noise, in the context of fish behavior in a flow field. In the model, each individual obtains measurements of the relative orientation of other individuals as well as the relative orientation of an external reference direction, the flow. Sensory noise is represented by the uncertainty in each individual's measurements. I vary the level of sensory noise, as well as the group size. Monte Carlo simulations numerically illustrate the influence of sensory noise and group size on internal (i.e., within the shoal) and external (i.e, with the flow) disagreement in

orientation. I find that in high noise conditions, the use of neighbor cues and group size improves rheotactic behavior. By relating the model to biological processes, I generate testable predictions about fish behavior.

The contributions of this chapter are (i) the extension of a noisy, non-Euclidean synchronization model to include a reference direction and unbounded sensory noise; and (ii) investigation of the influence of sensory noise and group size on synchronization, using novel measures of internal and external disagreement. The model generates testable experimental predictions, which may have implications for fish ecology, collective behavior, and flow sensing. While this study emphasizes shoals of fish, the general model framework may be applied to other animal and engineered collectives. A version of this chapter has been previously published in (Chicoli et al., 2015).

3.2 Noisy synchronization model

Starting with random initial phases drawn from a uniform distribution on the circle, each individual gathers measurements of the relative direction of the reference direction and of its neighbors' relative phases to determine the change in its own orientation. The measurements obtained by each individual contain additive sensory noise.

Consider a network (Mesbahi and Egerstedt, 2010) of N phase angles indexed by $k = 1, ..., N$ and coupled via an all-to-all, undirected communication graph $\mathcal{G} = (\mathcal{N},\mathcal{E})$ with nodes $\mathcal{N} = \{1, ..., N\}$ and edges $(l, k) \in \mathcal{E} \subseteq \mathcal{N} \times \mathcal{N}$ such that the graph $\mathcal{G}$ satisfies $(l, k) \in \mathcal{E}$ for all $l \neq k$. In the absence of noise, these angles synchronize with one another and with the reference direction; their dynamics are modeled as a stochastic difference equation (Higham, 2001; Papoulis and Pillai, 2002) (see Section 2.4). The reference direction is a special node in the graph, associated with the index $k = 0$ and, without loss of generality, is fixed at zero radians.

Noise is sampled from a VM distribution, where the noise concentration (see Section 2.3.1) depends of the values of k and l such that

$$\sigma_{kl} = \begin{cases} \sigma_0 & \text{when } k = 0, \\ 0 & \text{when } k = l, \text{ and} \\ \sigma & \text{otherwise.} \end{cases} \tag{3.1}$$

Figure 3.1 illustrates three VM distributions with low, moderate, and high sensory noise, respectively. When individual k compares its orientation to the reference direction, the noise is sampled from a VM distribution with concentration σ_0, and when fish k compares its orientation to another individual, the sensory noise is sampled with concentration σ. Sensory noise may be higher when visibility is poor (Meager

et al., 2006) or if bulk flow interferes with inter-individual communication (Chicoli et al., 2014).

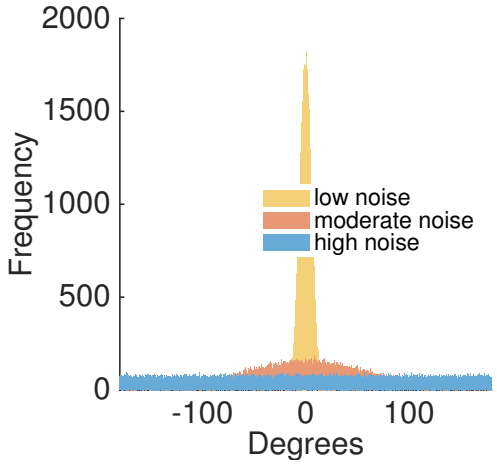

Figure 3.1: Example von Mises distributions with concentration values 10^2, 10^0 and 10^{-2}.

Let t represent the discrete time index. The orientation of individual k at time t is denoted by $\theta_k^t, k = 0, 1, ..., N$, where $\theta_0^t = 0$ represents the reference direction. Each orientation is updated according to the following stochastic difference equation:

$$\theta_k^{t+1} = \theta_k^t + \sum_{l=0}^{N} \kappa_{kl} \sin(\theta_l^t - \theta_k^t + \omega_{kl}^t), \tag{3.2}$$

where ω_{kl}^t represents the sensory noise value at time t with concentration value σ^{kl} as above and κ^{kl} is the coupling gain between pair k and l. Note that the sine term linearizes to $\theta_l^t - \theta_k^t + \omega_{kl}^t$ when the agreement is sufficiently small.

The gain κ_{kl} is of importance for the synchronization behavior of the model

3.2 (Kuramoto, 1975). Namely, $\kappa_{kl} > 0$ yields synchronization and $\kappa_{kl} < 0$ yields incoherent behavior. Here I specify $\kappa_{kl} > 0$ to vary based on

$$\kappa_{kl} = \begin{cases} \kappa_0 & \text{when } l = 0, \\ 0 & \text{when } l = k, \text{and} \\ \kappa & \text{otherwise.} \end{cases} \tag{3.3}$$

The values κ_0 and κ are coupled according to $N\kappa + \kappa_0 = 1$, so that as group size N increases, the influence of each neighbor decreases. I investigate several cases of κ_0 and κ values: for $\kappa_0 = 1$, there is no influence of the neighbors; for $\kappa_0 = 1/2$, the influence of the reference direction is equal to that of all neighboring fish; for $\kappa_0 = 0$, there is no influence of the reference direction, for $\kappa_0 = 1/3$ there is slight preference for neighbors, and for $\kappa_0 = 2/3$ there is preference for the reference direction.

Table 3.1 summarizes the model parameters. Each parameter combination was run for 500 Monte Carlo trials and each trial ran for 2,000 time steps. The University of Maryland supercomputing resources were used to conduct the research in this paper. Running through all group sizes for one parameter set takes twenty-four hours or more.

Table 3.1: Summary of model parameters

Model parameter	Symbol	Values
Group size	N	$2, 4, 8, 16, 32, 64, 128$
Conc., flow	σ_0	10^2,10^0, 10^{-2} rad.
Conc., neighbors	σ	10^2,10^0, 10^{-2} rad.
Gain, flow	κ_0	0, 1, $\frac{1}{2}$,$\frac{1}{3}$,$\frac{2}{3}$

3.3 Modeling Results

Figure 3.2 shows agent orientations over time, as well as the histogram of orientation distributions from four typical trials to illustrate the time course of each phase angle. Figures 3.2a,c depict the case when there is low noise in both the neighbor orientation and the reference direction; the group size is $N = 4$ and 32, respectively. Both of these simulations show strong alignment with the reference direction. Figure 3.2b,d shows simulations with moderate noise ($\sigma_0 = \sigma = 10^0$) in both the reference direction and in neighbor orientation. In these trials, there is no qualitative difference in synchronization based on group size.

3.3.1 No gain on reference direction

When $\kappa^0 = 0$, the reference direction is ignored. Figures 3.3a,b show the internal and external disagreement measures under various levels of neighbor noise ($\sigma = 10^2$, $\sigma = 10^0$, and $\sigma = 10^{-2}$). With no gain on the reference direction,

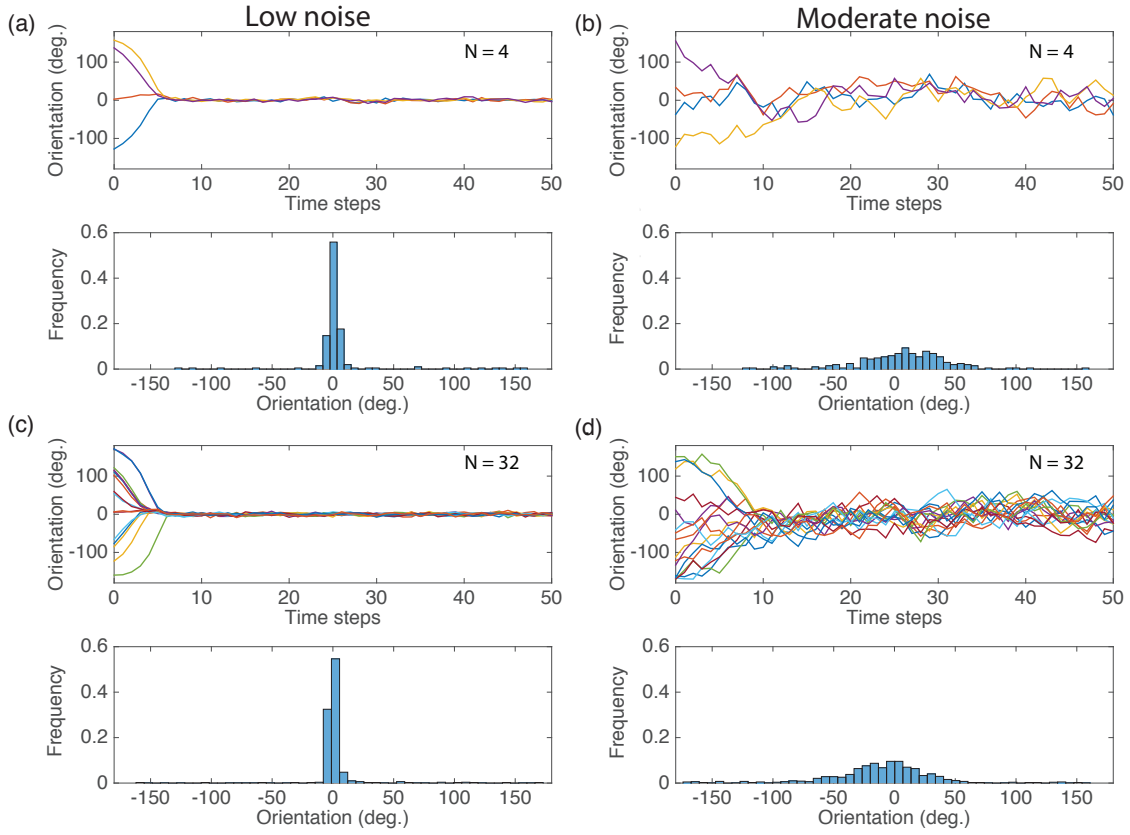

Figure 3.2: Typical runs (N=4, N=32) in the presence of low noise, $\sigma = \sigma_0 = 10^2$ (a,c) and moderate noise, $\sigma = \sigma_0 = 10^0$ (b,d).

individuals rheotact at chance levels (the disagreement in orientation on the circle for random values is approximately 0.7), regardless of what the noise is in neighbor orientation (Figure 3.3a). Internal disagreement decreases as group size increases in the presence of moderate sensory noise (Figure 3.3b, orange).

3.3.2 No gain on neighbor orientation

When $\kappa = 0$, neighbor orientation is ignored. Figures 3.3c,d depict the internal and external disagreement measures under various levels of noise in the reference direction ($\sigma_0 = 10^2$, $\sigma_0 = 10^0$, and $\sigma_0 = 10^{-2}$). External and internal disagreement values increase with increasing noise levels, indicating reduced synchronization. Although there is no effect of group size on either ED or ID, performance on both measures is better than chance, because all individuals have knowledge of the reference direction.

3.3.3 Equal gain on reference direction and neighbor orientation

When $\kappa_0 = 1/2$ (i.e., the influence of the reference direction equals that of all neighbors), results are organized based on the noise in the reference direction to assess how group size and noise in neighbor orientation affect the ED and ID values. There is no effect of group size when there is low noise in both the reference direction and neighbor orientation (Figures 3.4a,b yellow). However, when there is low noise in the reference direction, and moderate to high noise in neighbor orientation (Figures 3.4a,b orange and blue), the ED and ID values decrease with increasing group size, N. When there is moderate noise in the reference direction, there is a slight decrease in ED and no significant difference in ID values with increasing

group size (Figures 3.4c,d). Both ED and ID values decrease with decreasing noise levels in neighbor orientation. When there is high noise in the reference direction (Figures 3.4e,f), there is a decrease in ED with increasing group size for all values of neighbor orientation noise, σ, but no difference in the ID values. Both ED and ID values decrease with decreasing noise levels in neighbor orientation.

3.3.4 Higher gain on neighbor orientation

When $\kappa_0 = 1/3$ the results appear almost identical to the results of $\kappa_0 = 1/2$ (not shown). Agents have a slightly higher gain on neighbor orientation than the reference direction. When there is low to moderate noise in the reference direction and low noise in neighbor orientation, there is no effect of group size on ED or ID. When there is moderate to high neighbor noise, the ID and ED values decrease with increasing group size, N. The effect of group size in these cases is most prominent at the lowest group sizes. Both ED and ID values decrease with decreasing noise levels in neighbor orientation. When there is high noise in the reference direction, there is a decrease in ED with increasing group size for all values of neighbor orientation noise, σ, with the largest effects occurring when there is low to moderate noise in neighbor orientation. Both ED and ID values decrease with decreasing noise levels in neighbor orientation.

3.3.5 Higher gain on the reference direction

When $\kappa_0 = 2/3$ the agents have a slightly higher gain on the reference direction than on neighbor orientation. When there is low to moderate noise in the reference direction, there is little to no effect of group size. Both ED and ID values decrease with decreasing noise levels in neighbor orientation. When there is high noise in the reference direction, there is a decrease in ED with increasing group size N only when there is the lowest value of neighbor orientation noise, σ. When there is moderate and high neighbor noise the ED values are mostly random. Conversely, the ID values increase with increasing group size with low to moderate noise in neighbor orientation, especially at lower group sizes. This is shown next to the ID values of $\kappa_0 = 1/3$ for comparison (Figure 3.5).

3.4 Discussion

Grünbaum (1998) quantitatively demonstrated the effect of the many-wrongs principle (Simmons, 2004), which states that inherent noise in a system may be damped out through multiple samples. These results demonstrate the effects of social information on rheotaxis, a simple yet robust behavior found in fish and invertebrates. I find potential limitations of the many-wrongs principle, in the extreme cases when

the individuals are randomly aligned (for very high noise) or when perfectly aligned, social information does not improve taxis. Additionally, when there is higher gain on a noisy reference direction and moderate to high noise in neighbor orientation, as the group size increases, rheotaxis does not improve and shoal alignment decreases. By introducing noise in intra-shoal signaling as well as in an external reference, I investigate the relative roles of each cue.

I find that (i) under environmentally plausible conditions, the use of neighbor cues in groups improves rheotactic behavior; (ii) this improvement is limited to cases when there is high sensory noise in sensing either the flow direction or neighbor cues; and (iii) when there are external cues about the flow, fish align with each other, and the addition of neighbor cues do not improve intra-shoal alignment.

This work extends the engineering results of Mahmoudian and Paley (2011) by analyzing weak consensus on the N-torus with additive noise. The previous work analyzed solutions to weak consensus on the N-torus with additive noise bounded by $\pi/2$. I elaborate on this finding by numerically testing weak synchronization with unbounded noise levels, and find that with unbounded noise, individuals may still reach weak synchronization.

3.4.1 Effect of sensory noise on synchronization

When individuals have reliable information regarding the direction of the flow (which we interpret to be the reference direction), group size does not affect synchronization. However, when information regarding the flow direction is noisy, increasing group size improves synchronization to the flow. This result suggests that rheotacting fish may rely more on social information when their own information is uncertain. It has been previously shown that there may be costs to using socially acquired information if this information is incorrect (Giraldeau et al., 2002; Laland and Williams, 1998; Rieucau and Giraldeau, 2009). Thus when personal information is more accurate (i.e., when fish perceive the external or flow environment accurately), there may be a detriment to relying on noisy neighbor information. There is also some evidence that behaviors can change adaptively based on environmental context, including dynamic interactions between individuals (Kurvers et al., 2013; Torney et al., 2009; Viscido et al., 2005).

Rheotaxis is a robust and multi-sensory behavior (Bak-Coleman et al., 2013). However, the contribution of different sensory modalities to rheotactic behavior may vary by ecology. For example, fish in murky environments may rely more on other sensory modalities in order to compensate for the noisy visual information (Meager et al., 2006). This idea could be tested experimentally using a comparative study with

species of shoaling fish from different habitats, or by experimentally manipulating available cues, e.g., by conducting experiments in the dark or by temporarily blocking the lateral line (Brown et al., 2011; Trump et al., 2010).

3.4.2 Effect of group size on synchronization

These results rely on the assumptions that there is all-to-all communication between individuals that are identical. Neither assumption is realistic. Although I have chosen to investigate the all-to-all interaction case, in part to match the assumptions laid out by Mahmoudian and Paley (2011), the model described here is applicable to limited interaction topologies as well (Sepulchre et al., 2008).

Group size made the most significant improvement in the rheotaxis model when there was high noise in sensing the flow. In this case, information from many neighbors significantly improves synchronization to the reference direction when compared to the asocial case (Figures 3.3c,d) in which individuals with no neighbor information orient to the reference direction at chance levels. Once the group size increases past $N = 8$, there is a significant effect of group size on improving rheotactic performance (Figure 3.4e). Based on these results, group size has the largest benefit to shoals in noisy conditions. Testing this hypothesis experimentally may yield additional insights into the roles of multi-sensory integration and group behavior in rheotaxis.

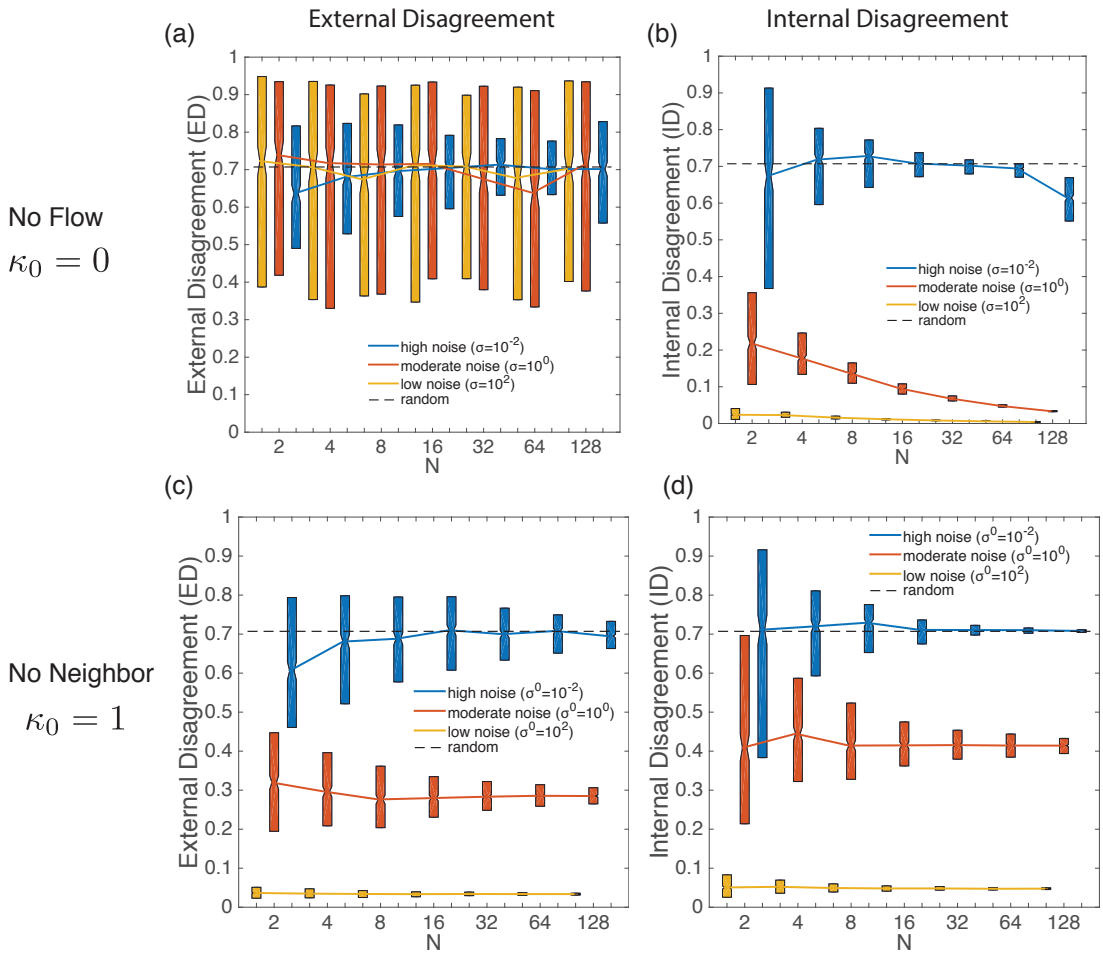

Figure 3.3: (a,b) Synchronization results when the gain on flow is zero ($\kappa_0 = 0$). (c,d) Gain on neighbors is zero ($\kappa_0 = 1$). (a,c) ED and (b,d) ID, over all group sizes, N and noise values. Noise values are as follows: (a,b) $\sigma = 10^2$ and (c,d) $\sigma_0 = 10^2$ (yellow), (a,b) $\sigma = 10^0$ and (c,d) $\sigma_0 = 10^0$ (orange online), and (a,b) $\sigma = 10^{-2}$ and (c,d) $\sigma_0 = 10^{-2}$ (blue). Length of bars represent the upper and lower quartiles.

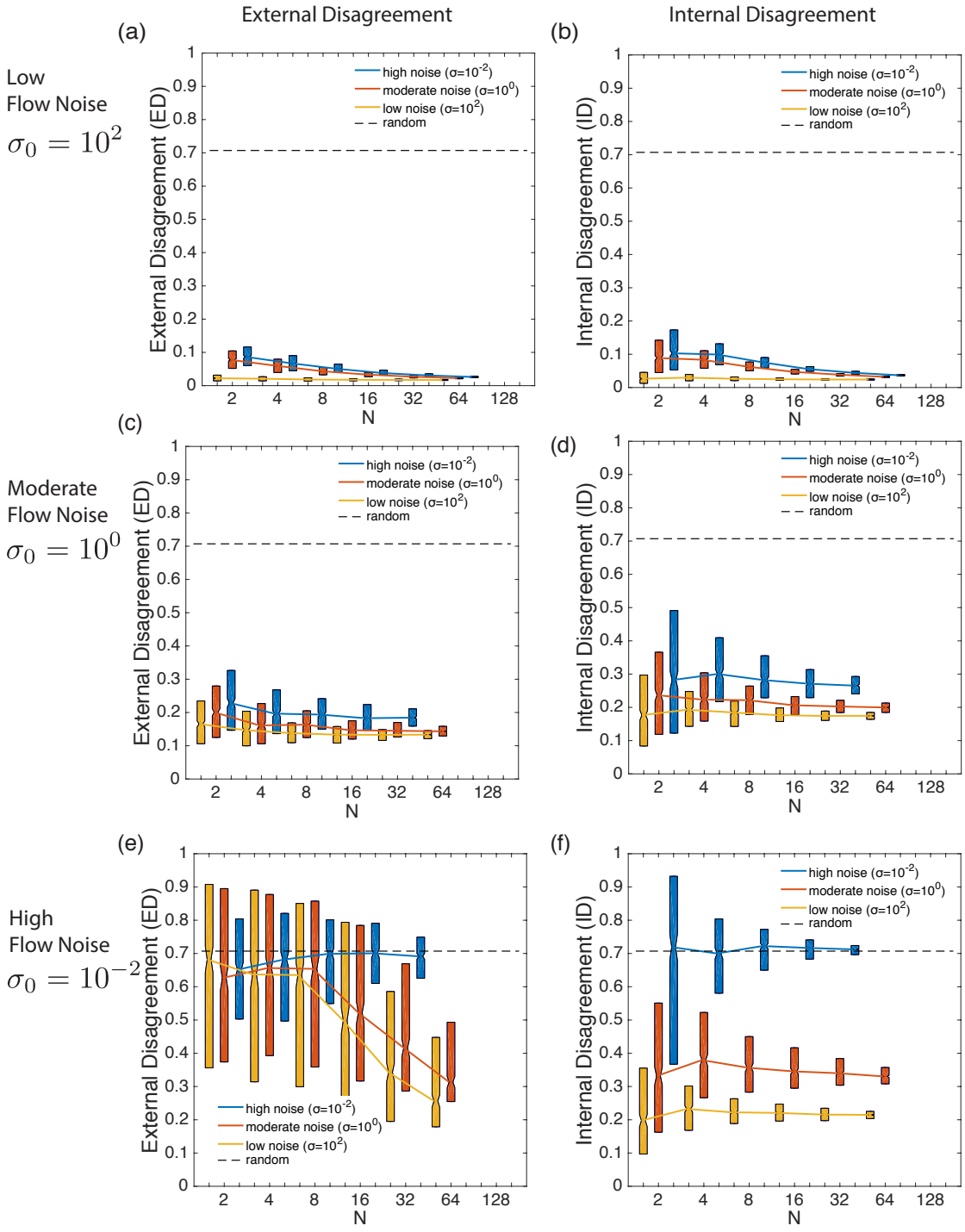

Figure 3.4: The effect of group size on synchronization results when there is both neighbor and flow information ($\kappa_0 = 1/2$) for low (a,b), moderate (c,d) and high (e,f) flow noise levels and for low (yellow), moderate (orange) and high (blue) levels of neighbor noise within each of these flow noise conditions. Length of bars represent the upper and lower quartiles.

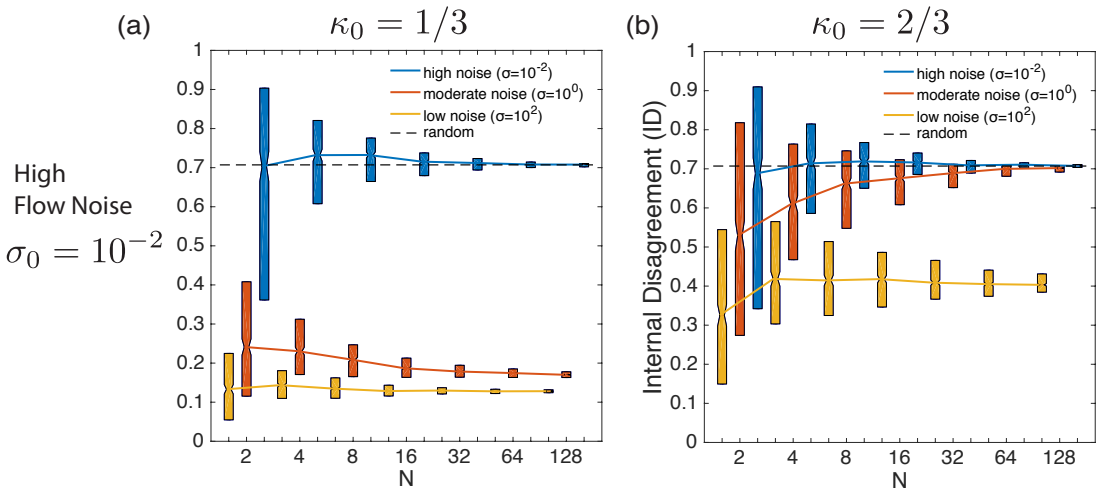

Figure 3.5: The effect of group size on internal disagreement (ID) when there is a slight preference for neighbor orientation ($\kappa_0 = 1/3$) (a), or a slight preference for the reference direction ($\kappa_0 = 2/3$) (b) in the presence of high flow noise ($\sigma_0 = 10^{-2}$). Low (yellow), moderate (orange) and high (blue) levels of neighbor noise is shown for each condition. Length of bars represent the upper and lower quartiles.

Chapter 4: Effects of flow speed and group size on rheotaxis and shoaling in giant danio

4.1 Introduction

This chapter experimentally tests the predictions established in Chapter 3, namely that group size will improve rheotactic performance under certain environmental conditions. Groups of giant danio, from one to thirty-two individuals were tested in flow speeds from 0 cm^{s-1} to 12 cm^{s-1}, and their positions and orientations during the trial were measured. I find that there is no effect of group size on rheotactic behavior for giant danio; however there is an effect of group size on shoaling behavior, as nearest-neighbor distance decreases with group size.

The contributions of this chapter are: (i) quantitative behavioral data of giant danio under different group size and flow speeds; (ii) presentation of a simple model of aggregation; and (iii) comparison of behavioral data to the proposed aggregation model as well as to previous theoretical data on group taxis.

4.2 Materials and methods

4.2.1 Experimental animal care

Fish were fed Tetramin flakes and pellets (Tetra, Melle, Germany) at the same time of day, once daily after trials had been completed. Fish were maintained at 21°–23° Celsius on a 14/10 light/dark hourly cycle.

4.2.2 Experimental set-up

Flow-tank experiments were carried out in 180 liter flow tank designed by Loligo systems (Loligo Systems, Tjele, Denmark). Fish were tested in part of the working area of the tank with dimensions 40 cm x 25 cm x 25 cm. Four collimators were used to establish laminar flow (Lagor et al., 2013). The original Loligo collimator was placed in the tank, plus two additional nomex honeycomb straighteners (Nomex, Ohio, United States), and an additional Loligo straightener. The collimators were placed 7 cm apart. The Hach FH950 portable flow meter (Hach, Colorado, US) was used to calibrate the flow tank and get a relation between speed of the motor in hertz and speed in cm^{s-1}. At the end of each day, a 25% water change was performed on the flow tank in order to reduce the accumulation of possible odor cues.

A dorsal view of the fish was recorded at 30 fps using a Casio EX-F1 camera

(Casio Worldwide), with a spatial resolution of 640 x 480 pixels. The camera was mounted 87.6 cm above the base of the working area. Four lights illuminated the working area. In order to minimize reflections of light off the water, the lights were angled towards the ceiling so only indirect, uniform light was cast onto the working area. A side view of the fish was additionally provided by a mirror placed three inches away from the tank, at a 45° angle. The mirror view was captured by the overhead Casio camera. However, in order to access the working area of the tank, the mirror had to be moved regularly, and thus the intrinsic mirror calibration may not be consistent between trials. For this reason, three-dimensional information was mainly used to verify tracking. Figure 4.1 illustrates the flow tank to scale, as well as the mirror and camera placement.

4.2.3 Experimental design

The experiment was a completely randomized, blocked design. Fish were selected for a particular group size pseudo-randomly from 250 fish in the lab. A random number generator in MATLAB was used to select random numbers of length one to the particular group size, out of the entire number of fish in the lab at the time (that had not run in a trial on the previous day). Groups were run in time blocks from 9:00–11:00, 11:00–13:00, 13:00–15:00 and 15:00–17:00. Each group size was run at

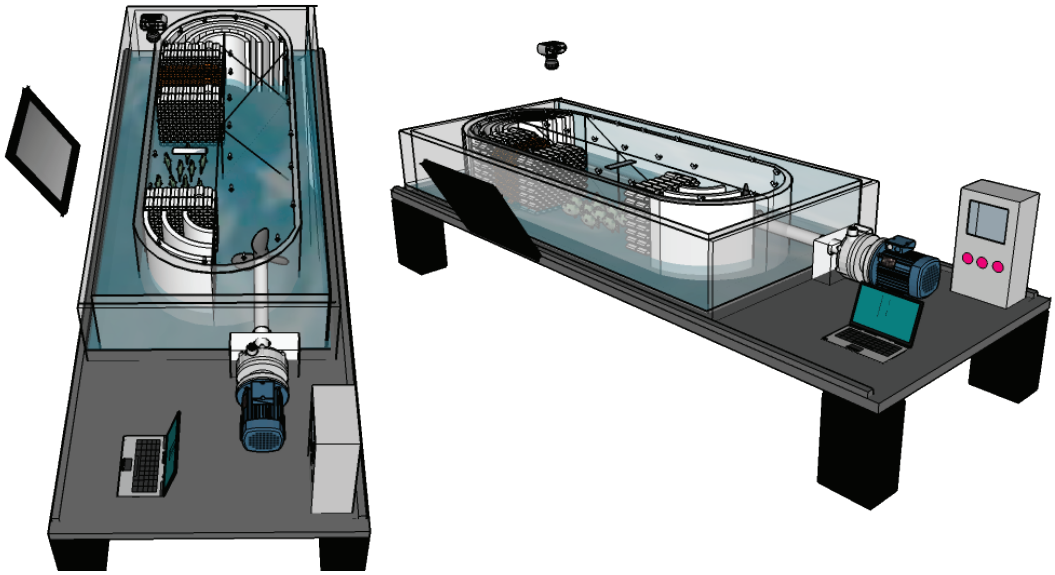

Figure 4.1: Experimental set-up, illustrating the Loligo flow tunnel, overhead camera and mirror placement.

least once in each time bock (plus one more trial in one of the time blocks) to control for possible time of day effects.

The experiment consisted of three independent variables: group size, flow speed and flow direction (increasing or decreasing). Levels of group size were one, two, four, eight, sixteen and thirty-two fish. Seven flow speeds were tested from 0 to 3 Hz (corresponding to approximately 0–12 cm^{s-1}) at intervals of .5 Hz. Each flow speed was presented twice in a given trial. The first presentation of each flow speed was at increasing intervals from 0 to 3 Hz. The second presentation of a given flow speed was decreasing from 3.0 to 0.0 Hz. The decreasing flow speed was used as a

control to test for any differences based on length of time in the tank, or potential order effects.

Five replicates of the experiment were conducted (i.e. for group size two, there were five unique sets of two fish). Multiple dependent variables of internal difference (ID), external difference (ED), nearest neighbor distance (NND), area of the group, density of the group, and standard deviation in x- and y-positions (cross-stream and stream-wise, respectively) were calculated.

Group size and flow speed are fixed factors. Flow direction is a nested within flow speed, and replicate is a random variable, coupled to group size, and nested within flow direction and flow speed. Group sizes of one and two fish were used as controls.

4.2.4 Experimental protocol

Trials were conducted during the day between 09:00 and 17:00. At the start of the day, extrinsic calibration was performed. Before the start of each trial, water quality and water temperature of the experimental tank and home tank was measured to ensure they did not differ in quality, and that the temperatures did not differ by more than two degrees. At the start of the trials, fish were transferred from their home tank to the experimental tank and placed in the working area to habituate for

thirty minutes in the tank, with the lights on and flow tunnel motor on and set to 0 Hz. Once the habituation period was over, fish were filmed for one minute at each flow speed (as well as filmed during the transitions between flow speeds). This is illustrated in the schematic in Figure 4.2.

The camera and flow tank motor could not be easily automated. An experimenter changed the flow speed and triggered the camera remotely from within the experimental room, hidden from sight by a curtain. Trials were conducted in silence, with the exception of some inevitable motor noise from the flow tank.

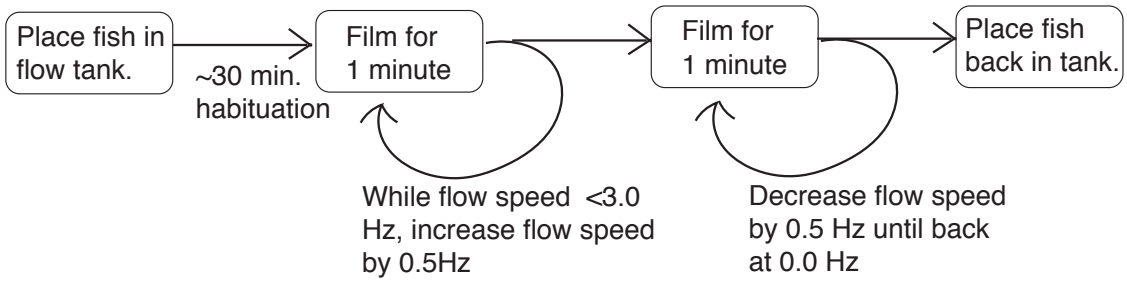

Figure 4.2: Experimental protocol

4.2.5 Statistical analysis

All statistical analyses were conducted in MATLAB and R (R Development Core Team, 2013, R 3.2.3, with RStudio Desktop 0.99.491).

The majority of the statistical analysis was performed using Linear Mixed Models. The full model in R was lmer(response.variable $\sim$ group.size $\times$ flow speed

$\times$ increasing + (flow speed + increasing | idx), where idx is the replicate tied to group size (i.e, 2 fish, replicate 1 and 4 fish, replicate 1, etc.). Data was not scaled before model fitting. Significance levels were set at p >0.05 or t >2. Flow speed and group size were initially run as factors in order to investigate potential non-linear trends in the data. No significant trends were found, so group size and flow speed were estimated to be linear variables for simplification. Diagnostic tests were performed on the model fits to verify model assumptions[1].

Rayleigh tests (Batschelet, 1981) were used to determine whether the phase order parameter distributions differed significantly from random in the absence of flow.

4.2.6 Aggregation model

This experimental data contains both orientation and positional information, whereas the model presented in Chapter 3 modeled orientation alone. Here, I developed a simple model of aggregation for which to compare the positional data from the experiment to.

Inspired by the rheotaxis model and notation in (Chicoli et al., 2015), consider

[1]Additionally, since the residuals were not perfectly normal, and there are small sample sizes, Bayesian models were also run in R assuming an inverse chi-squared prior based on the measured variance of the random variable. The main results did not differ from the lmer, and only the lmer results are reported here.

Figure 4.3: Sample data, showing fish, head and nose positions (green dots and stars, respectively) as well as fish orientation, and the direction into the flow.

the position $r_t^k = x_t^k + iy_t^k \in \mathbb{C}$ of agent $k = 1, ..., N$ at time t, expressed in complex notation for compactness. Let r^{kl} represent the pairwise coupling gain and ω_t^{kl} the interaction noise level. The collective model in discrete time is

$$r_k^{t+1} = r_k^t + \sum_{l \in N_k} \kappa_{kl}(r_l^t - r_k^t + \omega_{kl}^t). \tag{4.1}$$

Unlike the rheotaxis model, there is no reference direction in (Equation 4.1). Consequently, the constraint $\kappa_0 + Nk = 1$ reduces to $\kappa = N^{-1}$, where we assumed identical gains $\kappa_{kl} = \kappa$. Furthermore, let ω_{kl}^t be drawn from a zero-mean normal distribution

with identical variances σ^2 for all pairs k and l. We have

$$r_k^{t+1} = r_k^t + \frac{1}{N}\sum_{l \in N_k}(r_l^t - r_k^t + \omega_{kl}^t) = \frac{1}{N}\sum_{l \in N_k} r_l^t + \frac{1}{N}\sum_{l \in N_k}\omega_{kl}^t \triangleq \bar{r}^t + \frac{1}{N}\bar{\omega}^t, \qquad (4.2)$$

where $\bar{r}^t$ represents the centroid (average) position at time t and $\bar{\omega}_k^t$ is the total interaction noise on agent k at t divided by N. Since the sum of normally distributed random variables is normal with variance equal to the sum of the variances, $\bar{\omega}_k^t$ has variance $N\sigma^2/N^2 = \sigma^2/N$.

Therefore, the expected value of the position of agent k is the centroid position and its variance is σ^2/N, where σ^2 is the variance in the measurement noise of relative position in Equation 4.1. This observation implies the density of agents near the centroid increases with N and the expected nearest-neighbor distance is proportional to $1/N$ for complete interaction topologies.

4.3 Experimental Results

4.3.1 Effects of flow speed and group size on rheotaxis

I quantify rheotaxis by measuring the external disagreement (ED) measure. The ED is highly correlated with internal disagreement (ID) $r(346) = 0.8369$ and

$|p_\theta|$, $r(346) = 0.8691$.

As previously documented, giant danio show positive rheotaxis in a flow field, as indicated by a significant effect of flow speed on the ED (Table A.1). Additionally, the degree of rheotaxis increases with flow speed. Figure 4.4a shows the ED values over group sizes and flow speeds.

There was a significant interaction between flow direction and flow speed on ED values (Table A.1). As flow speed increases more fish rheotact and the ED value decreases as a result. The reverse trend occurs when flow speed decreases.

There were no significant effects of group size on the ED (Table A.1).

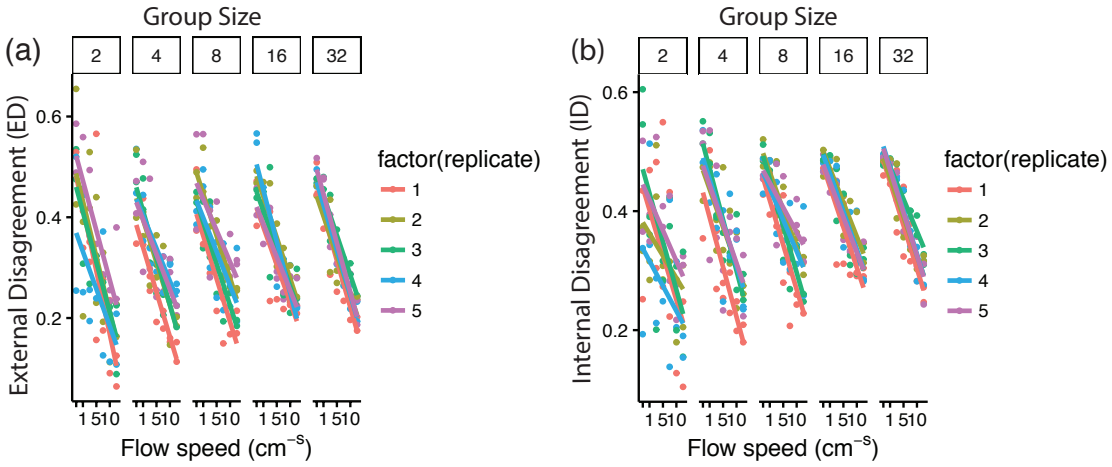

Figure 4.4: Effect of flow speed, group size and replicate on dependent variables of (a) ED, (b) ID. Increasing and decreasing flow speed changes are pooled together.

4.3.2 Effects of flow speed and group size on group alignment

Figure 4.5 shows polar histograms of fish orientation across group sizes and flow speeds. The orientations of giant danio in no-flow were compared to a uniform distribution. Group sizes of 8 and 32 were significantly different than a uniform distribution (Rayleigh tests, n = 49, $N = 2$: mean length = 0.1119, $p = .5438$, $N = 4$: mean length = 0.1577, $p = 0.2973$, $N = 8$: mean length = 0.3406, $p = 0.003$, $N = 16$: mean length = 0.069, p=0.7938, $N = 32$: mean length = 0.3583, $p = 0.0016$). There seems to be a tendency to orient towards 90° in the no-flow condition, which is likely due to the reflectivity of the wall in the working area of the flow tank.

Figure 4.4b shows the ID results over group sizes and flow speeds. At the lowest flow speeds, data are close to .7, which would indicate random orientations. This combined with the results from the Rayleigh test suggest giant danio weakly align their orientations.

There was a significant effect of flow speed on the ID. This is because as fish align independently with the flow, they by consequence align with each other as well. Tables A.2 shows the results of all independent variables on the ID.

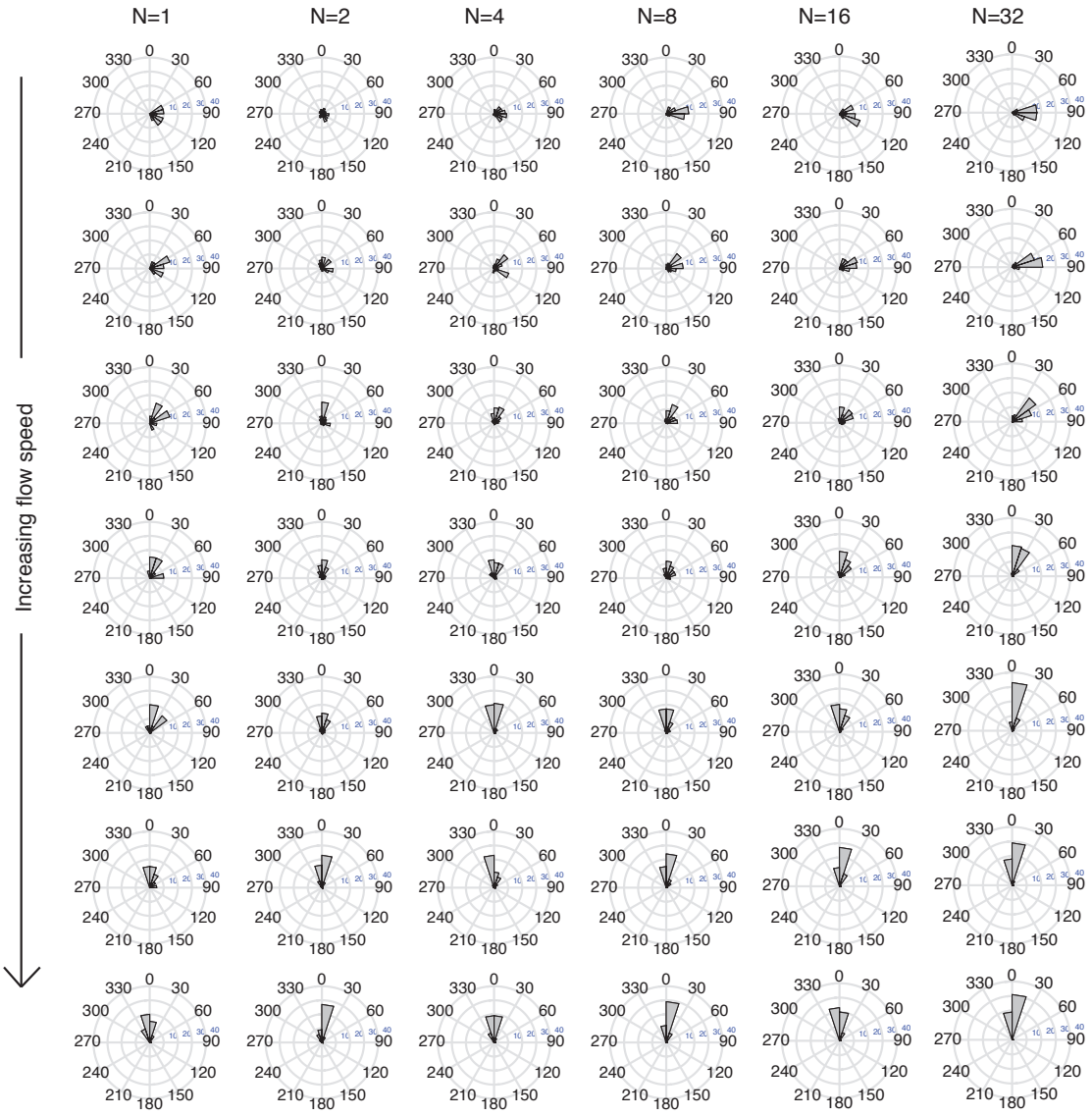

Figure 4.5: Rose histograms of fish orientation over group sizes and flow speeds. Note that these histograms are not scaled.

4.3.3 Effects of flow speed and group size on group aggregation

In order to investigate spatial data of the shoal, I first investigate the deviation in fish position. As group size increases, the standard deviation in both the x- and y- positions increase significantly (Tables A.3 and A.4). This is shown in Figure 4.6. There are also significant interactions between group size, flow speed, and flow direction in the y-direction (Table A.4) and a significant interaction of flow speed and direction in the x-direction (Table A.3).

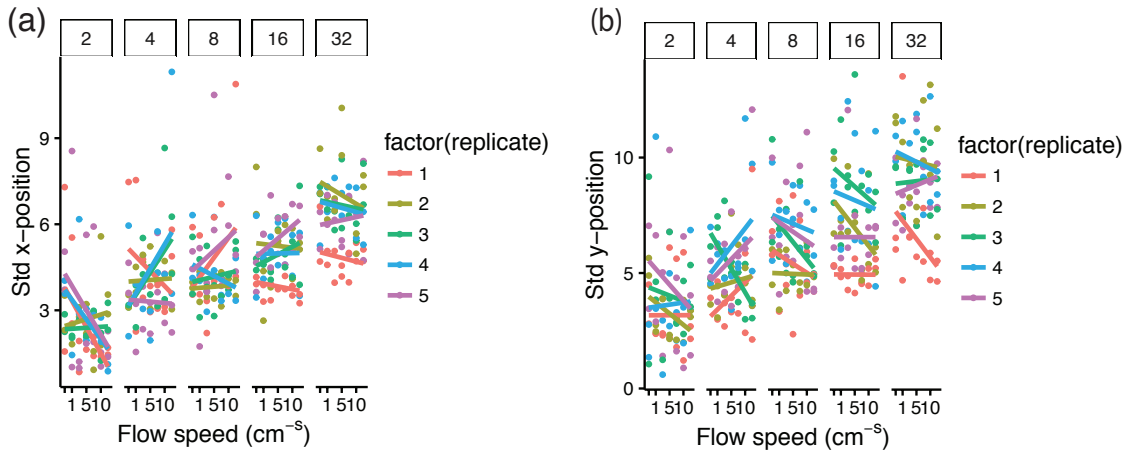

Figure 4.6: Effect of flow speed, group size and replicate on dependent variables of (a) std x-position, (b) std y-position. Increasing and decreasing flow speed changes are pooled together.

Nearest-neighbor distance decreases significantly as group size increases (Table A.5), as seen in Figure 4.7(a). There are are also significant interactions between group size and flow, and flow direction (Table A.5). Shoal density is not effected by

group size or flow speed (Table A.6 Figure 4.7(b)).

4.3.4 Space utilization

There is a possibility that the NND decreases with group size simply because there are more fish in the working area, and there is limited available space for the fish to spread themselves apart. To investigate this possibility, I calculated the area of the shoal (Table A.7, Figure 4.7(c)) based on the convex hull. Shoal area is correlated with the variation in the standard deviation in x-position $r(346) = 0.6955$ and y-position $r(346) = 0.764$ of shoal members. (Note, that in Figure 4.7(c) only group sizes 4–32 are valid and group size two is set to zero, because at least three points are required to compute a convex hull). As the group size increases, the total area taken up by the group increases. However, this is not due to lack of space. The average area of the 32 fish group size is approximately 500 cm^2, which is half the total available two-dimensional area available (1000 cm^2). Figure 4.7(d) shows a sample image from a 32 fish trial, demonstrating group aggregation.

4.3.5 Results of the aggregation model

An aggregation model was developed in order to fit to the spatial component of the experimental data. This model was not thoroughly evaluated, but several

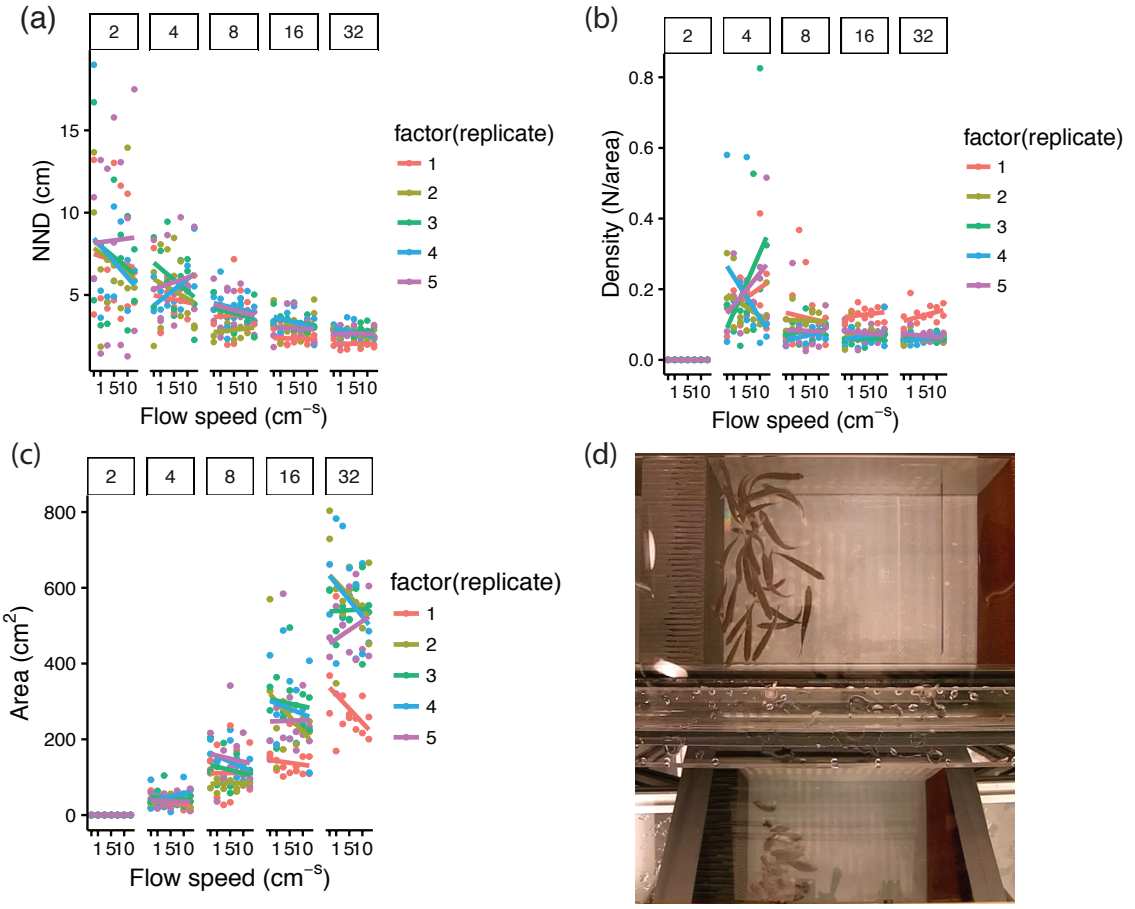

Figure 4.7: Effect of flow speed, group size and replicate on dependent variables of (a) NND (b) density of shoal, (c) area of shoal, and (d) image of experimental data with 32 fish demonstrating aggregation. For (a)-(c), increasing and decreasing flow speed changes are pooled together.

simulations were run using different interaction topologies. The results of these simulations are shown in Figure 4.8. The trend observed in the data, is a decrease in NND with group size at a rate of $1/\sqrt{(N)}$ (yellow triangle). When the model is run with limited interaction topologies, specifically when agents interact with their four

closest neighbors (red square), the NND decrease comes closer to what is observed in the data, as opposed to when run with an all-to-all interaction topology (blue cross). The trend for standard deviation (purple star) with a limited topology is also shown. Similarly to the experimental data, the standard deviation in xy-position increases with group size.

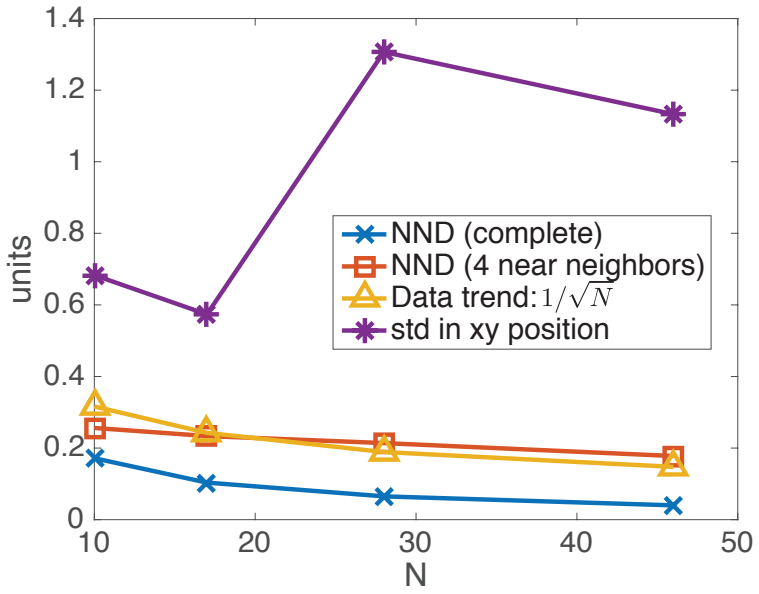

Figure 4.8: Aggregation model predictions in nearest neighbor distance. The yellow line with triangles shows the trend in the experimental data, in which NND decreases as a function of $1/\sqrt{N}$. The line with blue crosses shows the model results run with all-to-all interaction topology. The line with red squares shows the model run with a limited interaction topology of the four closest neighbors. The line with purple stars is the standard deviation in xy-position for the limited interaction topology.

4.4 Discussion

This study is the first, to the best of my knowledge, test the prediction that group size improves rheotaxis under different flow conditions. I varied group size with 1, 2, 4, 8, 16, and 32 giant danio and flow speeds from 0 cm^{-s} to 12 cm^{-s}. As expected, giant danio show positive rheotaxis that increases with increasing flow speed. Contrary to theoretical predictions, however, rheotaxis did not vary with group size under any of the flow conditions tested. I find that NND decreased with increasing group size, and developed a simple model similar to the previous noisy synchronization model of rheotaxis that predicts this trend.

4.4.1 Flow speed, group size and rheotaxis performance

Theoretical predictions from (Chicoli et al., 2015; Grünbaum, 1998; Torney et al., 2009) predict that in noisy sensory conditions, group size will improve taxis. One potential mechanism for a group benefit is the many-wrongs principle, which states that by averaging instantaneous movement decisions over neighbors, rather than averaging over time, individuals in a group can improve their performance. However, in this experiment, group size did not have an effect on rheotaxis.

There are several reasons why this may be. The first is that rheotaxis may be

too simple and robust of a behavior to show group size effects. Rheotaxis is multi-sensory behavior that can occur even in the complete absence of certain sensory modalities (Bak-Coleman et al., 2013). Additionally, group size effects depend on task difficulty. Sasaki et al. (2013) found that ant colonies outperform individuals when a sensory discrimination task is difficult, but not easy (although this particular result may involve a speed-accuracy trade-off).

Another potential explanation is that neighbor position is a more relevant cue for shoaling fish than neighbor orientation, and thus social information based on heading was largely unattended to. (Herbert-read et al., 2011) had found that in mosquitofish *Gambusia holbrooki*, attraction was the most important factor in fish shoaling, and that alignment only played a weak role in group cohesion. Additionally, Viscido et al. (2004) performed experiments on groups of four and eight giant danio, as well as simulated behavior using a model of repulsion, attraction and orientation. They found that only a weak alignment force was necessary in their simulations to reproduce experimental behavior (1–2% of the attraction/repulsion forces). These authors also suggest that alignment forces play a secondary role to positional cues during shoaling behavior. The data in this study also suggests that alignment forces between shoal mates may be weak. The experimental data here lies within the parameter space of the theoretical predictions in Chapter 3 — namely

the case when there are no explicit social interactions among group members. Since the synchronization model presented in Chapter 3 only includes interactions based on orientation and alignment, this would support the hypothesis that positioning is a more important factor in shoaling than alignment.

Finally, there is a methodological consideration. In this study, I reduced the strength of the flow signal. However, in a uniform flow field, there may not be much of a baseline noise factor. In this case the signal, once at detection threshold, would be easily perceived. Additionally, there is an increased probability that eddies or other turbulent structures will form at higher flow speeds, thereby potentially increasing noise as well as the signal. That said, establishing what noise means in a fluid environment is not a straightforward task, especially when interested in fish behavior. Behaviorally, fish prefer different flow environments based on the species, sex, and body size (Hockley et al., 2014; Liao and Cotel, 2005), but also on flow speed, turbulence and vortex structure (Lupandin, 2005). Additionally, turbulence may provide additional sensory cues for fish. Direct effects of turbulence on rheotactic performance have been measured in only two studies that I am aware of, one of which showed that rheotactic performance was enhanced in turbulence under both light and dark conditions (Pavlov et al., 2000) and one which showed no effect of turbulence (Trump and Mchenry, 2013).

4.4.2 Increased aggregation with group size

Nearest neighbor distances were found to decrease as group size increased, suggesting that fish may choose to stay closer together when there are more individuals to group with. Shelton et al. (2014) found a decrease in NND with group size in zebrafish *Danio rerio*. However, the authors found that when density was controlled for, NND of groups of four and eight fish were statistically similar. The amount of available space may be a factor in the results presented in this chapter, and should be further investigated. Soria et al. (2007) found that in the bigeye scad *Selar crumenophthalmus*, the nearest neighbor distance decreased when the group size increased, in contrast to the bobbed flagtail, *Kuhlia mugil*, where NND was constant. Viscido et al. (2004) did not find a change in NND between four and eight fish in giant danio. One possibility for the discrepancy between the results is that NND oscillates over time. Miller and Gerlai (2008) and Viscido et al. (2004) had recorded the danio groups for a much longer period of time. Another possibility is that in the previous study, only two groups sizes were used, and group size trends may not be as evident.

The observed decrease in NND with group size may be a result of positive feedback. Positive feedback is the amplification of events through recruitment or reinforcement (Bonabeau, 2007; Camazine et al., 2001), and positive feedback loops

are one of the main principles of collective behavior in animal groups (Sumpter, 2006). Some other examples of positive feedback in collective systems are well known, including ant pheromone trails that attract other ants (Bonabeau, 2007; Deneubourg and Gross, 1989) and the grouping of cockroaches to a shelter (Canonge et al., 2011; Jeanson and JeanLouis Deneubourg, 2007). In group behavior, this is also called local enhancement (i.e., when an individual is drawn to an area because of the presence of another individual) (Reader et al., 2003).

The aggregation model presented here, much like the rheotaxis model, is overly simplified. These models are not intended to fully describe fish behavior. Rather, these models capture aspects of shoaling and rheotactic behavior, can predict simple behavior under certain circumstances, and make very few assumptions. Figure 4.8 shows the predicted effects of the aggregation model on NND as group size increases. In an all-to-all interaction topology, NND decreases at a rate of approximately $1/N$. The experimental data shows a much slower decrease in NND, at a rate of approximately $1/\sqrt{N}$. Numerically analyzing the model for a limited interaction topology gets much closer of an estimate to the behavioral data. In addition to limited interaction topologies, the noise parameter in the model plays an important role. If the noise scales with the number of agents, the results also come closer to the experimental data. Both limited interaction topologies and noise values that scale with N

are biologically plausible.

Part II: Startle Response and Information Transmission

Chapter 5: Probabilistic information transmission in a network of coupled oscillators

5.1 Introduction

Groups of fish vary greatly in their shoaling behaviors from loose aggregations, to shoals and schools (see Section 1.4.1). However, many species of fish also exhibit dynamic shoaling behaviors that change over time (Miller and Gerlai, 2008; Viscido et al., 2004). Breder (1959) defined obligate shoaling fishes as those that are polarized constantly, and facultative shoaling fishes, which are those that are only polarized occasionally. This terminology is generally used to specify different shoaling behaviors as a result of different environmental contexts (e.g., shoaling in the presence of a threat) (Delcourt and Poncin, 2012). In this study, I use the term obligate to refer to shoals that are polarized before the presence of a threat and facultative to refer to shoals that seek to polarize once a threat is detected.

While differences in shoaling behavior have been observed in fishes, it is unclear

how the degree of polarization affects the response to predation. Individuals already aligned toward one another are able to respond more quickly to movement changes made by their neighbors (Couzin et al., 2002), and therefore respond more rapidly to the location of prey or unknown changes in their environment (Laland et al., 2011). Domenici and Blake (1997) hypothesized that when herring are shoaling, the ability of each fish to correct its trajectory following turns towards the stimulus is enhanced, and that shoaling fish may have an advantage when trying to correct their towards responses, as they may integrate information from the external stimulus with that from internal information from startled neighbors.

This study uses numerical simulation and modeling methods to test the hypothesis that strong alignment improves a shoal's response to a threat. To do so, I apply a simple model of epidemic contagion (see Section 2.6) to model the probability of response to a threat. This model is then paired with the dynamics of the synchronization model described in Chapter 3. With this joint model, I am able to investigate the spread of information through a network and study the resulting orientation dynamics resulting from interactions with other agents.

In order to compare between shoaling behaviors, I categorize agent behavior as either non-shoaling, obligate shoaling, or facultative shoaling. Additionally, I control for the individual effects of startling due to an external threat, or via neighbor cues,

by examining the responses of each shoaling type in both the presence or absence of social cues. When there are social cues from neighboring agents, these shoals are referred to as attentive. When there is no use of social cues, these shoals are referred to as inattentive. I then measure the proportion of fish startling over time, the directionality of the response, and the cohesion of the shoal after the startle response, in order to assess differences in response between different types of shoaling behavior.

The contributions of this chapter are (i) application of a probabilistic model of epidemics to the study of animal behavior; (ii) testing the biological hypothesis that shoal cohesion improves predator escape; (iii) quantification of the effect of attentiveness to startle propagation (via the variable P^{int}); and (iv) investigation of the variation in response based on network connectivity. This work has application to the study of collective behavior in fish shoals and other animal groups.

5.2 Methods

5.2.1 Coupled oscillator synchronization model

I use the synchronization model previously described in Chapter 3. For review, let t represent the discrete time index, and the orientation of individual k at time t is given by θ_k^t. When not startled, agents are steered according to the following

stochastic difference equation

$$\theta_k^{t+1} = \theta_k^t + \frac{\kappa}{N} \sum_{l=1}^{N} \sin(\theta_l^t - \theta_k^t + \omega_1), \tag{5.1}$$

where ω_1 represents sensory noise value at time t. Here the noise is drawn randomly from a Gaussian distribution, $N(0, \sigma_1)$ (degrees). The gain κ is of importance for the synchronization behavior of the model Kuramoto (1975). Namely, $\kappa > 0$ yields synchronization and $\kappa<0$ yields incoherent behavior.

5.2.2 Probabilistic model of information transmission

This model is a version of the SIR epidemic model, described in Section 2.6, and is also a discrete-time Markov chain. A discrete time Markov chain is a dynamical system composed of S discrete states. In this study, there are two states for each agent: a susceptible state, and an infected (or startled) state. These states and the transitions between them area based on the probabilities in the model (Figure 5.1). The state of each agent over time can also be represented as a cellular automata (Figure 5.2). In the cellular automata, each cell represents an agent k at a time step t. The color of the cell represents the agent's state.

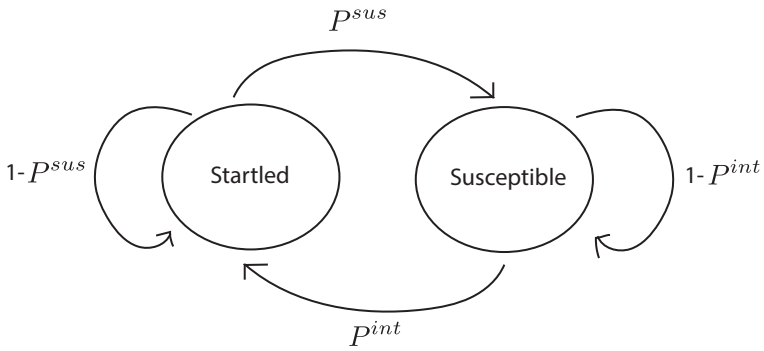

Figure 5.1: The transition diagrams illustrating how agents change state.

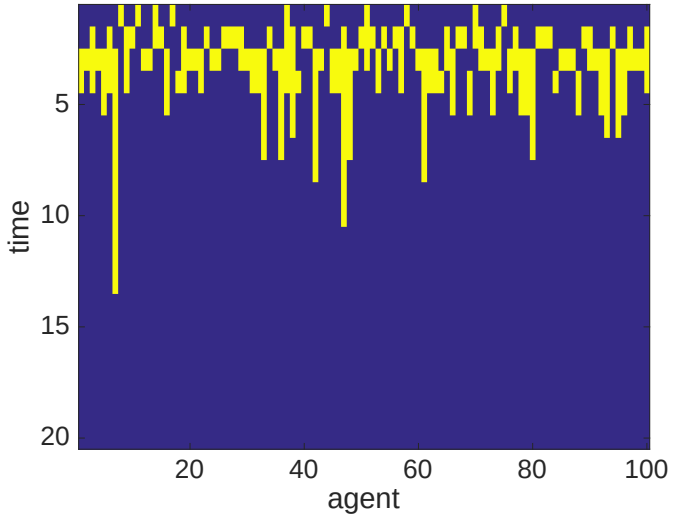

Figure 5.2: Image depicting change in agent state over time as a cellular automata. Blue indicates a non-startled state and yellow indicates a startled state. On the first time step, ten agents startle due to the external threat via P^{ext}. On subsequent time steps, the startle propagates throughout the shoal.

5.2.3 Behavioral Rules

Agents execute different behavioral rules depending on what signal initiated the startled state (external threat via P^{ext} or internal cue via P^{int}), and whether the startle has just been initiated or is sustained (P^{sus}).

When there is no disturbance or threat to the shoal, agents synchronize at a rate dependent on the gain of the synchronization model, κ. At time $t = 0$ agents have probability P^{ext} of responding to an external threat. When startled directly from a threat via P^{ext}, agents react to an impulse by instantaneously reorienting — with some variation due to noise — towards a reference direction, θ_s. Without loss of generality, the reference direction is considered to be the direction away from the threat, and is set at zero degrees. This is given by the equation

$$\theta_k^t = \theta_s + \omega_2, \tag{5.2}$$

where $\theta_s = 0°$, and ω_2 is the variability of directionality in the startle response drawn randomly from a Gaussian distribution, $N(0, \sigma_2)$ (degrees). This is a simplistic behavioral rule, but serves to simulate the rapid turning behavior of fish during an escape response.

At following time steps, $t > 0$, agents that are currently in a susceptible state

(they have not yet been startled) respond to startled neighbors with probability P^{int}. If startled from neighbor cues, agents react to an impulse directing them in the average orientation of their startled neighbors, given by

$$\theta_k^{t+1} = \sum_{l \in N_{k(startled)}} \theta_l^t + \omega_2 \tag{5.3}$$

Following the initial transition to a startled state, if agents remain in the startled state via P^{sus}, they follow the behavioral rules of the synchronization model as they would in the susceptible state. While sustaining a startled state agents may still continue to propagate the response.

5.2.4 Parameter space

Table 5.1 details the model parameters and the parameter values explored in this study. Simulations were run for 100 time steps. The startle model typically lasted no more than the first 10 time steps for the value of P^{sus} used.

5.2.5 Shoaling types

Three shoaling behaviors are investigated: obligate, facultative, and non-shoaling. Obligate shoaling agents are characterized by being initially polarized, and then continuing to follow the synchronization model. Facultative shoaling agents start in

Table 5.1: Parameter space of probabilistic startle model

Parameter	**Symbols**	**Values**
Probability of startling to threat	P^{ext}	0.05, .1, .5
Probability of startling to neighbor cues	P^{int}	0, 0.05, .1, .5
Probability of sustaining a response	P^{sus}	.5
Coupling gain between agents	κ	0, .2
Initial orientation (obligate)	θ_0	180°
Initial orientation (facultative, non-shoal)	θ_0	random
Standard deviation of noise in synchrony model	σ_1	2°
Standard deviation noise in startle response	σ_2	20°
Number of agents	N	100
Connectivity of random graph	c	1, .5, .2

random orientations, but in the presence of a threat follow the rules of the synchronization model. Non-shoaling agents do not follow the synchrony model.

In addition to these shoaling types, I also distinguish between attentive and inattentive shoals, based on the space they occupy in the probabilistic startle model. Namely, if $P^{int}>0$, the shoal is considered attentive, and the startle will spread, whereas if $P^{int}<0$, then the shoal is considered inattentive and the reaction to the threat does not spread throughout the group. The inattentive group also serves as a control to compare the effects of social information transmission within a group. Table 5.2 shows the parameter values for each shoaling type, and Figure 5.3 details the behavior of each shoal type in words.

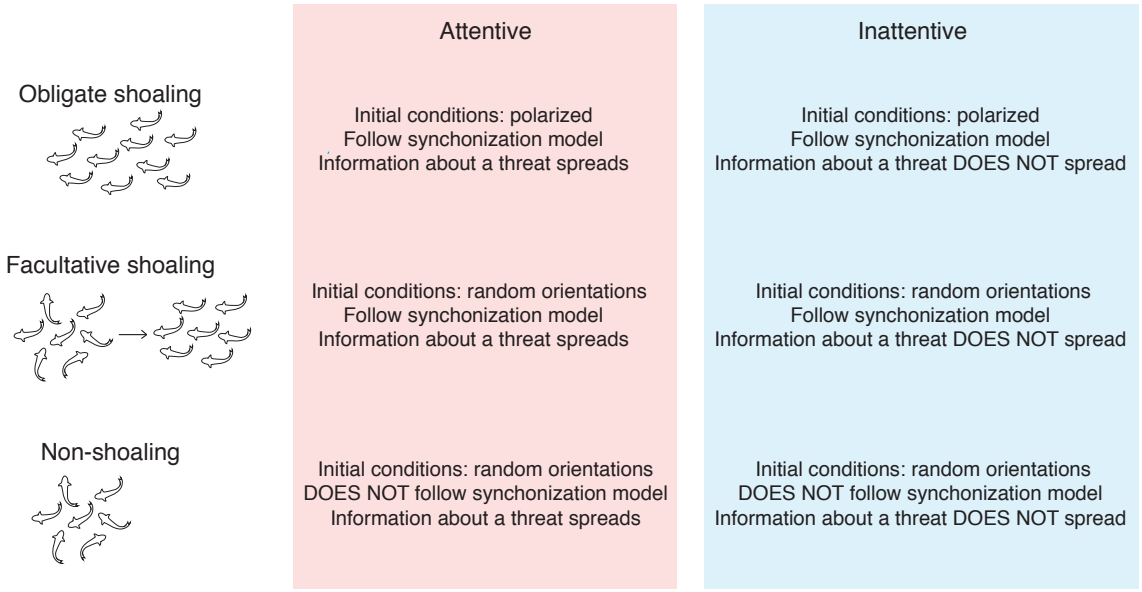

Figure 5.3: Categorization of shoaling behavior in the model.

Table 5.2: Shoaling categories

Behavior	**Initial conditions**	**Gain**	**Attentive, Inattentive**
obligate	polarized	$\kappa > 0$	$P^{int} > 0$, $P^{int} = 0$
facultative	random	$\kappa > 0$	$P^{int} > 0$, $P^{int} = 0$
non-shoaling	random	$\kappa = 0$	$P^{int} > 0$, $P^{int} = 0$

5.2.6 Analysis metrics

The proportion of the shoal startled is measured at each time step, which gives an indication of how many fish were startled (see Figure 5.4), as well as how rapidly the information spread. These results will be the same for all shoaling types because the interaction topology governing the results of the probability model is fixed, and does not interact with the synchronization model for the cases investigated here.

The orientation dynamics of the responses are measured over time as well and compared between the shoaling groups. I characterize a successful escape from the threat as orienting within $\pm$ 20° of the reference direction, and investigate two critical time points. The first time point is when all startles have just completed. The second time point is at the end of the simulation.

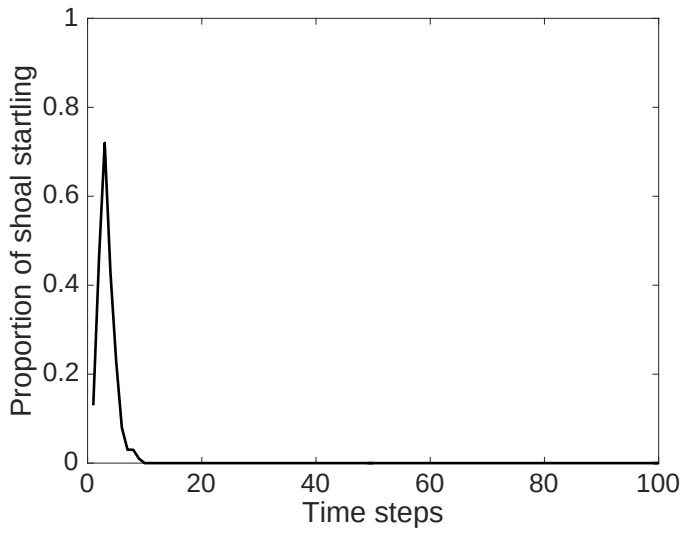

Figure 5.4: Exemplary plots depicting proportion of shoal startling over time.

5.3 Results

I combined a model of orientation synchronization based on coupled oscillators combined with a model of information propagation to predict how information would

be transferred through a group and how shoaling behavior would affect the dynamics of the startle response.

5.3.1 Startle propagation

I first examine the roles of topology, P^{int} and P^{ext} on the spread of information through the group. Figure 5.5 shows the average proportion of the shoal startling for given P^{int} and P^{ext} values, and three different network topologies, specified by percent connectivity.

As expected, more highly connected topologies have a higher proportion of agents responding to the threat. Additionally, the proportion of the shoal startling tends to increase with increasing values of P^{int} and P^{ext}. A non-intuitive exception to this result, is that at higher values of P^{int} (i.e, 0.5), there are more agents responding when P^{ext} is lower, as opposed to higher. This unexpected result can be attributed to the removal aspect of the SIR model, and the value of P^{sus}. If more fish startle due to P^{ext}, and the startle completes before it can spread, this would result in an overall reduced propagation of the response. This result indicates an interaction between the three probabilities in the model, and the proportion of agents startling.

The rate of information spreading happens fairly rapidly in all topology cases, with peak responses occurring in the first (when the connection topology is very low)

or second time step. The difference in peak number of responses between topologies can be seen in Figure 5.5. At low values of P^{int} and P^{ext} there is the greatest difference in the results between interaction topologies. At $P^{int} = 0$ the isolated effect of P^{ext} is shown.

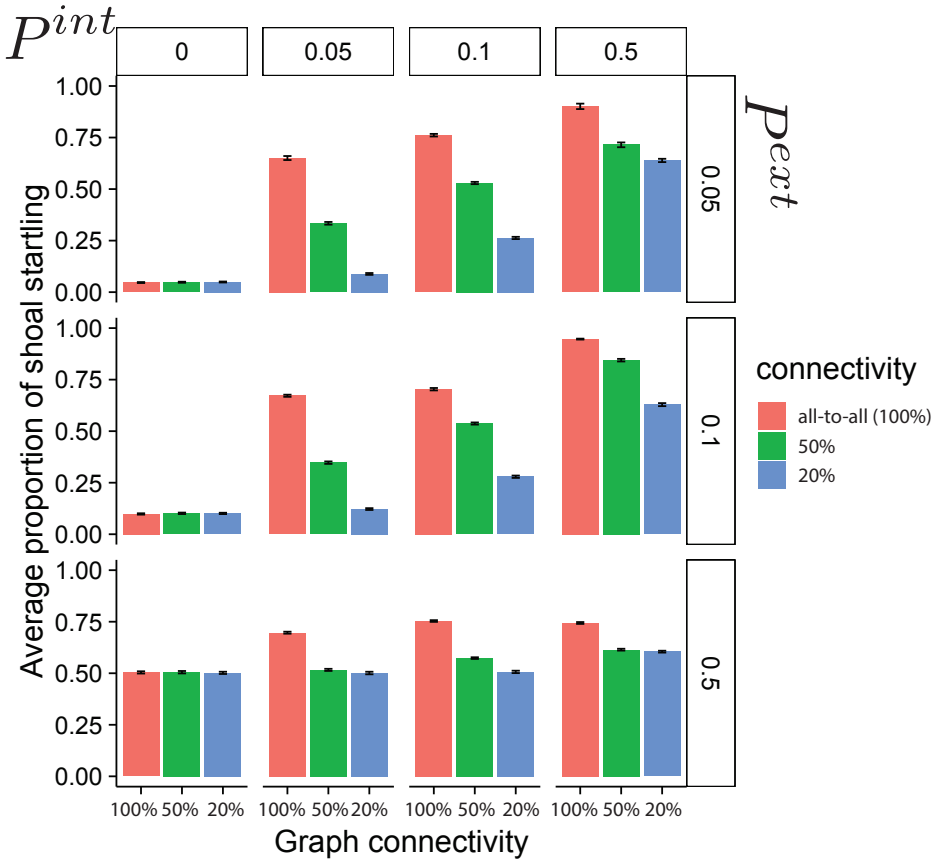

Figure 5.5: Bar plot illustrating the max proportion of the shoal startled (averaged over 300 Monte Carlo runs) for sample values of P^{ext} and P^{int}. Error bars are 95% confidence intervals.

5.3.2 Orientation dynamics

Next, I compare the response dynamics between shoaling groups, focusing on the results for the all-to-all interaction topology. Figures 5.6 and 5.7 show the average proportion of successful escapes at the time step when the last startle state ended (Figure 5.6) and the last time step in the simulation (Figure 5.7).

At the completion of the startle responses in the group, obligate shoaling agents show a higher proportion of the shoal escaping the threat as compared to facultative and non-shoaling groups. The exceptions to this are when the shoal is inattentive (no neighbor information), or when P^{ext} is high. When there is no social information, facultative and non shoaling groups show higher proportion of agents oriented away from the threat. However, this is due to the fact that these groups are initialized in a random orientation at the start of the simulations. So, by chance more agents are likely to be oriented away from the threat. Given that the average number of agents startling in all shoal groups is the same, the agents that startle in the obligate shoal group exhibit a more accurate response, according to this criteria (Figure 5.6).

Figure 5.7 illustrates the proportion of agents oriented to the reference direction at the end of the simulation. There are noticeably more facultative shoaling agents oriented towards the reference direction than obligate shoaling agents, and approximately 10% more than immediately following the startle responses, suggest-

ing that non-startled agents were recruited to the direction away from the threat, but at a much slower rate. In comparison, there are significantly fewer obligate shoaling agents oriented towards the reference direction at the end of the simulation than immediately following the startle responses, suggesting a strong influence of the role of non-startled agents in determining the orientation during the synchrony model.

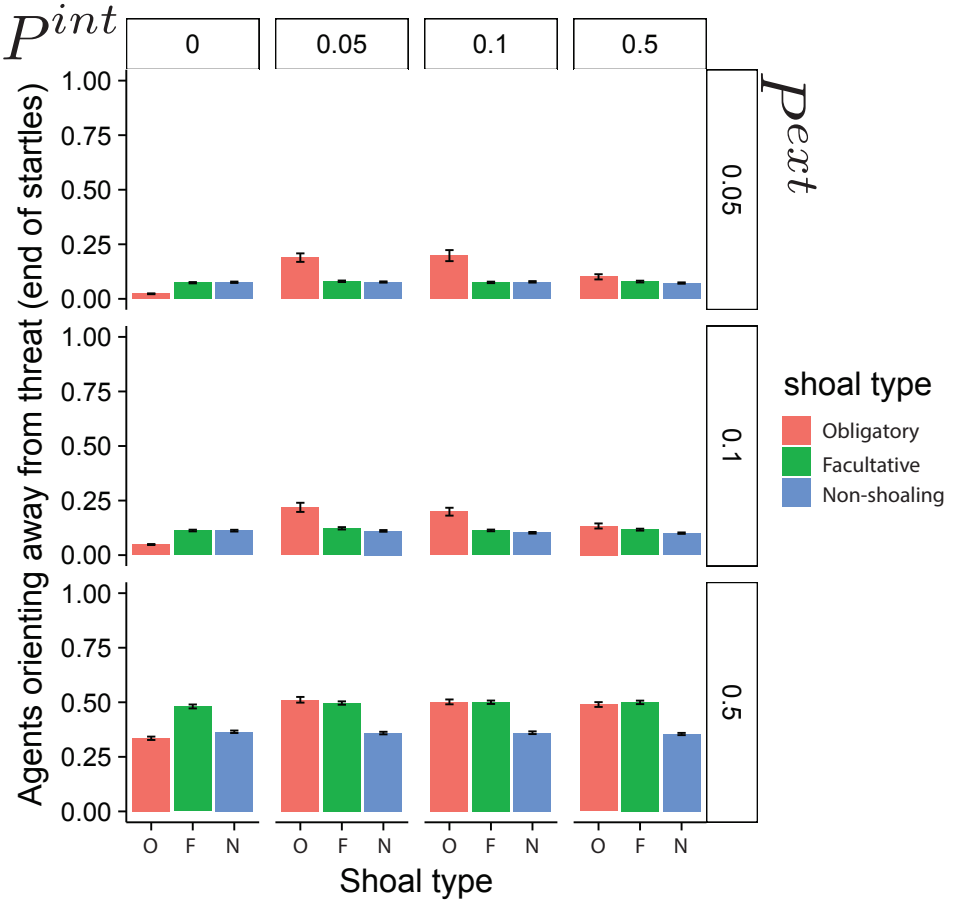

Figure 5.6: Bar plot illustrating the average proportion (over 300 Monte Carlo runs) of the shoal oriented $\pm 20°$ from the reference direction at the time of the last startle response. Error bars are 95% confidence intervals.

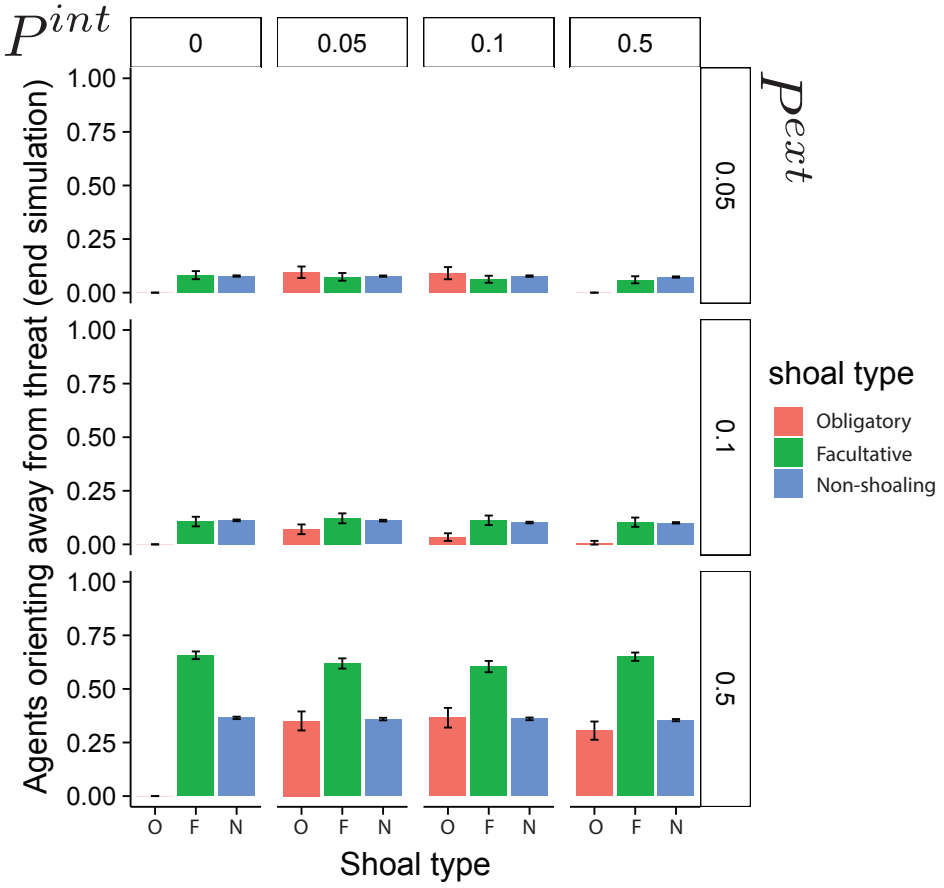

Figure 5.7: Bar plot illustrating the average proportion (over 300 Monte Carlo runs) of the shoal oriented $\pm 20°$ from the reference direction at the last time step of the simulation. Error bars are 95% confidence intervals.

Thus, obligate shoaling agents respond much more rapidly than facultative shoaling agents to a threat (0- 20% more of the shoal escaping at the end of the last startle response). Facultative shoaling fish, however, are able to exert stronger influence on their shoal-mates orientation through the synchronization model. Figure 5.8 depicts waterfall plots of histograms of agent orientation over time, normalized by

30,000 (100 agents $\times$ 300 Monte Carlo runs) and bound between 0 and π.

5.4 Discussion

In this study, I use an epidemic model paired with a model of coupled oscillators to model information transmission in groups of fish. I examine potential differences in startle response behavior based on shoaling properties and investigate the spread of information transmission through a group using a model of contagion. To the best of my knowledge this is the first study to apply an epidemic model to the study of fish startle response behavior and the first to numerically analyze potential effects of polarization on startle response behavior.

I find differences in startle response behavior between shoaling types. This is true even for attentive obligatory and facultative shoals, where the only difference between them is the initial orientation of the shoal when the threat is introduced. The results of the model reinforce the idea that there are benefits of polarized shoaling (Couzin et al., 2002). The model also predicts that randomly oriented shoals may better at transferring information to uninformed individuals, leading to a slower, but more accurate response. A speed-accuracy trade-off may be a strategy used by fish shoals in the response to a predator (Domenici and Blake, 1997).

I investigated different values of P^{ext} and P^{int}, which varies the number of

informed individuals and the rate of information transmission among group members. The model proposed here could thus be used to vary group size and the number of informed individuals over the parameter space to assess the conditions under which knowledgeable individuals have the most influence. A small number of knowledgeable individuals has been previously shown to elicit a response from both small and large groups (Gueron et al., 1996; Huse et al., 2002; Mirabet et al., 2008; Reebs, 2000). However, in smaller groups, a greater proportion of knowledgeable individuals is needed to elicit a response (Couzin et al., 2005; Huse et al., 2002), and it is more likely that inaccurate decisions will be made (Ward et al., 2008).

In this study, low probabilities of P^{ext} and P^{int} were used. The greater the number of connections between agents, the lower this number needs to be to avoid saturation of the response. It may also be possible to scale this parameter with distance or number of neighbors, such that an agent may have a high probability of interacting with close neighbors, but reduced probability of being startled by more distant neighbors. Additionally, the parameter P^{sus} was kept fixed for this study. However, the value of P^{sus} has bee shown to play an important role in the timing of epidemic spreading.

While I use a very simple version of the model to investigate startle response behavior in shoals, the model is powerful given its simplicity and also quite generaliz-

able. As it is, the joint model proposed herein includes two behaviors (synchronizing and startling), that occur on different time scales, and may involve separate network interactions. This model may be used to test other hypotheses regarding startle response behaviors in fish, including information transmission based on location within a shoal, different network interactions, and heterogenous groups. It is important to note that the synchronization model and the probabilistic startle model operate independently in this study, but may interact depending on how the interaction topology between agents is specified. Additionally, this model may be used to investigate different information-transmission or decision-making behaviors in animal groups.

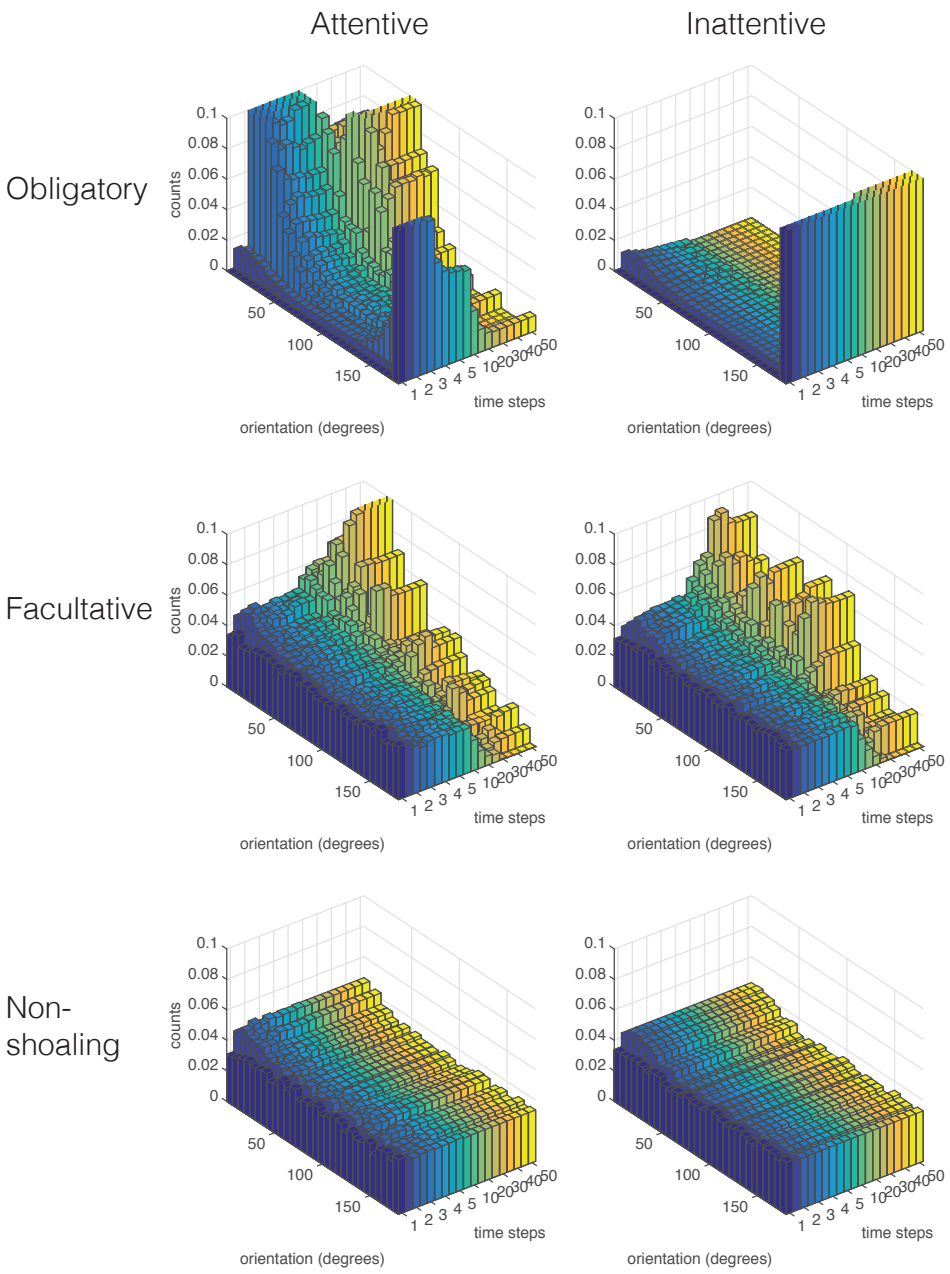

Figure 5.8: Waterfall plots displaying orientation histograms over time for all three shoaling types, $P^{ext} = 0.05$, $P^{ext} = 0.05$ Note the time scale plots the first five time steps when most startles occur, then plots once every 10 time steps up until 50, by which time the startles have long ended.

Chapter 6: Effect of flow on group structure, startle response and information transmission

6.1 Introduction

This chapter quantifies startle response rates to an external threat (a visual looming stimulus) for solitary and groups of eight fish in flow and no-flow conditions. The data is fit to the probabilistic model of information transmission from Chapter 5 that includes socially transmitted information. This model predicts the number of fish responding in both the flow and no-flow conditions. The aims of this study were to determine the effects of flow on the collective transmission of threat information within groups of fish, as measured by the number of fish responding to an external threat, as well as to investigate the effect of flow on information transmission.

Fishes use a variety of sensory modalities to receive information from a predator or other fish in the school, including vision (Dill, 1974; Guthrie and Muntz, 1993), olfaction (Ferrari and Chivers, 2006; Mathuru et al., 2012) and lateral line sensing

(McHenry et al., 2009; Mirjany et al., 2011). Although the extent to which ambient currents might affect the ability of fishes to detect predators either directly or indirectly is unknown, currents would be expected to have a large impact on the flow-sensing lateral line system. For example, local hydrodynamic disturbances produced from the C-start escape maneuvers of fishes in response to a predator are capable of stimulating the lateral line of nearby fish in a school (Tytell et al., 2008), but the ability of fishes to detect these local flows may be masked by the presence of ambient water motions, such as those in a stream (Coombs et al., 2001; Engelmann et al., 2002). On the other hand, the fact that flow elicits rheotactic behavior means that fishes are more likely to be aligned in a common direction, which is typically upstream. Individuals already aligned toward one another are able to respond more quickly to movement changes made by their neighbors (Couzin et al., 2002) and therefore respond more rapidly to the location of prey or unknown changes in their environment (Laland et al., 2011). Rheotacting fishes should thus have less directional noise, meaning that deviations from the polarized direction such as startle responses may be more easily detected via vision or the lateral line. Additionally, increased alignment has the effect of minimizing relative motion between adjacent fish, thus reducing hydrodynamic and optical-flow noise generated by the movements of nearby fish.

Behavioral results indicate that (i) school formation is altered in flow such that fish orient upstream while spanning out in a crosswise direction; (ii) the probability of at least one fish detecting the looming visual stimulus is higher in flow than no flow for both solitary and groups of eight fish, but (iii) the probability of three or more individuals responding is higher in no flow than flow. Taken together, the behavioral results indicate a higher probability of stimulus detection in flow but a higher probability of internal transmission of information in no flow. Behavioral results were well-predicted by a computational model of collective fright response that included the probability of both direct (based on classic Signal Detection Theory) and indirect (i.e. via interactions among group members) detection of external (threat) signals. This model provides a new theoretical framework for analyzing the collective transfer of information among groups of fish and other organisms. A version of this work has been previously published (Chicoli et al., 2014).

6.2 Experimental design

The experiment was a multi-way design with two within-subjects variables (flow condition and looming speed) and one between-subjects variable (social context). Both flow condition and social context had two levels: flow present (7 cm^{-s}) or flow absent (0 cm^{-s}) and solitary (1 individual) or social (group of 8), respectively.

To assess the probability of startle response, fish were exposed to blank trials (no stimulus) and five different looming speeds (20, 40, 80, 160 and 320 cm^{-s}). Different loom speeds were used so that stimulus-response functions could be generated.

Both blank and stimulus trials of varying loom speeds were presented randomly with inter-stimulus intervals ranging from 3 to 10 min. Eight replicates of solitary and grouped individuals were presented twice with each stimulus in both the flow and no-flow conditions in a repeated-measures, counter-balanced blocked design (half of the replicates were exposed to the flow condition first and the other half exposed to the no-flow condition first). Before the start of each trial, I measured the water temperature of the experimental tank to ensure that the temperatures did not deviate from the home tank or change over time by more than 2° C. Fish were then transferred from the holding tank to the experimental tank using a plastic-lined net, which provided a cushion of water around the fish, in order to minimize stress and possible damage to the lateral line system. Trials were conducted during the day between 09:00 and 17:00 on two consecutive days with one day of tests in flow and the other in no-flow. Each replicate was tested at the same time of day to help avoid potential confounds from order and time-of-day effects.

I automated the experiments using custom scripts in Linux (OpenSuse version 11.2) and Matlab to create movies of the stimulus presentation as well as a 30 min

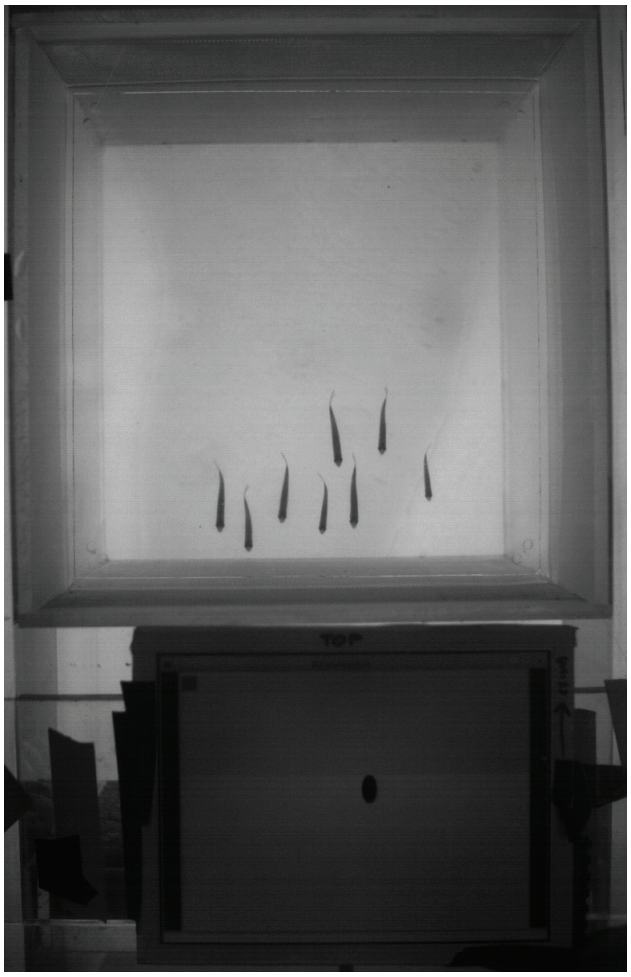

Figure 6.1: Experimental arena depicted working area, and verification screen, showing a stimulus. The side of the screen where the black square is located is the side where the stimulus is being shown.

acclimation period. During habituation and inter-trial intervals, the monitors displayed blank white screens. The stimulus movie was played on VLC media player (videolan.org) at 60 fps from a single Linux computer with an extended desktop display. This display was split three ways by a multi-monitor adapter (Dell Multi-

monitor hub adapter, DP-to-DVI, 64XHK) to the left and right side monitors, as well as to a small verification screen (Figure 6.1). (The verification screen displayed movies being shown on either screen, with a black square in either the upper-left or upper-right corner corresponding to the active monitor.) To coordinate data capture with the timing of stimulus presentation, the camera was triggered through a data acquisition board (National Instruments USB-6525, http://www.ni.com), via a five-volt signal to a video-capture module connected to the camera (Midas 2.0 AD2M Module for auto-download/auto-reset/auto-triggering, http://xcitex.com). I recorded behavior was recorded for 8 s, which is the maximum recording time of the camera hardware. However, this is enough time to capture startle responses, even taking into consideration the variability in latency and duration (Meager et al., 2006).

6.3 Experimental approach

6.3.1 Experimental set-up

I carried out these experiments at Bowling Green State University in the laboratory of Dr. Sheryl Coombs. The flow tank there was a rectangular, plexiglass channel (154 × 28 × 35 cm) filled to a depth of 25 cm (Figure 6.2) and similar in design to that described by (Vogel and Labarbera, 1978). I tested fish in the cen-

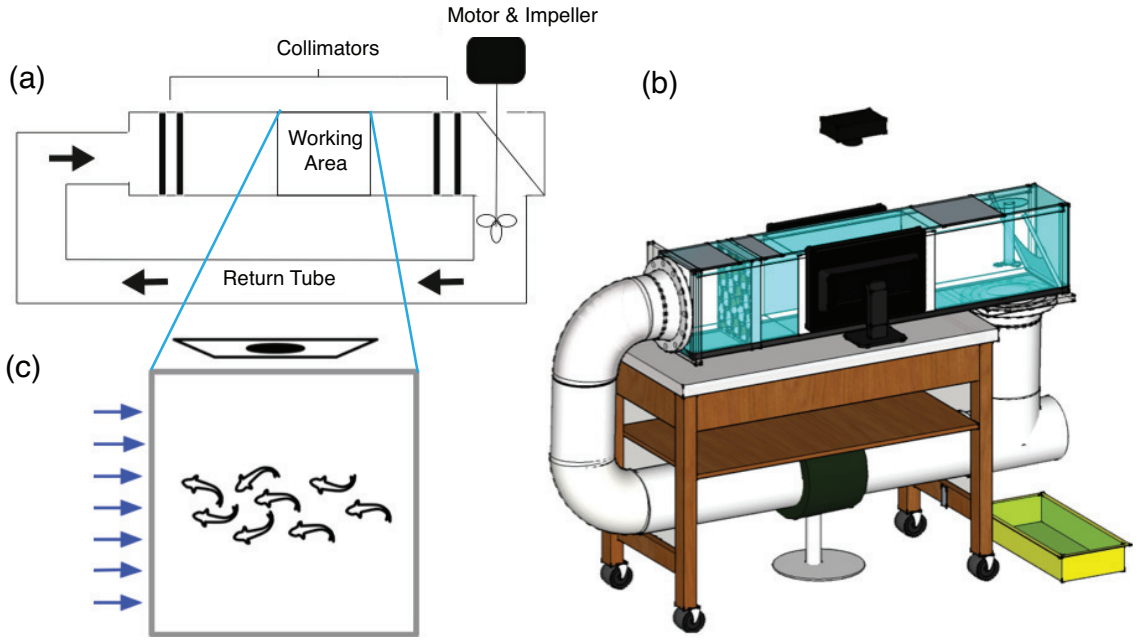

Figure 6.2: (a) Schematic of the flow tank (adapted from (Vogel and Labarbera, 1978). An impeller drives water through a return tube. The collimators reduce turbulence and fish were tested in the 25.4 × 25.4 cm working area. The working area is backlit with evenly distributed fluorescent lighting. (b) Top view of the working area during a flow trial. Arrows illustrate the direction of flow. (c) Three-dimensional illustration of the flow tank with overhead mounted camera, connected to a computer outside the experimental room. Stimuli are presented to either side of the tank by the computer monitors attached to a computer that generates the stimulus movies (Chicoli et al., 2014).

tre of the flow tank in a removable compartment with dimensions of equal length (25 × 25 cm) to avoid possible directional bias. Water in the flow tank was circulated through a 20.32 cm (8 in.) polyvinyl chloride return pipe via a 12.7 cm (5 in.) aluminum impeller blade attached to a chem-stirrer (IKA Laborteknik RW 20DZM http://www.ika.com). Water circulation was facilitated with a baffle placed at the

downstream end of the tank. Turbulence created by the chem-stirrers was reduced with two coarse collimators consisting of plastic egg crates (3 cm thick with 1 cm pores) placed at the upstream and downstream end of the flow tank. Additionally, a fine collimator composed of drinking straws (3 cm in length) was located between the upstream coarse collimator and the working compartment. The flow tank had been calibrated using dye to create a curve for converting impeller speed (rpm) to flow velocity (cm^{-s}). The flow speed used (7 cm^{-s} or 468 revolutions per minute) corresponds to two body lengths per second (BL^{-s}). Although flow speeds normally encountered by giant danio in the wild are not well characterized, this speed is sufficient to evoke rheotactic behavior and was probably well within the range of flow speeds encountered in their natural habitats (McClure et al., 2006).

Two 43 cm liquid crystal display (LCD) monitors (Dell P170S, 60 Hz) were placed on each side of the flow tank's working area for stimulus display. An additional 20 cm monitor (Accele Electronics, Inc. Accelevision 20 cm LCD module LCD3LVGA, http://www.iatft.com) was placed outside the working area, for verification of the stimulus display. A dorsal view of the fish were recorded at 400 fps using a high-speed camera (Itronx DRS Data and Lightning RDT high-speed camera, http://www.itronx.com), with a spatial resolution of 1280 × 1024 pixels. The working area was backlit with a 34-watt bulb diffused 1/4 stop by an optical diffuser

to provide uniform, upwelling light within the tank.

6.3.2 Stimulus design

A looming stimulus is a two dimensional image of an approaching object. A definitive characteristic of a looming stimulus is that as collision becomes imminent, both angular size and speed grow non-linearly with time, while time to collision decreases linearly with time. For two dimensional stimuli, the time to collision is defined as the moment when the angular size $\theta(t)$ subtended by the silhouette on the retina reaches 180° (Gibson, 1958). (Note here that θ refers to angular size of the image subtended on the retina to coincide with previous literature. However, throughout the dissertation, θ will refer to the heading of a fish). The looming image may also collide with the eye-plane of the observer, and in that case the calculations are termed time to passage, and are based on relative change of angle between the object and the observer line of sight.

Looming stimuli consisted of a computer-generated series of black-on-white disks that increased in size to give the appearance of a constant approach velocity Dill (1974) until they reached a maximum size of 15 cm, and positioned so that the entire stimulus was present on the monitor. Five stimuli with various approach speeds (20, 40, 80, 160 and 320 cm^{-s}) were generated in Matlab (2007, R2007a Mathworks,

Natick, MA, USA, http://www.mathworks.com). The stimulus speeds fall within the range of swimming speeds of the giant danios' natural predators (Shahnawaz et al., 2010).

6.3.3 Statistical analysis

Statistical analysis was performed in the stats package in R (version 2.14). General linear mixed models (GLMM) for binomial response assessed how well the factors of flow condition, group size and stimulus speed predicted the frequency of startle responses. Groups were included in the model as a random factor. Differences in vector strength between flow and no-flow were compared using Wilcoxon rank tests. Rayleigh tests (Batschelet, 1981) were used to determine whether the phase order parameter distributions differed significantly from random. An equality of variance F-test was used to assess differences in school structure between flow and no-flow, in both the x and y directions. For all statistical tests, significance level was set to $P<0.05$.

6.3.4 Model of information transmission

The probabilistic model predicts how information flows through a network (see Section 2.6 and Chapter 5) and gives insight into the experimental results, even

though the interaction network and interaction probability P^{int} cannot be measured directly from the experimental data. Thus, the experimental data was fit to the model to assess where the results lie in the model parameter space, as well as to compare differences in information transmission between flow and no-flow trials.

In order to fit the model to the data, a fast probabilistic optimization technique known as simulated annealing (Aarts, E. H. L., Korst, J. H.M.&van Laarhoven, 2003) was applied. This method mimics the physical process of gradually cooling a physical material to decrease defects, effectively minimizing the system energy (the cost function). By occasionally accepting points that raise the cost function, this algorithm avoids being trapped in local minima in early iterations and is able to explore globally for better solutions. The cost function in this case was the average mean-squared error between the model fit for the cumulative probability distribution of startle responses and the number (1–8) of simulated fish responding over five simulation runs (looped over 20 instances of the data).

The inputs to the simulated annealing algorithm was the position of all the fish from the experimental data at the start of the stimulus, a topology network specifying fish interactions, and a fixed value for the model variable P^{sus}. Let the parameter P^{sus} represent the duration of a startle, and let $P^{sus} = 100$ ms, which is an average duration for a startle response (although startle speeds and durations often

exhibit variability (Eaton et al., 1977)). The model was optimized to find the values of P^{ext} and P^{int} that minimized the cost function. Multiple simulated annealing runs were conducted using a Boltzmann cooling schedule (Aarts, E. H. L., Korst, J. H.M.&van Laarhoven, 2003). Simulated annealing runs were terminated when the cost function did not change beyond a given tolerance.

I investigated several instances of metric and topological distance topologies for neighbor interaction (see Section 2.4).

6.4 Results

6.4.1 Alignment in flow and no flow

I computed the phase order parameter p_θ for groups of fish in flow and no flow. I refer to the magnitude of the phase order parameter during the first time step (frame) as the initial vector strength; the average over all time steps (video frames) of an undisturbed school I refer to as the time-averaged vector strength (Figure 6.3a,b). A two-tailed, paired Wilcoxon signed-rank test indicated that the time-averaged vector strength was significantly higher in the flow condition (Mdn = 0.92, n = 88) than the no-flow condition (Mdn = 0.42, n = 83, Z = -6.97, P<0.001). Moreover, fish headings in flow were not randomly distributed with respect to the upstream direction (mean vector direction = 3°; V test, V = -22.1, P<0.95), whereas those in

no-flow were randomly distributed (mean vector direction = 166°; V test, V = 79.9, P<0.001). Thus, the upstream rheotactic behavior in flow enhances the degree of inter-fish alignment. Nevertheless, the distribution of orientations was significantly non-random in both the flow (Rayleigh test; Z = 78.9, P<0.001) and no-flow group conditions (Rayleigh test; Z = 7.25,P<0.001) suggesting that groups of fish were partially aligned even in the absence of flow due to their inherent schooling behavior.

Since the proclivity of fish to head upstream may have biased the direction from which looming stimuli were received, individual orientation with respect to the stimulus location was measured at the onset of each stimulus trial (Figure 6.3c,d). As expected, fish heading upstream in flow were more frequently oriented at 90° or 270° with respect to the stimulus, given that they were always presented from one of two computer monitors on either side of the tank (Figure 6.3c). In contrast, fish in no-flow were more randomly oriented with respect to the stimulus direction (Figure 6.3d). However, the response frequency of fish to the startle stimulus in the no-flow condition did not appear to depend on stimulus direction; the response probability was uniformly distributed (Rayleigh test; Z = 2.01, P<0.05), binned data with bin spacing of .35 radians). Rayleigh tests could not be carried out on the flow trials, since the flow data had multiple modes, which violates the necessary statistical assumptions.

6.4.2 Neighbor position and school structure

Two-dimensional neighbor distance in BL was calculated for each individual at each time step during stimulus presentation when no fish were startling. I collected data from the start of the stimulus until the first reaction, if one was detected, or until the end of the stimulus presentation. No differences were observed in behavior or position even in the presence of a stimulus, unless a startle response occurred that disturbed the school. A two-tailed, paired Wilcoxon signed-rank test indicated that the nearest-neighbor distance was larger in flow (Mdn = 0.70, n = 88) than in no-flow (Mdn = 0.69, n=83, Z =-2.97, P<0.5). However, the actual size of the difference (0.01 BL, i.e., approximately 3–4 mm) was very small. There was no significant difference found in a measure of density given by the ratio of the distance of first and second nearest neighbors in flow (Mdn = 0.68, n = 88) or no-flow (Mdn = 0.68, n = 83, Z = -0.19, P<0.05). The spread of neighbor position was calculated (Figure 6.4a,b) by creating a two-dimensional histogram and fitting a bivariate Gaussian distribution to the data. The overall shape of the groups in flow was elongated in the crosswise direction, being more oblong (Figure 6.4a) than circular (Figure 6.4b). The shape differences along the transformed x and y axes were tested with an equality of variance test (x direction: F = 1.29; df = 2327 (flow) and df = 2491 (no-flow); P<0.001; y direction: F = 1.11; P<0.05). It was also

observed that fish in the flow condition tended to spend most of their time upstream (Figure 6.4c) whereas fish in the no-flow condition were largely located downstream (Figure 6.4d).

6.4.3 Response probability

No startle responses were observed during the control (blank) trials and, across all conditions, the fastest looming speeds (80, 160 and 320 cm^{s-1}) were all significantly better at predicting startle responses than the 20 cm^{s-1} stimuli (80 cm^{s-1}: Z = 3.39, $P<.001$; 160 cm^{s-1}: Z = 2.93, $P<.003$; 320 cm^{s-1}: Z = 3.4, $P<.001$). In general, the probability that at least one fish responded to the looming stimulus increased as a function of stimulus speed for both solitary and grouped fish in both flow and no-flow conditions (Figure 6.5). In addition, the probability of one fish responding was generally greater in the flow condition (filled symbols) compared to the no-flow (open symbols) condition (Figure 6.5).

A general linear mixed model was run in R, using flow condition, solitary vs. grouped state and stimulus speed in order to predict response probability. Results of this model are summarized in Table 6.1. Only the three highest loom speeds (80, 160 and 320 cm^{s-1}) were used in this analysis to ensure that stimulus levels were detectable across all conditions. The effect of replicate groups was controlled for by

adding it as a random factor in the model. No evidence of interaction between the two factors of flow condition and social context was found (Z = -0.138, P>0.8, AIC = 645.4). Flow and solitary/group states were significant predictors of response frequency (flow: Z = 2.42, P<0.05; group size: Z = 4.21, P<0.001), i.e., the probability of at least one fish responding was greater for grouped compared to solitary fish and in flow compared to no-flow.

6.4.4 Model including social information fits experimental data

Although there was a higher probability of at least one fish responding to each of the $80, 160$ or 320 cm^{s-1} loom stimuli in the flow condition compared to the no-flow condition, the mean number of grouped fish responding in flow (M = 2.65, n = 88) and no flow (M = 2.53, n = 83) did not differ (Mann-Whitney U-test, Z = -0.38, P<0.7). Thus, while there was a higher probability of at least one fish responding in flow compared to no flow, a greater number of fish responded in no flow. This observation indicates higher probabilities of stimulus detection in flow but higher probability of internal information transmission in no flow, as shown in the pooled frequency distributions of the number of fish responding in flow (Figure 6.6a) and no-flow (Figure 6.6b) conditions. A G-test comparing these frequency distributions in flow and no flow indicates that the two distributions are statistically different

(G= 4.44, df = 1, P <0.05). The differences in the number of fish responding can be further distinguished by fitting the frequency distributions with polynomial models to show higher probabilities of one or two fish responding in the flow condition, but lower probabilities of three or more fish responding as compared to the no-flow condition (Figure 6.6c). The flow condition does not appear to have an effect at higher numbers of fish responding (7–8 fish), which may be due to very small sample sizes (in only a few trials did the entire school startle).

Table 6.1: Linear mixed-effects model investigating the effect of stimulus speed, group size and flow condition on response. Replicate groups were controlled for as a random effect

						95% C.I.	
Fixed Effect	Level	Value	S.E.	z-value	P-value	Lower bound	Upper bound
Intercept		-2.2533	0.4102	-5.493	<0.001	-3.0573	-1.4492
Stimulus speed	40	0.63420	0.4089	-1.524	>0.05	0.1677	1.5771
	80	1.4171	0.4169	3.399	<0.001	-0.1784	1.4246
	160	1.2065	.4121	2.928	<0.005	0.5999	2.2343
	320	1.6823	0.4209	3.996	<0.001	0.3988	2.0142
Flow		0.8724	0.3595	2.426	<0.05	0.8574	2.3368
Group size n =8		0.8724	0.3595	2.426	<0.05	0.8574	2.3368
Group:Flow		0.0619	0..5129	-0.138	>0.05	-0.0943	1.0671

Next, the data were fitted to a probabilistic model of startle response that included the affect of socially transmitted information (see Methods). Figure 6.7 shows sample fits of the model outcomes (simulated data) to the experimental data

for the flow (Figure 6.7a) and no-flow (Figure 6.7b) conditions. The shaded regions illustrate the range of typical outputs of the model based on one standard deviation from the mean output. The parameters for the model that best fit the data were optimized using simulated annealing (see Methods). The model values determined by this optimization approach are shown in Figure 6.8, for both nearest-neighbor and proximity-based topologies for flow (black squares) and no flow (open circles). The results indicate that, regardless of the network topology, the probability of detecting an external threat P^{ext} is higher in the flow condition than the no-flow condition, as was seen in the experimental results. However, the model predicts that the probability of detecting and responding to neighboring fish, P^{int} is higher in the no-flow condition than in the flow condition, which could not be observed directly from the experiments. Additionally, the results of the model suggest that P^{ext} does not depend on the interaction topology, whereas P^{int} decreases exponentially as the presumed number of interacting neighbors increases.

6.5 Discussion

To the best of my knowledge, this study is the first to examine school structure, startle response probability, and information transmission in the environmental context of a flow field (Rieucau et al., 2014a). For many species, social interaction

and predator avoidance are important parts of behavioral ecology and several studies have attempted to model and understand how schooling fish might handle predator avoidance (Lemasson et al., 2009; Wood and Ackland, 2007; Zheng et al., 2005). However, these studies lack a key ecological factor (flow) that fishes often experience in their natural habitats. Flow brings with it benefits (e.g., drifting prey) as well as challenges, such as hydrodynamic noise and disruption of positional stability. It was demonstrated that (i) the polarity and two-dimensional shape of grouped fish in the flow condition are altered relative to the no-flow condition such that fish orient upstream while spanning out in a cross-stream direction; (ii) the probability that at least one fish responds to a looming visual stimulus is higher in flow than in no flow; and (iii) the number of fish responding to the looming stimulus is higher in no flow than flow. Furthermore, a computational model of collective startle response was developed that predicted the results; the model indicated that, relative to no flow, flow impairs the transmission of social information in the form of propagated startle responses.

6.5.1 The effect of flow on group formation and polarity

It is well-known that fishes exhibit rheotactic behaviors in the presence of flow (Arnold, 1974; Lyon, 1904). Thus, the finding that the flow condition caused

solitary fish and grouped fish to orient predominantly upstream is not new. The change in the two-dimensional shape of the group in the flow condition, however, is a new finding that may have implications for threat detection in flow, although fish tend to elongate their shape in their direction of travel (Bumann et al., 1997). Given that fish in flow tended to be located further upstream than those in no flow (Figure 6.4), it is possible that the observed cross-stream distribution in flow was the result of a wall effect. That is, the upstream barrier might have prevented fish from moving further upstream, causing them to span out in a cross-stream direction. Although wall effects cannot be ruled out, they seem less likely given that the data analysis excluded all instances in which individuals were less than 1 BL away from the wall. Alternatively, fish may position themselves in order to increase rheotactic performance. Rheotaxis is a robust behavior with many potential benefits, including enhanced detection of prey and energy conservation (Arnold, 1974; Montgomery et al., 1997). Visual (optical-flow) cues appear to be sufficient for rheotaxis under many conditions (reviewed in Arnold (1974)). By positioning themselves laterally to each other, fish may be obtaining enhanced visual cues (about other fish) that would otherwise be absent.

Interestingly, Partridge (1980) showed that ablation of the lateral line affects the structure of saithe *Pollachius virens* schools in a manner that appears to be

similar to the effects of flow observed in this study on group structure of giant danio. That is, lateral-line-impaired satire showed an increase in the frequency of neighbors directly alongside at about 90° compared to control groups (all senses intact) or visually deprived groups. Thus, it is conceivable that the flow conditions of this experiment may have had similar disabling effects on the lateral line. That is, the surrounding ambient flow may have masked the ability of giant danio to detect the flow signals generated by neighboring fish. In this regard, there is both behavioral (Coombs et al., 2001) and physiological evidence (Chagnaud et al., 2007; Englemann et al., 2002) that unidirectional (DC) flow does indeed compromise the ability of the lateral line to detect oscillatory (AC) flows, such as those generated by a swimming fish (Kalmijn, 1988). This general scenario is consistent with the finding that social transmission of information may be greater in no flow than in flow (Figure 6.8).

6.5.2 Startle response probability and information transmission

For both individual and groups of eight fish, the probability of at least one fish responding was higher in flow. This result was somewhat unexpected, given that fish in the flow condition were expending much more energy by swimming into the flow. The simplest explanation is that because the orientations of fish in no-flow were random over time, the stimulus may have been positioned outside the visual field of

the fish (i.e., in the blind zone), thus reducing the overall probability of detection. This is in contrast to the flow condition, where rheotaxis induced by the flow field allowed the stimuli to largely lie within the visual field (Figure 6.3).

Although there was a higher probability of at least one fish responding in the flow condition, results showed lower probabilities of four or more fish responding in flow as compared to the no-flow condition. Explanations as to why fish in the flow condition did not appear to be responding may deal with both detection abilities and response abilities or proclivities. Fish in the flow condition were expending more energy than they would in no flow to swim against the flow and to maintain position so that they were not displaced downstream. The decision to respond to the looming stimulus was thus more costly in flow than in no flow. Thus, it may be possible that fish in flow were detecting signals from their neighbors regarding a threat, but that their threshold criterion for responding was higher. Given that the individual probability of response was higher in flow for solitary fish, an increased threshold for response is an unlikely explanation. Another explanation is that the crosswise distribution of fish into side-by-side positions may have prevented those in the interior of the group from having a direct line of sight to the looming stimuli, partially occluding the vision of fish on the interior of the school. This is also unlikely, given the small working area and the size of the looming stimulus. Finally, flow

signals produced by the movements of neighboring fish were weaker (because fish were further apart and flow signals attenuate very steeply with distance) and/or masked by the ambient flow, making the transmission of hydrodynamic information from one individual to the next more difficult.

Fishes use a variety of sensory modalities to receive information regarding the presence of a threat, including vision (Dill, 1974; Guthrie and Muntz, 1993), olfaction (Ferrari and Chivers, 2006; Mathuru et al., 2012), and lateral line sensing (McHenry et al., 2009; Mirjany et al., 2011). The predatory stimulus used in these experiments was purely visual. While the presence of any unimodal cue may be strong enough to elicit a startle response, the use of multi-modal cues has been shown to improve accuracy in predator detection in the mosquitofish, *Gambusia holbrooki* (Ward et al., 2010). Fish in a school may gain additional visual, hydrodynamic, and olfactory cues from their neighbors that support the presence of a threat, or be in conflict with it (e.g., neighbors not responding to the looming stimulus). Thus, if hydrodynamic and visual cues from neighboring individuals are masked or occluded in the flow condition, fish may have a lower probability to respond. This may be true even for giant danio detecting the looming stimulus if they additionally receive conflicting information from other fish that do not respond.

After the publication version of this study came out (Chicoli et al., 2014),

another study performed startle response experiments in the Hawaiian stream goby in flow and no-flow conditions (Diamond, 2015). These researchers also found effects of flow on the probability of responding, and came to a similar conclusion that flow may mask important hydrodynamic signals important for responding to a threat directly, or for responding to neighbor cues.

6.5.3 Variability of startle responses

Experimental analysis of the response latencies of startling fishes have provided evidence that certain fish are more likely to respond to a potential threat than others (Marras and Domenici, 2013). The wide range of response latencies (207 - 907 ms) measured in this study is indicative of substantial variability in responsiveness. Whether or not this variability can be attributed to individual performance differences or stimulus differences (e.g. the orientation of the fish re: the looming stimulus) is uncertain. The tracking software used in this study does not allow the maintenance of individual identities to be preserved between trials, so it was not possible to determine whether some individuals were more likely to respond than others. Moreover, the latency measures cannot distinguish between responses elicited by the looming stimulus itself vs. those that may have been elicited by the startle responses of other fish. Indeed, several startle responses occurred after the looming stimulus

ended, suggesting the possibility of the latter.

From a mechanistic perspective, it is interesting to note that the range of response latencies measured in this study is very similar to that measured from freely swimming goldfish *C. auratus* in response to looming stimuli shown to be effective at eliciting Mauthner cell-mediated escape responses (Preuss et al., 2006). A site of multisensory integration, the Mauthner cell relies on the sum of all of its sensory inputs in order to reach the threshold level for firing and initiating the escape response (Korn and Faber, 2005). Whereas the visual input is indirectly relayed to the Mauthner cell from a visual processing region of the midbrain, both lateral line and auditory inputs are direct from the sense organs themselves (Zottoli et al., 1995). Thus, the transmission of information from the visual system is slower and delayed relative to that from mechanosensory systems. Moreover, different senses in different species have different influences on the probability of M cell firing (Canfield and Rose, 1996). In goldfish, for example, visual or auditory inputs alone are capable of exciting the M cell, whereas lateral line inputs may bias the probability of a response but only in combination with inputs from other senses. Thus, at least some of the variability in startle response latency may be explained in terms of the relative contributions of different senses, which in this study involves vision (via the looming stimulus), as well as the potential for auditory and lateral line senses (via the movements of

nearby startled fish).

6.5.4 Modeling information transmission

While social information cannot be measured directly from the experimental data, it can be hypothesized that the increased number of fish responding in the no-flow condition may be a result of increased information transmission. To test this hypothesis, a probabilistic model to predict the number of fish startling was developed. Fitting the model to the data indicated increased internal information transmission P^{int} in the no-flow case for all topologies. The results of the model agree with the prediction that social information transmission is higher in the no-flow condition. It is not well understood how fishes transmit information between individuals, or what interaction networks fishes are using. For the analysis here, both neighbor-based and proximity-based topologies were used to determine when fish might be interacting with each other. Fishes may also use a sensory-based topology (Strandburg-Peshkin et al., 2013), however the results of the model presented are robust to network topology, in that for all network topologies simulated, the same pattern of values P^{int} higher in no flow and P^{ext} higher in flow was observed (Figure 6.8).

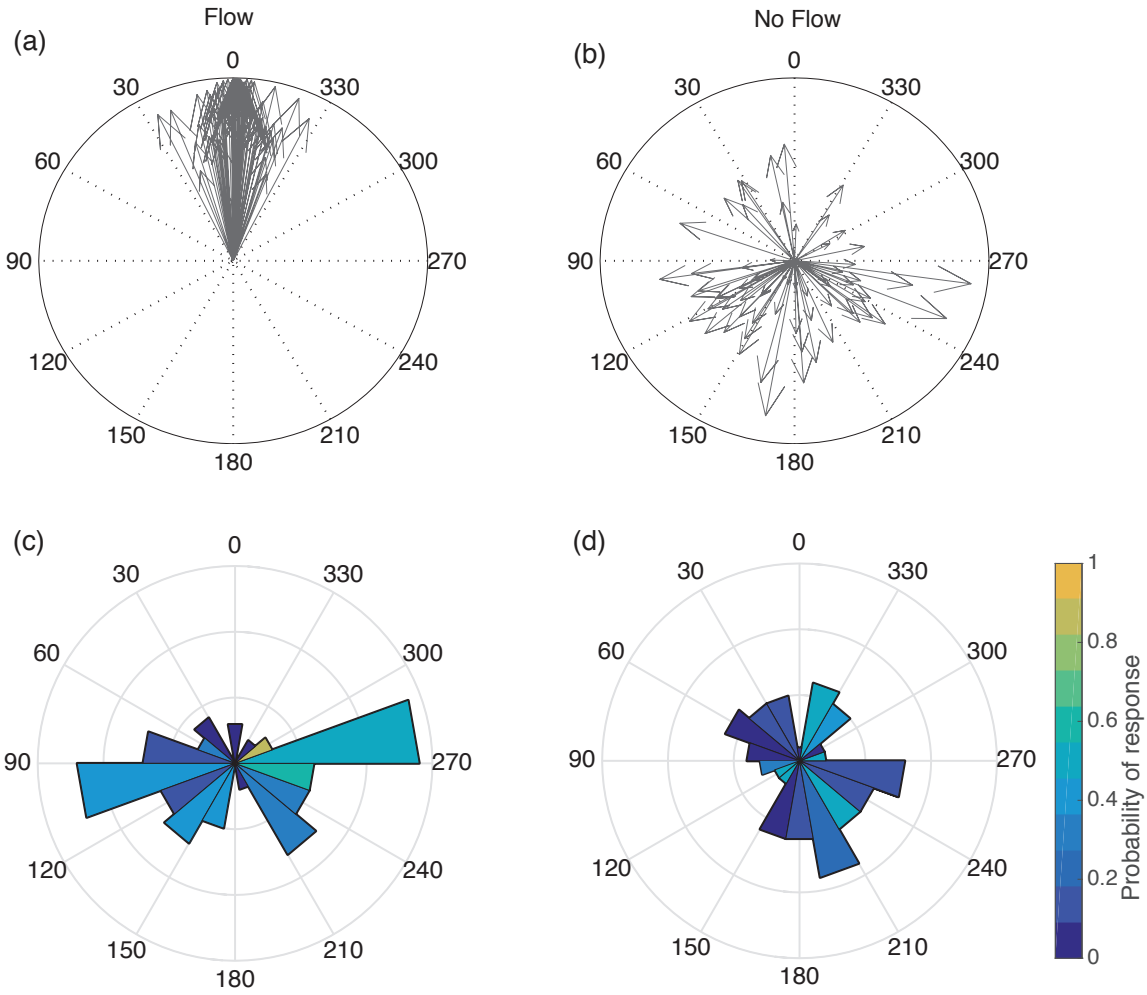

Figure 6.3: Time-averaged vector strength and direction associated with groups of eight fish in flow (a) and no-flow (b), where the orientation 0° is in the upstream direction. Vector strength ranges from 0 to 1, with 1 being the highest degree of alignment. Probability of individuals in solitary trials responding to a looming stimulus according to orientation with respect to the stimulus location at stimulus onset in flow (c) and no-flow (d), where the orientation 0° is in the stimulus direction. Length of rose histogram indicates the frequency with which individual fish are oriented in any given direction at the time of stimulus onset, whereas the color indicates the probability of a response, computed from the total number of solitary trials (Chicoli et al., 2014).

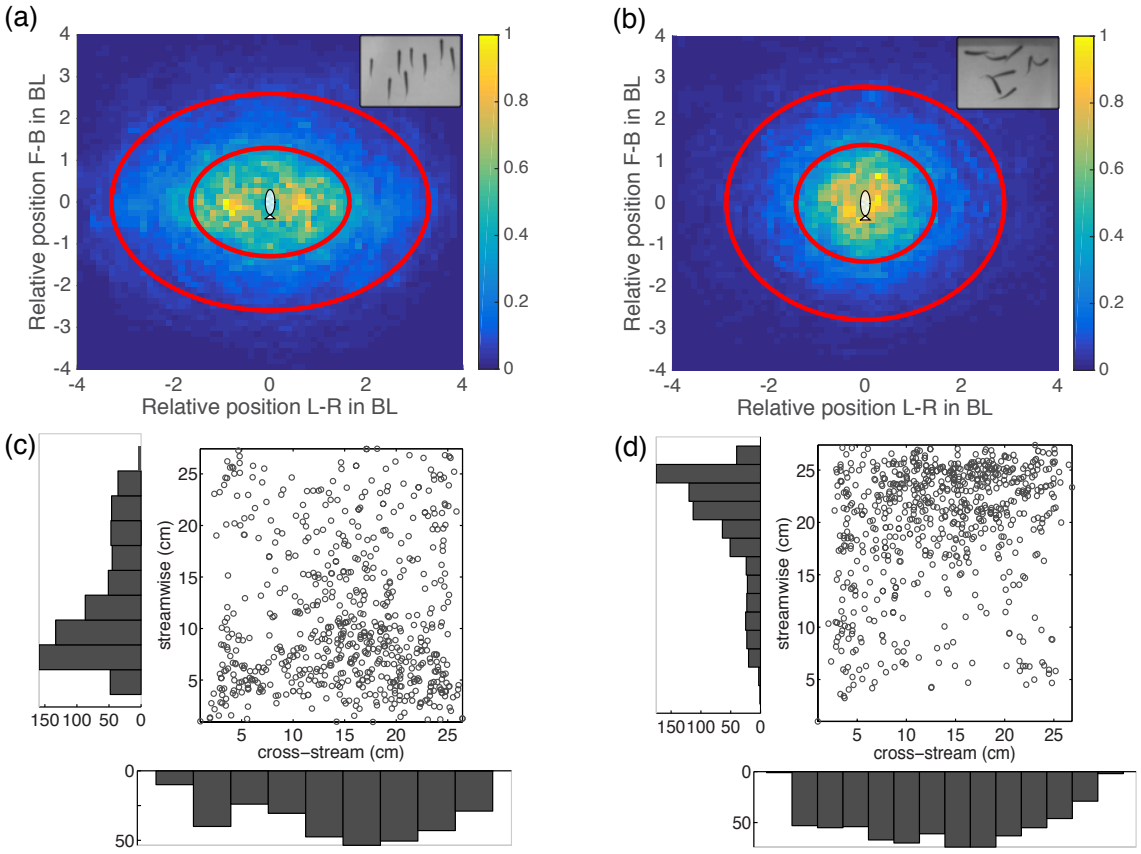

Figure 6.4: (a) and (b) Probability density functions of relative position. Color corresponds to the number of points in each bin, normalized by the bin with the most points. Red circles are one standard deviation away from the mean, white circles are the average nearest-neighbor distance. (a) flow (b) no-flow; (c) and (d) Scatterplots and corresponding histograms of individual position in the tank (Chicoli et al., 2014).

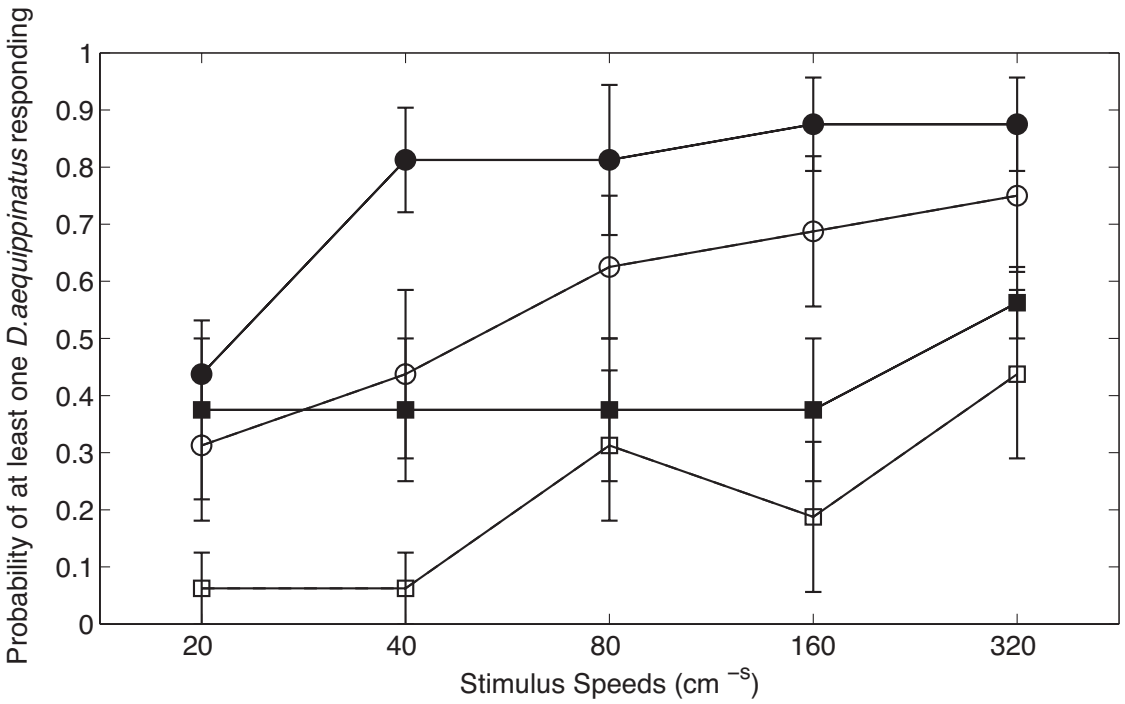

Figure 6.5: Response probabilities of at least one fish startling at various stimulus speeds in individual (squares) and groups of eight fish (circles). Error bars are the standard error of the mean. There were eight blocks for each condition and, within each of the blocks, each stimulus was shown twice (16 measurements per point). Filled black symbols indicate flow and empty symbols indicate no-flow (Chicoli et al., 2014).

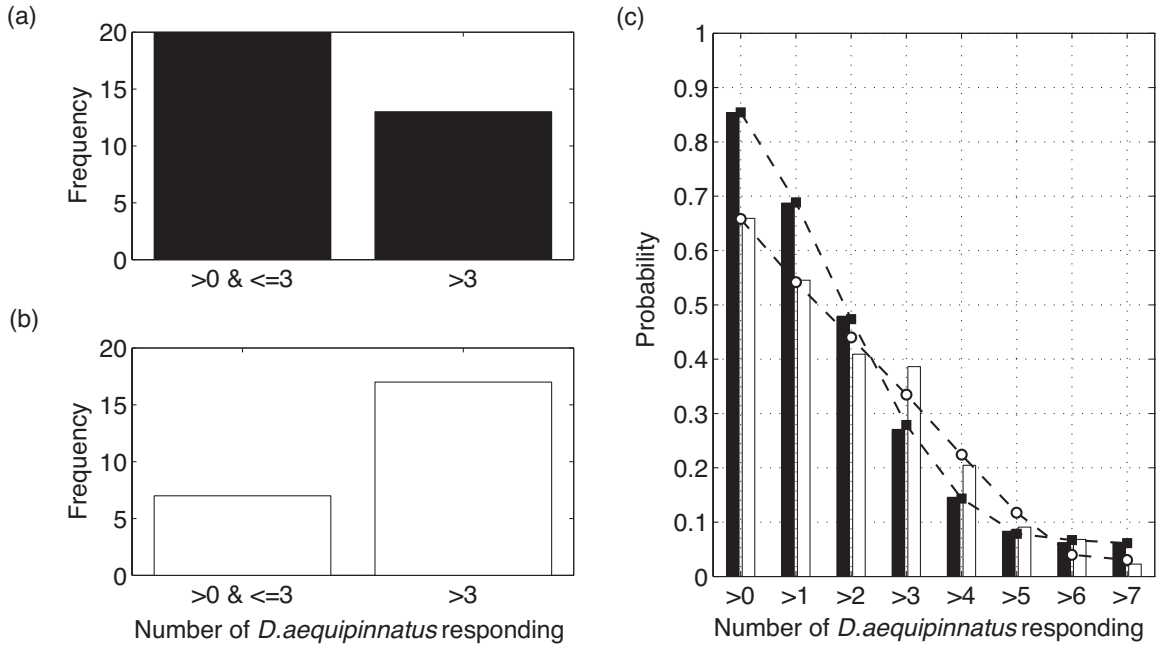

Figure 6.6: Frequency distributions of the number of giant danio responding in (a) flow and (b) no flow. (c) Cumulative probability distribution of the number of fish responding (black squares are flow trials, empty squares are no-flow trials). Dotted lines with corresponding black and empty symbols for flow and no-flow, respectively, show polynomial model fits to the distributions

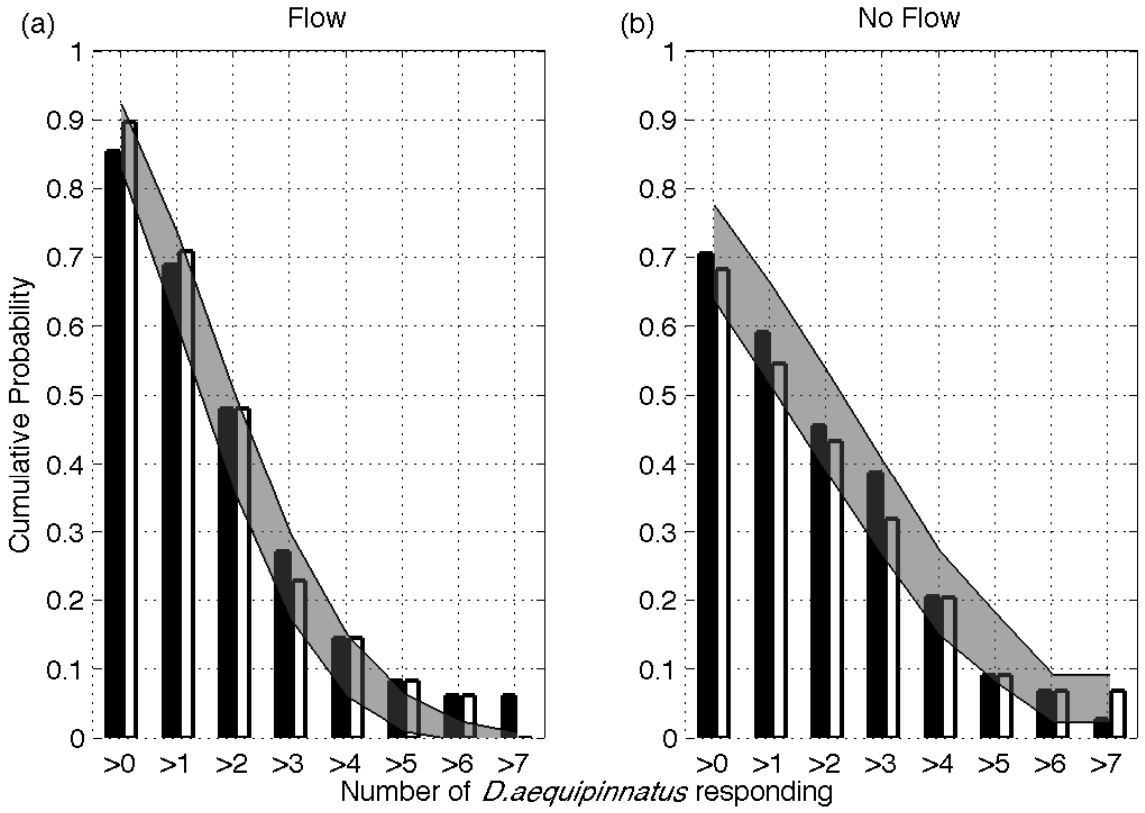

Figure 6.7: Example of an optimal fit of a probabilistic model (empty bars, simulated data) to the cumulative probability distributions of a certain number of giant danio startling in (a) flow and (b) no flow (black squares, experimental data; grey shaded region, mean fit of the model $\pm s.d.$

.

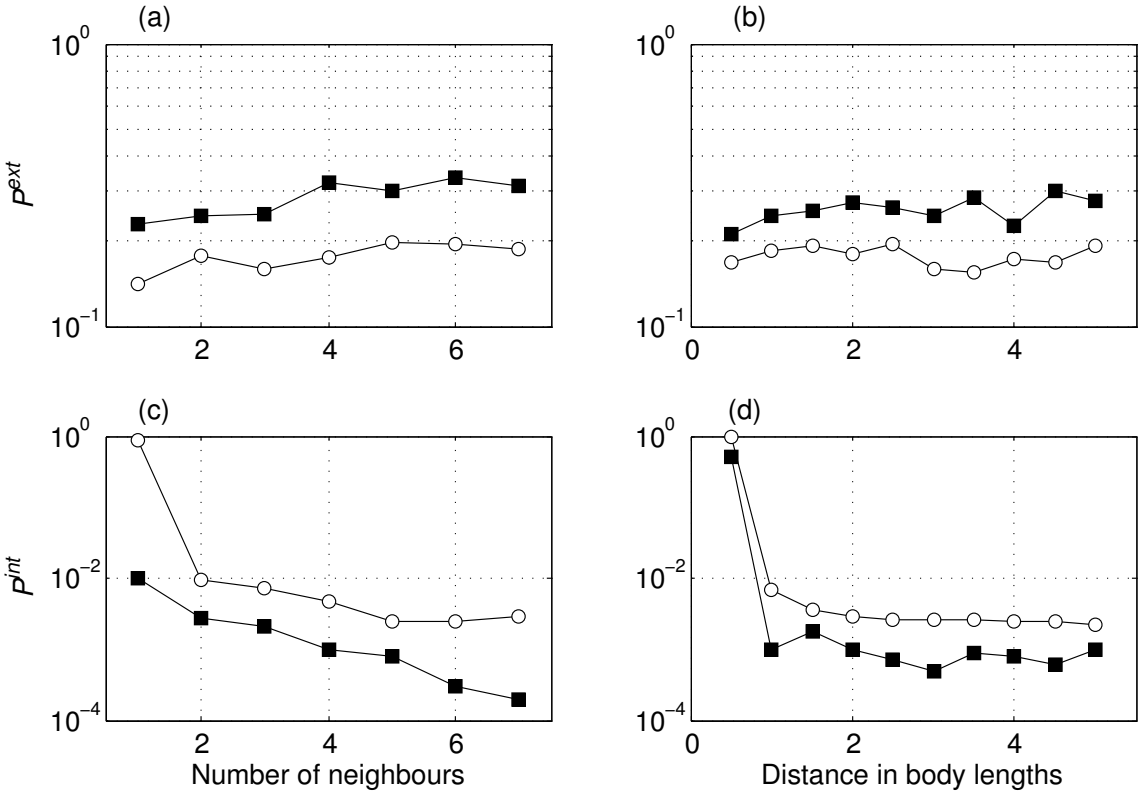

Figure 6.8: Semi-log plots of optimized values of P^{ext} (the probability of directly responding to a threat) and P^{int} (the probability of responding to cues from other individuals) in flow (black squares) and no flow (white circles) for (a) and (c) n-neighbor and (b) and (d) metric distance topologies. In the n-neighbour topology, fish receive signals from the closest n number of neighbors, whereas in the metric distance topology networks, fish receive signals from all neighboring fish within a given radial distance.

Summary and Conclusions

Chapter 7: Conclusions and suggestions for future work

Each of the preceding chapters detailing original work in this thesis has a section discussing the results and implications of that work. This chapter provides a brief summary of the contributions of this dissertation, and suggest potential areas for ongoing and future work.

7.1 Summary of contributions

This dissertation couples mathematical modeling and behavioral experiments to investigate the effects of group size and different flow conditions on both rheotaxis, and startle response behaviors in fish.

Chapter 3 develops a noisy synchronization model that includes a reference direction, and unbounded sensory noise in order to model rheotaxis behavior. The reference direction corresponds to the direction of the flow, and the noise term is placed on each agent's ability to sense either the relative flow direction, or the relative direction of its neighbors. Varying the noise term in the model manipulates the

accuracy of information each agent receives. This model allows for comparisons of behavior and performance given different sensory conditions and certainty about the environment. When applied to rheotaxis, the model indicates that orientation to the reference direction can occur (albeit weakly) even in the presence of sensory noise, and predicts that group size only improves behavior in high sensory noise conditions (i.e., when an individual agent has high uncertainty regarding the direction of the flow).

Chapter 4 tests the predictions of Chapter 3 by varying group size and flow speed and quantifying the resulting rheotactic and shoaling behaviors in giant danio. I find that small groups from 2–32 giant danio do not show any effect of group size on rheotaxis, corresponding to the results from the synchronization model when there is no neighbor interaction. However, there was a decrease in NND as group size increased, which is predicted by a limited interaction topology model of aggregation.

Chapter 5 proposes a probabilistic model of information transmission in groups, and couples this model with the coupled oscillator dynamics of Chapter 3. To the best of my knowledge, this is the first application of SIR models commonly used in computer science and epidemiology to the investigation of the spread of information transmission in collective groups of animals (other than humans). This model specifies probabilities for responding to an external threat, being startled by neighbors,

and remaining in a startled state. The probability model alone yields results that resemble a cellular automata, with two explicit states: startled and non-startled. When paired with the coupled oscillator system behavioral dynamics can be evaluated. Importantly, the parameter space of the oscillator model was categorized into non-shoaling, facultative shoaling and obligate shoaling types, based on the level of alignment of group members. The model predicts faster spreading of the startle response in previously polarized groups (obligatory shoalers), and slower, but more accurate responses in facultative shoalers.

Chapter 6 experimentally investigates the effects of flow on shoal structure, response probability, and information transmission in groups of eight giant danio compared to solitary fish. There was a greater probability of at least one fish responding in the flow condition, but the responses did not spread as far or as often through the group indicating lower probability of information transmission. The cumulative probability distributions of the number of fish responding was fit to the model in Chapter 5. The lateral line has been shown behaviorally and physiologically to be masked by bulk flow (Englemann et al., 2002). Given this, it is possible that the lateral line was masked by the flow in the flow condition, resulting in the decrease in information transmission. This suggests that the lateral line may be important for information transmission in shoals.

7.2 Ongoing work and suggestions for future research

7.2.1 Synchronization in noisy environments

The noisy synchronization model in Chapter 3 demonstrated that weak consensus could still occur in the presence of unbounded noise. It would be interesting to perform numerical and analytical solutions when these assumptions do not hold. The most immediate next step would be to run the model under different interaction topologies, other than all-to-all, that are more biologically plausible. Additionally, more complex graph types may be introduced to test the limits of synchronization. (Skardal et al., 2015) previously investigated frustrated and heterogenous networks in which synchronization is likely to erode. By characterizing the conditions that lead to the erosion of synchronization, it may be possible to mitigate these effects in both natural and unmanned systems. In biology, hypotheses may be generated when a synchronized group of fish or other animals may dissolve or break apart. For future research involving group dynamics, it may also be interesting to explore associative memory models (in addition to heterogenous populations), such that agents can dynamically associate with the other connected agents. It has been well established that fish can recognize and preferentially associate with certain individuals (Krause et al., 2000). Thus a dynamic, heterogenous graph may be formed based on a mem-

ory of which agents have better knowledge of a reference direction. (The reference direction in Chapter 3 represented the direction of the flow, however the reference direction can be generalized to any direction of interest such as when foraging or navigating).

7.2.2 Group size benefits

Chapter 4 laid out several potential hypotheses for why there was no observed group size effect on rheotaxis. Namely, that giant danio may be attending to either a limited interaction topology, may only be attending to neighbor positional information, or that the task was overly simple. It would be interesting to explore these hypotheses further. One potential experiment to potentially increase the difficulty of the task would be to perform a similar experiment, but have a conflicting signal, for example optical flow cues, in the opposing direction of a flow field.

The studies in this dissertation involve small groups of fish or agents. Experimentally, a maximum of 32 fish were tested, and in simulation, a maximum group size of 128 was used. However, in large marine shoals, the number of individuals in the group can be in the thousands. It is quite likely that many of the experimental laboratory results may not apply to these vary large groups (Rieucau et al., 2014a).

7.2.3 Information transmission in groups

The studies in this dissertation suggest that the lateral line may be an important factor in rapid information transmission for shoals of fish. Experiments could be performed that explicitly test this hypothesis. One way to do this would be to temporarily block the lateral line (LL) with gentamicin or cobalt chloride. While these methods have been show to kill the hair cells of the lateral line with some probability (Brown et al., 2011; Trump et al., 2010), although verification of hair cell death with dye (DASPEI) is necessary. LL+ and LL- may then be exposed to a visual stimulus. The results from the lateral line ablated groups could then be compared to the group behavior in uniform flow. The prediction would be that if the flow masks the lateral line of fish, then fish behavior in flow would be similar to that of lateral line ablated groups.

In the startle response experiment in this dissertation, it is impossible to know which fish were startled by the looming stimulus and which were startled by the reaction of neighboring fish. Because a visual looming stimulus was used with free-swimming fish, there is no way to be sure if or when a given individual fish detected the stimuli. In order to investigate information transmission with regards to startle response in fish, a few 'informed' fish should be startled while the other naïve fish would then only be responding to cues from neighboring fish. One method to do

this might be to classically condition fish to startle in response to a conditioned stimulus. In classical, or Pavlovian conditioning, an unconditioned stimulus (US) which naturally elicits a response, is paired with a neutral stimulus, that under normal conditions would not elicit any response. When the neutral stimulus is paired with the unconditioned stimulus, they can become associated, causing the previously neutral stimulus to now elicit a reaction. The previously neutral stimulus becomes the conditioned stimulus (CS). Fish have been trained using positive reward to expect food following the flashing of a light (Stienessen and Parrish, 2013). Aversive training techniques can also be used (Soria et al., 1993), and may include showing images of predators, exposing the fish to aversive chemical stimuli or using shock. Thus, it may be possible to train fish to elicit an escape response (not necessarily M-cell driven) and assess how the response spreads throughout a group.

Another potential way to experimentally measure information transmission through a group might be possible to implant a small pizoelectric device to slightly shock a single fish (or several) but it may be quite difficult to be sure the electricity does not propagate through the water.

7.2.4 Modeling multi-sensory integration

Multi-sensory integration and the sensory cues used for group behaviors was an important aspect in the behavioral studies conducted in this dissertation, but as not a focus of modeling work. It would be of interest in future studies to attempt to model the role of different sensory input on group behavior to better make predictions or tease apart the relative roles of different visual, hydrodynamic or chemical cues used in information transmission in groups. One way to do this in the startle model may be to incorporate known information about the neurobiology of the startle response of fish into the model. As started in Chapter 6, the Mauthner cell is an integrate and fire neuron, that receives multi-modal input. Rather than having a two-state model of startles and non-startled, the model may be modified to capture the integration of information, perhaps such that a certain threshold must be met before an agent enters into the startled state.

Additionally, there are neurobiological effects of the environment that can influence the excitability of the M-cell through neuromodulation. Additionally, a previous stimulus may also cause a decrease in the probability of response, called pre-pulse inhibition (Medan and Preuss, 2011, 2014). Both of these mechanisms play a role in M-cell responses, and can be included in the startle model by adding additional states.

7.2.5 Individual differences

Another topic of interest is individual differences. While I have largely considered shoals of fish as being composed of homogenous individuals, there is huge variation among individual fish in terms of behavior (Burns et al., 2012; Krause et al., 2000; Marras and Domenici, 2013; Nakayama et al., 2012). Fish may be individually marked with a visual implant elastomer) (VIE) (Northwest Marine Technology Co.) to analyze the behavior of each fish individually over trials, and new advances in computer vision harness the power of machine learning to detect individuals even if the individual is lost from frames or occluded (Perez-Escudero et al., 2014). Investigating individual differences influences information transmission and decision-making in groups is a topic that is deserving of more research. From a theoretical perspective, heterogenous groups can also be simulated in the models discussed in this dissertation.

Appendix A

Table A.1: Linear mixed effects model investigating the effect of group size, flow speed and flow direction on external disagreement (ED). Replicate groups were controlled for as a random effect.

Scaled residuals				
Min	1Q	Median	3Q	Max
-2.7733	-0.5327	-0.0171	0.5297	4.1099
Random effects				
Groups	Name	Variance	Std.Dev	Corr.
idx	Intercept	9.714e-04	0.0311	
	flow speed	4.240e-06	0.00201	-0.27
	increasing	1.209e-03	0.0347	0.66,0.90
Residual		3.168e-03	0.0562	
Fixed effects				
		Estimate	Std. Error	t-value
Intercept		0.4669	0.0172	**27.117**
group size		0.0007	0.0010	0.760
flow speed		-0.038	0.0032	**-11.648**
increasing		0.0417	0.0231	1.808
group size: flow speed		-0.0001	0.0001	-0.554
group size:increasing		-0.0003	0.0013	-0.232
flow speed:increasing		-0.0104	0.0045	**-2.277**
group size:flow speed:increasing		0.0003	0.0002	1.277

Table A.2: Linear mixed effects model investigating the effect of group size, flow speed and flow direction on internal disagreement (ID). Replicate groups were controlled for as a random effect.

Scaled residuals				
Min	1Q	Median	3Q	Max
-3.3788	-0.5261	0.0039	0.5852	3.6728
Random effects				
Groups	Name	Variance	Std.Dev	Corr.
idx	Intercept	4.734e-04	0.0217	
	flow speed	4.998e-07	0.0007	0.10
	increasing	1.168e-04	0.0108	0.55,0.89
Residual		3.199e-03	0.0565	
Fixed effects				
		Estimate	Std. Error	t-value
Intercept		0.4753	0.0159	**29.897**
group size		-0.0017	0.0009	1.799
flow speed		-0.0289	0.0032	**-8.942**
increasing		0.0066	0.020	0.319
group size: flow speed		-0.0001	0.0001	-0.826
group size:increasing		0.0004	0.0012	0.327
flow speed:increasing		-0.0055	0.0046	-1.212
group size:flow speed:increasing		0.0002	0.0002	0.839

Table A.3: Linear mixed effects model investigating the effect of group size, flow speed and flow direction on standard deviation in x-position (cross-stream). Replicate groups were controlled for as a random effect.

Scaled residuals				
Min	1Q	Median	3Q	Max
-2.1664	-0.5980	-0.1323	0.4455	4.2518
Random effects				
Groups	Name	Variance	Std.Dev	Corr.
idx	Intercept	0.06407	0.2531	
	flow speed	0.0260	0.1612	0.41
	increasing	0.2362	0.4760	0.04,-0.90
Residual		1.6448	1.282	
Fixed effects				
		Estimate	Std. Error	t-value
Intercept		2.784	0.3370	**8.261**
group size		0.1144	0.0204	**5.609**
flow speed		0.1304	0.0881	1.480
increasing		0.9019	0.4914	1.835
group size: flow speed		-0.0045	0.0053	-0.854
group size:increasing		-0.0307	0.0295	-1.038
flow speed:increasing		-0.2607	0.1044	**-2.497**
group size:flow speed:increasing		0.0089	0.0062	1.418

Table A.4: Linear mixed effects model investigating the effect of group size, flow speed and flow direction on the standard deviation in y-position (stream-wise). Replicate groups were controlled for as a random effect.

Scaled residuals				
Min	1Q	Median	3Q	Max
-2.1478	-0.6618	-0.1255	0.4255	3.6915
Random effects				
Groups	Name	Variance	Std.Dev	Corr.
idx	Intercept	1.416e+00	1.1900	
	flow speed	1.1514e-08	0.000	-1.00
	increasing	3.572e-01	.597636	-0.55,0.55
Residual		3..191e+00	1.7863	
Fixed effects				
		Estimate	Std. Error	t-value
Intercept		3.937	0.5820	**6.765**
group size		0.2163	0.0352	**6.140**
flow speed		0.1397	0.1022	1.368
increasing		1.3396	0.06776	1.977
group size: flow speed		-0.0150	0.0062	**-2.429**
group size:increasing		-0.1212	0.0407	**-2.971**
flow speed:increasing		-0.4250	0.1454	**-2.922**
group size:flow speed:increasing		0.0267	0.0087	**3.045**

Table A.5: Linear mixed effects model investigating the effect of group size, flow speed and flow direction on NND. Replicate groups were controlled for as a random effect.

Scaled residuals				
Min	1Q	Median	3Q	Max
-2.9523	-0.4041	-0.0430	0.2750	5.3543
Random effects				
Groups	Name	Variance	Std.Dev	Corr.
idx	Intercept	1.2524	1.1191	
	flow speed	0.0026	0.051	-1.00
	increasing	0.0349	0.1867	1.00
Residual		4.4253	2.1037	
Fixed effects				
		Estimate	Std. Error	t-value
Intercept		5.514	0.636	**8.669**
group size		-0.0891	0.0385	**-2.316**
flow speed		0.1642	0.1213	1.353
increasing		2.050	0.7711	2.658
group size: flow speed		-0.0104	0.0073	-1.415
group size:increasing		-0.1114	0.0464	**-2.401**
flow speed:increasing		-0.5846	0.1712	**-3.413**
group size:flow speed:increasing		0.0286	0.0103	**2.769**

Table A.6: Linear mixed effects model investigating the effect of group size, flow speed and flow direction on shoal density. Replicate groups were controlled for as a random effect.

Scaled residuals				
Min	1Q	Median	3Q	Max
-4.0024	-0.2490	-0.0810	0.1258	7.6848
Random effects				
Groups	Name	Variance	Std.Dev	Corr.
idx	Intercept	0.0027	0.0517	
	flow speed	0.0026	0.051	.01
	increasing	0.0349	0.1867	0.34,-0.94
Residual		0.0042	0.0650	
Fixed effects				
		Estimate	Std. Error	t-value
Intercept		6.872e-02	2.284e-02	**3.008**
group size		-7.753e-05	1.383e-03	-0.056
flow speed		4.817e-03	4.797e-03	1.004
increasing		2.292e-02	2.585e-02	0.887
group size: flow speed		-9.090e-05	2.904e-04	-0.313
group size:increasing		-1.240e-04	1.556e-03	-0.080
flow speed:increasing		-4.360e-03	5.299e-03	-0.823
group size:flow speed:increasing		7.752e-05	3.195e-04	0.243

Table A.7: Linear mixed effects model investigating the effect of group size, flow speed and flow direction on shoal area. Replicate groups were controlled for as a random effect.

Scaled residuals				
Min	1Q	Median	3Q	Max
-3.2662	-0.3833	-0.0462	0.1936	4.9202
Random effects				
Groups	Name	Variance	Std.Dev	Corr.
idx	Intercept	3272.643	57.207	
	flow speed	2.881	1.697	-0.1
	increasing	147.865	12.160	0.02,-1.00
Residual		3987.622	63.148	
Fixed effects				
		Estimate	Std. Error	t-value
Intercept		-35.4281	23.6873	-1.496
group size		19.8910	1.4341	**13.870**
flow speed		3.6188	3.6495	0.992
increasing		25.8551	23.3801	1.106
group size: flow speed		0.2210	2.904e-04	**-3.242**
group size:increasing		-4.8562	1.4022	**-3.451**
flow speed:increasing		-6.7547	5.1422	-1.314
group size:flow speed:increasing		0.8003	0.3102	**2.580**

Bibliography

Aarts, E. H. L., Korst, J. H.M.&van Laarhoven, P. J. M. (2003). Simulated annealing. In Aarts, E. & Lenstra, J. K., editor, *Local Search in Combinatorial Optimization*, pages 91–120. Princeton, NJ: Princeton University Press.

Aoki, I. (1980). An analysis of the schooling behavior of fish: Internal organization and communication process. *Bulletin of the Ocean Research Institute -University of Tokyo*, 12.

Arnold, G. P. (1974). Rheotriopism in fishes. *Biological Reviews*, 49(4):515–576.

Axelson, B. E., Nilssen, T. A., Fossum, P., Kvamme, C., and Nøttestad, L. (2001). Pretty patterns but a simple strategy: predator–prey interactions between juvenile herring and Atlantic puffins observed with multibeam sonar. *Canadian Journal of Zoology*, 79(9):1586–1596.

Bak-Coleman, J., Court, A., Paley, D., and Coombs, S. (2013). The spatiotemporal dynamics of rheotactic behavior depends on flow speed and available sensory information. *The Journal of Experimental Biology*, 216(Pt 21):4011–24.

Baker, C. F. and Montgomery, J. C. (1999). Lateral line mediated rheotaxis in the Antarctic fish Pagothenia borchgrevinki. *Polar Biology*, 21(5):305–309.

Ballerini, M., Cabibbo, N., Candelier, R., Cavagna, A., Cisbani, E., Giardina, I., Lecomte, V., Orlandi, A., Parisi, G., Procaccini, A., Viale, M., Zdravkovic, V., and Others (2008). Interaction ruling animal collective behavior depends on topological rather than metric distance: Evidence from a field study. *Proc. Nat. Acad. Sciences*, 105(4):1232–1237.

Bartolini, T., Butail, S., and Porfiri, M. (2015). Temperature influences sociality and activity of freshwater fish. *Environmental Biology of Fishes*, 98(3):825–832.

Batschelet, E. (1981). *Circular statistics in biology.* Academic Press, New York, NY, USA.

Berdahl, A., Torney, C. J., Ioannou, C. C., Faria, J. J., and Couzin, I. D. (2013). Emergent sensing of complex environments by mobile animal groups. *Science (New York, N.Y.)*, 339(6119):574–6.

Bertram, B. C. R. (1978). Living in groups: predators and prey. *Behavioural ecology*, pages 64–96.

Billings, L., Spears, W. M., and Schwartz, I. B. (2002). A unified prediction of computer virus spread in connected networks. *Physics Letters A*, 297(3-4):261–266.

Biro, D., Nagy, M., Akos, Z., and Vicsek, T. (2010). Hierarchical group dynamics in pigeon flocks. *Nature*, 464(7290):890–3.

Bonabeau, E. (2007). Understanding and Managing Complexity Risk. *MITSloan Management Review*, (48416):1–9.

Bouguet, J. (2008). Camera calibration toolbox for Matlab.

Breder, C. (1959). Studies on the social groupings of fishes. *Bulletin of the Museum of American Natural History*, 117:393–482.

Breder, C. M. (1967). On the survival value of fish schools. *Zoologica*, 52(2):25–40.

Brown, A. D., Mussen, T. D., Sisneros, J. A., and Coffin, A. B. (2011). Reevaluating the use of aminoglycoside antibiotics in behavioral studies of the lateral line. *Hearing research*, 272(1-2):1–4.

Bumann, D., Krause, J., and Rubenstein, D. (1997). Mortality risk of spatial positions in animal groups: The danger of being in the front. *Behavior*, 134:1063–1076.

Burns, A. L. J., Herbert-Read, J. E., Morrell, L. J., and Ward, A. J. W. (2012). Consistency of leadership in shoals of mosquitofish (Gambusia holbrooki) in novel and in familiar environments. *PloS one*, 7(5):e36567.

Butail, S. and Paley, D. A. (2011). Three-dimensional reconstruction of the fast-start swimming kinematics of densely schooling fish. *J. Royal Society Interface*, 9(66):77–88.

Cahn, P. H., Atz, E. H., and Shaw, E. (1965). Lateral-line nerve differentiation correlated with schooling in the marine fish Menidia. *American zoologist*, 5:142.

Cahn, P. H. and Phyllis, C. (1972). Sensory factors in the side-to-side spacing and positional orientation of the tuna, Euthynnus affinis, during schooling. *Fishery bulletin*, 70(I):197–204.

Camazine, S., Deneubourg, J.-L., Franks, R., Sneyd, J., Theraulaz, G., and Bonabeau, E. (2001). *Self-organization in biological systems*. Princeton University Press.

Canfield, J. G. and Rose, G. J. (1996). Hierarchical Sensory Guidance of Mauthner-Mediated Escape Responses in Goldfish (*Carassius auratus*) and Cichlids (*Haplochromis burtoni*) (Part 2 of 2). *Brain, Behavior, and Evolution*, 48(3):147–156.

Canonge, S., Deneubourg, J. L., and Sempo, G. (2011). Group living enhances individual resources discrimination: The use of public information by cockroaches to assess shelter quality. *PLoS ONE*, 6(6):e19748.

Carton, A. G. and Montgomery, J. C. (2003). Evidence of a rheotactic component in the odour search behaviour of freshwater eels. *Journal of Fish Biology*, 62:501–516.

Chagnaud, B., Bleckmann, H., and Hofmann, M. (2007). Karman vortex street detection by the lateral line. *Journal of comparative physiology. A, Neuroethology, sensory, neural, and behavioral physiology*, 193(7):753–763.

Chapman, M. R. and Kramer, D. L. (1996). Guarded resources: the effect of intruder number on the tactics and success of defenders and intruders. *Animal Behavior*, 52(1):83–94.

Chicoli, A., Bak-Coleman, J., Coombs, S., and Paley, D. A. (2015). Rheotaxis performance increases with group size in a coupled phase model with sensory noise. *European Physical Journal: Special Topics*, 224(17-18):3233–3244.

Chicoli, A., Butail, S., Lun, Y., Bak-Coleman, J., Coombs, S., and Paley, D. A. (2014). The effects of flow on schooling *Devario aequipinnatus*: school structure, startle response and information transmission. *Journal of Fish Biology*, 84(5):1401–1421.

Codling, E. A., Pitchford, J. W., and Simpson, S. D. (2007). Group navigation and the "many-wrongs principle" in models of animal movement. *Ecology*, 88(7):1864–70.

Conradt, L., Krause, J., Couzin, I. D., and Roper, T. J. (2009). Leading According to Need in Self-Organizing Groups. *The American Naturalist*, 173(3).

Conradt, L. and Roper, T. J. (2003). Group decision-making in animals. *Nature*, 421(6919):155–8.

Conradt, L. and Roper, T. J. (2005). Consensus decision making in animals. *Trends in ecology & evolution*, 20(8):449–56.

Cont, R. and Bouchaud, J.-P. (1997). Herd behavior and aggregate fluctuations in financial markets. *Macroeconomic Dynamics*, page 29.

Coombs, S., Braun, C. B., and Donovan, B. (2001). The Orienting Response of Lake Michigan Mottled Sculpin is Mediated by Canal Neuromasts. *Journal of Experimental Biology*, 204(2):337–348.

Couzin, I. D., Ioannou, C. C., Demirel, G., Gross, T., Torney, C. J., Hartnett, A., Conradt, L., Levin, S. A., and Leonard, N. E. (2011). Uninformed individuals promote democratic consensus in animal groups. *Science (New York, N.Y.)*, 334(6062):1578–80.

Couzin, I. D., Ioannou, C. C., Demirel, G., Gross, T., Torney, C. J., Hartnett, A., Conradt, L., Levin, S. A., and Leonard, N. E. (2012). Democratic Consensus in Animal Groups. *Science*, 1578(2011).

Couzin, I. D., James, R., Mawdsley, D., Croft, D. P., and Krause, J. (2006). Social Organization and Information Transfer in Schooling Fishes. In Krause, J., Brown, C., and Laland, K. N., editors, *Fish Cognition and Behavior*, chapter 9, pages 166–187. Blackwell Publishing.

Couzin, I. D., Krause, J., Franks, N. R., and Levin, S. A. (2005). Effective leadership and decision-making in animal groups on the move. *Nature*, 433(February):513–516.

Couzin, I. D., Krause, J., James, R., Ruxton, G. D., and Franks, N. R. (2002). Collective memory and spatial sorting in animal groups. *Journal of Theoretical Biology*, 218(1):1–11.

de Berg, M., van Kreveld, M., Overmars, M., and Schwarzkopf, O. (2008). Computational Geometry.

Delcourt, J. and Poncin, P. (2012). Shoals and schools: back to the heuristic definitions and quantitative references. *Reviews in Fish Biology and Fisheries*.

Deneubourg, J. L. and Gross, S. (1989). Collective Patterns and Decision Making. *Ethology, Ecology, and Evolution*, (1):295–311.

Diamond, K. (2015). *Environmental effects on fish escape responses: Impact of flow on the escape performance of the Hawaiian stream goby* Sicyopterus stimpsoni . PhD thesis, Clemson University.

Dijkgraaf, S. (1963). The functioning and significance of the lateral-line organs. *Biological Reviews*, 38(1):51–105.

Dill, L. M. (1974). The escape response of the zebra danio (*Brachydanio rerio*) II. The effect of experience. *Animal Behaviour*, 22(3):711–722.

Domenici, P. and Blake, R. W. (1997). The kinematics and performance of fish fast-start swimming. *Journal of Experimental Biology*, 200(8):1165–1178.

Domenici, P., Lefrançois, C., and Shingles, A. (2007). Hypoxia and the antipredator behaviours of fishes. *Philosophical transactions of the Royal Society of London. Series B, Biological Sciences*, 362(1487):2105–2121.

Eaton, R. C., Bombardieri, R. A., and Meyer, D. L. (1977). The Mauthner-initiated startle response in teleost fish. *Journal of Experimental Biology*, 66(1):65.

Eaton, R. C. and Emberley, D. S. (1991). How stimulus direction determines the trajectory of the Mauthner-initiated escape response in a teleost fish. *The Journal of Experimental Biology*, 161(1):469–87.

Eaton, R. C., Lee, R. K. K., and Foreman, M. B. (2001). The Mauthner cell and other identified neurons of the brainstem escape network of fish. *Progress in Neurobiology*, 63(4):467 – 485.

Engelmann, J., Hanke, W., and Bleckmann, H. (2002). Lateral line reception in still- and running water. *Journal of Comparative Physiology A: Neuroethology, Sensory, Neural, and Behavioral Physiology*, 188(7):513–526.

Englemann, J., Hanke, W., and Bleckmann, H. (2002). Lateral line reception in still- and running wate. In *Journal of Comparative Physiology A*, volume 188, pages 513–526.

Epps, B. P. and Techet, A. H. (2007). Impulse generated during unsteady maneuvering of swimming fish. *Experiments in Fluids*, 43(5):691–700.

Fang, F. (2003). Phylogenetic analysis of the Asian cyprinid genus Danio (Teleostei, Cyprinidae). *Copeia*, 2003(4):714–728.

Faria, J. J., Codling, E. A., Dyer, J. R., Trillmich, F., and Krause, J. (2009). Navigation in human crowds; testing the many-wrongs principle. *Animal Behaviour*, 78(3):587–591.

Ferrari, M. C. O. and Chivers, D. P. (2006). Learning threat-sensitive predator avoidance: how do fathead minnows incorporate conflicting information? *Animal Behaviour*, 71(1):19–26.

Fisher, N. I. (1993). *Statistical analysis of circular data*. Cambridge University Press.

Flock, A. (1965). Electron microscopic and electrophysiological studies on the lateral line canal organ. *Acta Otolaryngology*, 199:1–90.

Fukami, Y., Furukawa, T., and Asada, Y. (1965). Excitability Changes of the Mauthner Cell During Collateral Inhibition. *The Journal of General Physiology*, 48:581–600.

Galton, F. (1907). The wisdom of crowds. *Nature*, 75(1949):450–451.

Gardiner, J. M. and Atema, J. (2007). Sharks need the lateral line to locate odor sources: rheotaxis and eddychemotaxis. *The Journal of Experimental Biology*, 210:1925–1934.

Gerlotto, F., Bertrand, S., Bez, N., and Gutierrez, M. (2006). Waves of agitation inside anchovy schools observed with multibeam sonar: a way to transmit information in response to predation. *ICES Journal of Marine Science*, 63(8):1405–1417.

Gibson, J. J. (1958). Visually Controlled Locomotion and Visual Orientation in Animals.

Giraldeau, L., Valone, T. J., and Templeton, J. J. (2002). Potential disadvantages of using socially acquired information. *Philosophical transactions of the Royal Society of London. Series B, Biological sciences*, 357(1427):1559–66.

Godin, J.-G. J., Classon, L. J., and Abrahams, M. V. (1988). Group Vigilance and Shoal Size in a Small Characin Fish. *Behaviour*, 104(1):29–40.

Godin, J.-G. J. and Morgan, M. J. (1985). Predator Avoidance and School Size in a Cyprinodontid Fish, the Banded Killifish (Fundulus diaphanus Lesueur). *Behavioral Ecology and Sociobiology*, 16(2):105–110.

Goodwin, R. A., Politano, M., Garvin, J. W., Nestler, J. M., Hay, D., Anderson, J. J., Weber, L. J., Dimperio, E., Smith, D. L., and Timko, M. (2014). Fish navigation of large dams emerges from their modulation of flow field experience. *Proceedings of the National Academy of Sciences of the United States of America*, 111(14):5277–82.

Goulet, J., Engelmann, J., Chagnaud, B. P., Franosch, J.-M. P., Suttner, M. D., and Van Hemmen, J. L. (2008). Object localization through the lateral line system of fish: theory and experiment. *Journal of comparative physiology. A, Neuroethology, sensory, neural, and behavioral physiology*, 194(1):1–17.

Grünbaum, D. (1998). Schooling as a strategy for taxis in a noisy environment. *Evolutionary Ecology*, 12:503–522.

Gueron, S., Levin, S. A., and Rubenstein, D. I. (1996). The Dynamics of Herds: From Individuals to Aggregations. *Journal of Theoretical Biology*, 182(1):85–98.

Guthrie, D. M. and Muntz, W. R. A. (1993). The role of vision in fish behaviour. In Pitcher, T. J., editor, *Behaviour of Teleost Fishes*, pages 89–128. Chapman Hall, London.

Hamilton, W. D. (1971). Geometry for the selfish herd. *Journal of Theoretical Biology*, 31(2):295–311.

Hammar, L., Andersson, S., Eggertsen, L., Haglund, J., Gullström, M., Ehnberg, J., and Molander, S. (2013). Hydrokinetic turbine effects on fish swimming behaviour. *PloS one*, 8(12):e84141.

Helbing, D., Buzna, L., Johansson, A., and Werner, T. (2005). Self-Organized Pedestrian Crowd Dynamics: Experiments, Simulations, and Design Solutions. *Transportation Science*, 39(1):1–24.

Hemelrijk, C. K., Reid, D. A. P., Hildenbrandt, H., and Padding, J. T. (2014). The increased efficiency of fish swimming in a school. *Fish and Fisheries*, 8(8).

Herbert-read, J. E., Perna, A., Mann, R. P., Schaerf, T. M., Sumpter, D. J. T., and Ward, A. J. W. (2011). Inferring the rules of interaction of shoaling fish. *Proceedings of the National Academy of Sciences*, 108(46):18726–18731.

Higham, D. J. (2001). An Algorithmic Introduction to Numerical Simulation of Stochastic Differential Equations. *SIAM Review*, 43(3):525–546.

Hockley, F. A., Wilson, C. A. M. E., Brew, A., and Cable, J. (2014). Fish responses to flow velocity and turbulence in relation to size, sex and parasite load. *Journal of the Royal Society, Interface*, 11:20130814.

Huang, M. and Manton, J. H. (2009). Coordination and consensus of networked agents with noisy measurements: Stochastic algorithms and asymptotic behavior. *SIAM Journal on Control and Optimization*, 48(1):134–161.

Huse, G., Railsback, S., and Feronö, A. (2002). Modelling changes in migration pattern of herring: collective behaviour and numerical domination. *Journal of Fish Biology*, 60(3):571–582.

Inada, Y. and Kawachi, K. (2002). Order and Flexibility in the Motion of Fish Schools. *Journal of Theoretical Biology*, 214(3):371–387.

Ioannou, C., Tosh, C., Neville, L., and Krause, J. (2007). The confusion effect from neural networks to reduced predation risk. *Behavioral Ecology*, 19(1):126–130.

Ioannou, C. C., Guttal, V., and Couzin, I. D. (2012). Predatory fish select for coordination in prey. *Science*, 337(6099):1212–1215.

Jadbabaie, A., Lin, J., and Morse, A. S. (2003). Coordination of groups of mobile autonomous agents using nearest neighbor rules. *IEEE Trans. on Automatic Control*, 48(6):988–1001.

Jeanson, R. and JeanLouis Deneubourg (2007). Conspecific Attraction and Shelter Selection in Gregarious Insects. *The American Naturalist*, 170(1):47–58.

Kalmijn, A. J. (1988). Hydrodynamic and acoustic field detection. *Sensory biology of aquatic animals*, pages 83–130.

Kanter, M. J. and Coombs, S. (2003). Rheotaxis and prey detection in uniform currents by Lake Michigan mottled sculpin (*Cottus bairdi*). *Journal of Experimental Biology*, 206(Pt 1):59–70.

Kermack, W. O. and McKendrick, A. G. (1927). A Contribution to the Mathematical Theory of Epidemics. *Proceedings of the Royal Society of London. Series A115*, 115(772):700–721.

Kleerekoper, H. (1978). Chemoreception and its interaction with flow and light perception in the locomotion and orientation of some elasmobranchs. In Hodgsen, E. and Matthewson, R., editors, *Sensory Biology of Sharks, Skates and Rays*, pages 269–329. CRC Press, Inc., Arlington, VA.

Kolpas, A., Busch, M., Li, H., Couzin, I. D., Petzold, L., and Moehlis, J. (2013). How the spatial position of individuals affects their influence on swarms: a numerical comparison of two popular swarm dynamics models. *PloS one*, 8(3):e58525.

Korn, H. and Faber, D. S. (2005). The Mauthner cell half a century later: a neurobiological model for decision-making? *Neuron*, 47(1):13–28.

Krakauer, D. (1995). Groups confuse predators by exploiting perceptual bottlenecks: a connectionist model of the confusion effect. *Behavioral Ecology and Sociobiology*, 36:421–429.

Krause, J., Hoare, D., Krause, S., Hemelrijk, C. K., and Rubenstein, D. I. (2000). Leadership in fish shoals. *Science*.

Krause, J. and Ruxton, G. D. (2002). *Living in Groups*. Oxford University Press.

Kuramoto, Y. (1975). Self-entrainment of a population of coupled non-linear oscillators. In *International symposium on mathematical problems in theoretical physics*, pages 420–422. Springer.

Kurvers, R. H. J. M., Wolf, M., and Krause, J. (2013). Humans use social information to adjust their quorum thresholds adaptively in a simulated predator detection experiment. *Behavioral Ecology and Sociobiology*, 68(3):449–456.

Lachlan, R., Crooks, L., and Laland, K. (1998). Who follows whom? Shoaling preferences and social learning of foraging information in guppies. *Animal behaviour*, 56(1):181–90.

Lagor, F. D., Devries, L. D., Waychoff, K. M., and Paley, D. A. (2013). Bio-inspired Flow Sensing and Control : Autonomous Rheotaxis Using Distributed Pressure Measurements. *Journal of Unmanned System Technology Bio-inspired*, 1:78–88.

Laland, K. N., Atton, N., and Webster, M. M. (2011). From fish to fashion: experimental and theoretical insights into the evolution of culture. *Philosophical transactions of the Royal Society of London. Series B, Biological sciences*, 366(1567):958–968.

Laland, K. N. and Williams, K. (1998). Social transmission of maladaptive information in the guppy. *Behavioral Ecology*, 9(5):493–499.

Landeau, L. and Terborgh, J. (1986). Oddity and the confusion effect in predation. *Animal Behaviour*, 34:1372–1380.

Lauder, G. V. and Madden, P. G. A. (2006). Learning from fish: kinematics and experimental hydrodynamics for roboticists. *International Journal of Automation and Computing*, 3(4):325–335.

Lee, S.-H., Pak, H. K., and Chon, T.-S. (2006). Dynamics of prey-flock escaping behavior in response to predator's attack. *Journal of Theoretical Biology*, 240(2):250–9.

Lemasson, B. H., Anderson, J. J., and Goodwin, R. A. (2009). Collective motion in animal groups from a neurobiological perspective: the adaptive benefits of dynamic sensory loads and selective attention. *Journal of Theoretical Biology*, 261(4):501–10.

Leonard, N. E., Shen, T., Nabet, B., Scardovi, L., Couzin, I. D., and Levin, S. A. (2012). Decision versus compromise for animal groups in motion. *Proceedings of the National Academy of Sciences of the United States of America*, 109(1):227–32.

Liao, J. C. and Cotel, A. J. (2005). Effects of turbulence on fish swimming in aquaculture. In Palstra, A. P. and Planas, J. V., editors, *Swimming Physiology of Fish*, chapter 5. Springer Verlag.

Lima, S. L. (1995). Collective detection of predatory attack by social foragers: fraught with ambiguity? *Animal Behaviour*, 50:1097–1108.

Lupandin, A. I. (2005). Effect of Flow Turbulence on Swimming Speed of Fish. *Biology Bulletin*, 32(5):461–466.

Lyon, E. P. (1904). On rheotropism. I.Rheotropism in fishes. *American Journal of Physiology–Legacy Content*, 12(2):149.

Magurran, A. E. (1986). The development of shoaling behaviour in the European minnow, *Phoxinus phoxinus*. *Journal of fish biology*, 29(sA):159–169.

Magurran, A. E. and Higham, A. (1988). Information transfer across fish shoals under predation threat. *Ethology*, 78(78):153–158.

Mahmoudian, N. and Paley, D. A. (2011). Synchronization on the N-torus with noisy measurements. *Proceedings of the 2011 American Control Conference*, pages 4014–4019.

Mardia, K. and Jupp, P. (1999). *Directional Statistics*. Wiley.

Marras, S. and Domenici, P. (2013). Schooling fish under attack are not all equal: some lead, others follow. *PloS one*, 8(6):e65784.

Mathuru, A. S., Kibat, C., Cheong, W. F., Shui, G., Wenk, M. R., and Friedrich, R. W. (2012). Report Chondroitin Fragments Are Odorants that Trigger Fear Behavior in Fish. *Current Biology*, 22:1–7.

Mayden, R., Tang, K. L., Conway, K., Freyhof, J., Chamberlain, S., Haskins, M., Schneider, L., Sudkamp, M., Wood, R. M., Agnew, M., Bufalino, A., Sulaiman, Z., Masaki, M., Saitoh, K., and He, S. (2006). Phylogenetic relationships of *Danio* within the order Cypriniformes: a framework for comparative and evolutionary studies of a model species. *Journal of Zxperimental zoology. Part B, Molecular and Developmental Evolution*, 306(1):1–7.

McClure, M. M., McIntyre, P. B., and McCune, A. R. (2006). Notes on the natural diet and habitat of eight danionin fishes, including the zebrafish Danio rerio. *Journal of Fish Biology*, 69(2):553–570.

McHenry, M. J., Feitl, K. E., Strother, J. A., and Van Trump, W. J. (2009). Larval zebrafish rapidly sense the water flow of a predator's strike. *Biology Letters*, 5(4):477–9.

McNamara, J. M. and Houston, A. I. (1992). Evolutionarily stable levels of vigilance as a function of group size. *Animal Behaviour*, 43:641–658.

Meager, J. J., Domenici, P., Shingles, A., and Utne-Palm, A. C. (2006). Escape responses in juvenile Atlantic cod *Gadus morhua* L.: The effects of turbidity and predator speed. *Journal of Experimental Biology*, 209(20):4174.

Medan, V. and Preuss, T. (2011). Dopaminergic-induced changes in Mauthner cell excitability disrupt prepulse inhibition in the startle circuit of goldfish. *Journal of neurophysiology*, 106(6):3195–204.

Medan, V. and Preuss, T. (2014). The Mauthner-cell circuit of fish as a model system for startle plasticity. *Journal of Physiology Paris*, 108(2-3):129–140.

Mesbahi, M. and Egerstedt, M. (2010). *Graph Theoretic Methods in Multiagent Networks*. Princeton University Press, New Jersey.

Milinski, M. (1984). A predator's cost of overcoming the confusion-effect of awarming prey. *Animal Behaviour*, 32:1157–1162.

Miller, N. Y. and Gerlai, R. (2008). Oscillations in shoal cohesion in zebrafish (*Danio rerio*). *Behavioral Brain Research*, 193(1):148–151.

Miller, R. C. (1922). The significance of the gregarious habit. *Ecology*, 3:122–126.

Mirabet, V., Fréon, P., and Lett, C. (2008). Factors Affecting Information Transfer from Knowledgeable to Naive Individuals in Groups. Behavioral Ecology and Sociobiology,. *Behavioral Ecology and Sociobiology*, 63(2):159–171.

Mirjany, M., Faber, D. S., and Preuss, T. (2011). Characteristics of the anterior lateral line nerve input to the Mauthner cell. *Journal of Experimental Biology*, 214:3368–3377.

Montgomery, J., Coombs, S., and Halstead, M. (1995). Biology of the mechanosensory lateral line in fishes. *Reviews in Fish Biology and Fisheries*, 5(4):399–416.

Montgomery, J. C., Baker, C. F., and Carton, A. G. (1997). The lateral line can mediate rheotaxis in fish. *Nature*, 389(6654):960–963.

Moreau, L. (2005). Stability of multiagent systems with time-dependent comunication links. *IEEE Trans. on Automatic Control*, 50(2):169–182.

Nabet, B., Leonard, N. E., Couzin, I. D., and Levin, S. A. (2009). Dynamics of Decision Making in Animal Group Motion. *Journal of Nonlinear Science*, 19:399–435.

Nakayama, S., Harcourt, J. L., Johnstone, R. a., and Manica, A. (2012). Initiative, personality and leadership in pairs of foraging fish. *PloS one*, 7(5):e36606.

Neumeister, H., Szabo, T. M., and Preuss, T. (2008). Behavioral characterization of sensorimotor gating in the goldfish startle response. *Journal of Neurophysiology*, 99:1493–1502.

Neumeister, H., Whitaker, K. W., Hofmann, H. A., and Preuss, T. (2010). Social and Ecological Regulation of a Decision-Making Circuit. *Journal of neurophysiology*, 104:3180 –3188.

Ojima, D. and Iwata, M. (2009). Central administration of growth hormone-releasing hormone triggers downstream movement and schooling behavior of chum salmon (Oncorhynchus keta) fry in an artificial stream. *Comparative Biochemistry and Physiology - A Molecular and Integrative Physiology*, 152(3):293–298.

Olszewski, J., Haehnel, M., Taguchi, M., and Liao, J. C. (2012). Zebrafish Larvae Exhibit Rheotaxis and Can Escape a Continuous Suction Source Using Their Lateral Line. *PloS one*, 7(5).

Orlean, A. (1995). Bayesian interactions and collective dynamics of opinion: Herd behavior and mimetic contagion. *Journal of Economic Behavior & Organization*, 28(2):257–274.

Paley, D. A., Leonard, N. E., Sepulchre, R., Grunbaum, D., and Parrish, J. K. (2007). Oscillator models and collective motion: Spatial patterns in the dynamics of engineered and biological networks. *IEEE Control Systems Magazine*, 27(4):89–105.

Papoulis, A. and Pillai, S. (2002). *Probability, Random Variables and Stochastic Processes*. McGraw Hill Publishing Company.

Partridge, B. L. (1980). The Three-Dimensional Structure of Fish Schools. *Behavioral Ecology and Sociobiology*, 6(4):277–288.

Partridge, B. L. and Pitcher, T. J. (1980). The Sensory Basis of Fish Schools: Relative Roles of Lateral Line and Vision. *Journal Of Comparative Physiology*, 135(4):315–325.

Patrtridge, B. L., Johansson, J., and Kalish, J. (1983). The structure of schools of giant bluefin tuna in Cape Cod Bay. *Environmental Biology of Fishes*, 9:253–262.

Pavlov, D. S., Lupandin, A. I., and Skorobogatov, M. A. (2000). The effects of flow turbulence on the behavior and distribution of fish. *Journal of Ichthyology*, 20:232–261.

Peck, A. L. (1970). *Aristotle. History of Animals. Books IV-V1.* Harvard University Press, Cambridge, Massachusetts.

Perez-Escudero, A., Vicente-Page, J., Hinz, R. C., Arganda, S., and de Polavieja, G. G. (2014). idTracker: tracking individuals in a group by automatic identification of unmarked animals. *Nature methods*, 11(7):743–748.

Pitcher, T. (1983). Heuristic definitions of fish shoaling behaviors. *Animal Behaviour*, 31(2):611–613.

Pitcher, T. J. (1980). Some ecological consequences of fish school volumes. *Freshwater Biology*, 10:539–544.

Pitcher, T. J., Magurran, a. E., and Winfield, I. J. (1982). Fish in larger shoals find food faster. *Behavioral Ecology and Sociobiology*, 10(2):149–151.

Pitcher, T. J. and Parrish, J. K. (1993). Functions of shoaling behavior in teleosts. In Pitcher, T. J., editor, *Behavior of Teleost Fishes*, chapter 12, pages 363–440. Springer, 2nd edition.

Preparata and Shamos (1985). *Computaional Geometry. An Introduction.* Springer-Verlag.

Preuss, T. and Faber, D. S. (2003). Central cellular mechanisms underlying temperature-dependent changes in the goldfish startle-escape behavior. *The Journal of neuroscience*, 23(13):5617–26.

Preuss, T., Osei-Bonsu, P. E., Weiss, S. A., Wang, C., and Faber, D. S. (2006). Neural Representation of Object Approach in a Decision-Making Motor Circuit. *New York*, 26(13):3454 –3464.

Pulliam, H. R. (1973). On the advantages of flocking. *Journal of theoretical biology*, 38(2):419–422.

Radakov, D. (1973). *Schooling and the ecology of fishes.* J. Wiley.

Reader, S. M., Kendal, J. R., and Laland, K. N. (2003). Social learning of foraging sites and escape routes in wild Trinidadian guppies. *Animal Behaviour*, 66(4):729–739.

Reebs, S. G. (2000). Can a minority of informed leaders determine the foraging movements of a fish shoal? *Animal Behavior*, 59(2):403–409.

Reynolds, C. W. (1987). Flocks, Herds, and Schools: A Distributed Behavioral Model. *Computer Graphics*, 21(4):25–34.

Rieucau, G., Boswell, K. M., De Robertis, A., Macaulay, G. J., and Handegard, N. O. (2014a). Experimental evidence of threat-sensitive collective avoidance responses in a large wild-caught herring school. *PloS one*, 9(1):e86726.

Rieucau, G., Fernö, A., Ioannou, C. C., and Handegard, N. O. (2014b). Towards of a firmer explanation of large shoal formation, maintenance and collective reactions in marine fish. *Reviews in Fish Biology and Fisheries*, pages 21–37.

Rieucau, G. and Giraldeau, L. (2009). Persuasive companions can be wrong: the use of misleading social information in nutmeg mannikins. *Behavioral Ecology*, 20(6):1217–1222.

Rosbash, M., Stoleru, D., and Peng, Y. (2004). Coupled oscillators control morning and evening locomotor behaviour of Drosophila. *Letters to Nature*, 431(October):862–868.

Rubenstein, M., Cornejo, A., and Nagpal, R. (2014). Programmable self-assembly in a tthousand-robot swarm. *Science*, 345(6198):795–799.

Ryer, C. H. and Olla, B. L. (1991). Information transfer and the facilitation and inhibition of feeding in a schooling fish. *Environmental Biology of Fishes*, 30(3):317–323.

Sasaki, T., Granovskiy, B., Mann, R., Sumpter, D., and Pratt, S. (2013). Ant colonies outperform individuals when a sensory discrimination task is difficult but not when it is easy. *Proceedings of the National Academy of Sciences*, 110(34):13769–13773.

Schmicl, T. and Crailsheim, K. (2008). Trophallaxis within a robotic swarm: bio-inspired communication among robots in a swarm. *Autonomous Robots*, 25(1-2):171–188.

Sepulchre, R., Paley, D. A., and Leonard, N. E. (2008). Stabilization of planar collective motion with limited communication. *IEEE Trans. on Automatic Control*, 53(3):706–719.

Shahnawaz, A., Venkateshwarlu, M., Somashekar, D. S., Santos, K., and Santosh, K. (2010). Fish diversity with relation to water quality of Bhadra River of Western Ghats (India). *Environmental Monitoring and Assessment*, 161(1-4):83–91.

Shaw, E. (1970). Schooling in fishes: Critique and review. In Aronson, L. R., Tobach, E., and Lehrman, D. S., editors, *Schooling in fishes: Critique and review*, Development and Evolution of Behavior, pages 452–480. Freeman, San Francisco, CA.

Shaw, E. (1978). Schooling Fishes: The school, a truly egalitarian form of organization in which all members of the group are alike in influence, offers substantial benefits to its participants. *American Scientist*, 66(2):166–175.

Shelton, D. S., Price, B. C., Ocasio, K. M., Martins, E. P., Shelton, D. S., Price, B. C., Ocasio, K. M., and Martins, E. P. (2014). Density and Group Size Influence Shoal Cohesion , but Not Coordination in Zebrafish (*Danio rerio*). *Journal of Comparative Psychology*, 129(1):72–77.

Simmons, A. (2004). Many-wrongs: the advantage of group navigation. *Trends in Ecology & Evolution*, 19(9):453–5.

Simons, A. M. (2004). Many wrongs: the advantage of group navigation. *Trends in ecology & evolution*, 19(9):453–455.

Skardal, P. S., Taylor, D., Sun, J., and Arena, A. (2015). Erosion of synchronization: Coupling heterogeneity and network structure. *Physica D: Nonlinear Phenomena*, in press(correced proof).

Soria, M., Freon, P., and Chabanet, P. (2007). Schooling properties of an obligate and a facultative fish species. *J. Fish Biology*, 71(5):1257–1269.

Soria, M., Gerlotto, F., and Fréon, P. (1993). Study of learning capabilities of tropical clupeoids using an artificial stimulus. *ICES Mar. Sci. Symp*, 196:17–20.

Stienessen, S. C. and Parrish, J. K. (2013). The effect of disparate information on individual fish movements and emergent group behavior. *Behavioral Ecology*, 24(5):1150–1160.

Strandburg-Peshkin, A., Twomey, C. R., Bode, N. W. F., Kao, A. B., Katz, Y., Ioannou, C. C., Rosenthal, S. B., Torney, C. J., Wu, H. S., Levin, S. A., and Couzin, I. D. (2013). Visual sensory networks and effective information transfer in animal groups.

Sumpter, D. J. T. (2006). The principles of collective animal behaviour. *Philosophical Transactions of the Royal Society B: Biological Sciences*, 361(1465):5–22.

Sumpter, D. J. T., Krause, J., James, R., Couzin, I. D., Ward, A. J. W., and Hall, G. (2008). Consensus Decision Making by Fish. *Current Biology*, 18(22):1773–1777.

Sumpter, D. J. T., Mann, R. P., and Perna, A. (2012). The modelling cycle for collective animal behaviour. *Interface Focus*, 2(6):764–773.

Thorpe, J. E., Ross, L. G., Struthers, G., and Watts, W. (1981). Tracking Atlantic salmon smolts, *Salmo salar* L., through Loch Voil, Scoltand. *J.Fish Biol*, 19:519–537.

Torney, C., Neufeld, Z., and Couzin, I. D. (2009). Context-dependent interaction leads to emergent search behavior in social aggregates. *Proceedings of the National Academy of Sciences*, 106(52):22055–22060.

Treherne, J. E. and Foster, W. A. (1981). Group Transmission of Predator Avoidance-Behavior in a Marine Insect – The Trafalgar effect. *Animal Behaviour*, 29:911–917.

Trump, W. J. V., Coombs, S., Duncan, K., and McHenry, M. J. (2010). Gentamicin is ototoxic to all hair cells in the fish lateral line system. *Hearing research*.

Trump, W. J. V. and Mchenry, M. J. (2013). The lateral line system is not necessary for rheotaxis in the Mexican blind cavefish (\emph{Astyanax fasciatus}). *Integrative and Comparative Biology*, 53(5):799–809.

Turner, R. H. and Killian, L. M. (1957). *Collective behavior*. Prentice Hall, Oxford, England.

Tytell, E. D., Standen, E. M., and Lauder, G. V. (2008). Escaping Flatland: three-dimensional kinematics and hydrodynamics of median fins in fishes. *Journal of Experimental Biology*, 211:187–195.

Tytler, P., Thorpe, J. E., and Shearer, W. M. (1978). Ultrasonic tracking of the movements of Atlantic salmon smolts (*Salmo salar* L) in the estuaries of two Scottish rivers. *J. Fish Biology*, 12:575–586.

Vabø, R. and Nøttestad, L. (1997). An individual based model of fish school reactions: predicting antipredator behaviour as observed in nature. *Fisheries Oceanography*, 6(3):155–171.

Viehman, H. A. and Zydlewski, G. B. (2015). Fish Interactions with a Commercial-Scale Tidal Energy Device in the Natural Environment. *Estuaries and Coasts*, 38(1):241–252.

Viscido, S. V., Parrish, J. K., and Grünbaum, D. (2004). Individual behavior and emergent properties of fish schools: A comparison of observation and theory. *Marine Ecology Progress Series*, 273:239–249.

Viscido, S. V., Parrish, J. K., and Grünbaum, D. (2005). The effect of population size and number of influential neighbors on the emergent properties of fish schools. *Ecological Modelling*, 183(2-3):347–363.

Vogel, S. and Labarbera, M. (1978). Simple Flow Tanks for Research and Teaching. *BioScience*, 28(10).

Ward, A. J. W., Hoare, D. J., Couzin, I. D., Broomt, M., and Krause, J. (2010). The effects of parasitism and body length on positioning within wild fish shoals. *Society*, 71(1):10–14.

Ward, A. J. W., Sumpter, D. J. T., Couzin, I. D., Hart, P. J. B., and Krause, J. (2008). Quorum decision-making facilitates information transfer in fish shoals. *Proceedings of the National Academy of Sciences*, 105(19):6948–6953.

Weihs, D. (1973). Hydrodynamics of fish schooling. *Nature*, 241:290– 291.

Weiss, S. A., Preuss, T., and Faber, D. S. (2009). Phase encoding in the Mauthner system: Implications in left-right sound source discrimination. *The Journal of Neuroscience*, 29(11):3431–41.

Windsor, S. P., Norris, S. E., Cameron, S. M., Mallinson, G. D., and Montgomery, J. C. (2010). The flow fields involved in hydrodynamic imaging by blind Mexican cave fish (*Astyanax fasciatus*). Part I : open water and heading towards a wall. *Journal of Experimental Biology*, 4:3819–3831.

Wood, A. J. and Ackland, G. J. (2007). Evolving the selfish herd: emergence of distinct aggregating strategies in an individual-based model. *Proceedings of the Royal Society B: Biological Sciences*, 274(1618):1637–42.

Yang, Y., Klein, A., Bleckmann, H., and Liu, C. (2011). Artificial lateral line canal for hydrodynamic detection. *Applied Physics Letters*, 99(2):023701.

Zhang, F., Lagor, F. D., Yeo, D., Washington, P., and Paley, D. A. (2015). Distributed flow sensing for closed-loop speed control of a flexible fish robot. *Bioinspiration & Biomimetics*, 10(6):65001.

Zheng, M., Kashimori, Y., Hoshino, O., Fujita, K., and Kambara, T. (2005). Behavior pattern (innate action) of individuals in fish schools generating efficient collective evasion from predation. *Journal of Theoretical Biology*, 235(2):153–167.

Zhu, Q., Wolfgang, M. J., and Yue, D. K. P. (2002). Three-dimensional flow structures and vorticity control in fish-like swimming. *Journal of Fluid Mechanics*, 468:1–28.

Zottoli, S. J., Bentley, A. P., Prendergast, B. J., and Rieff, H. I. (1995). Comparative studies on the Mauthner cell of teleost fish in relation to sensory input. *Brain, Behavior, and Evolution*, 46(3):151–164.